Retinal perfusion changes in radiation retinopathy-post brachytherapy for choroidal melanoma

by

Kalpana Rose

A thesis
presented to the University of Waterloo
in fulfillment of the
thesis requirement for the degree of
Doctor of Philosophy
in
Vision Science

Waterloo, Ontario, Canada, 2017

Examining Committee Membership

The following served on the Examining Committee for this thesis. The decision of the Examining Committee is by majority vote.

External Examiner	NAME	Toke Bek
	Title	Professor
Supervisor	NAME	Christopher Hudson
	Title	Professor
Internal Member	NAME	Trefford Simpson
	Title	Professor
Internal-external Member	NAME	Mungo Marsden
	Title	Associate Professor
Other Member	NAME	Elizabeth Irving
	Title	Professor

Author's declaration

This thesis consists of material all of which I authored or co-authored: see Statement of Contributions included in the thesis. This is a true copy of the thesis, including any required final revisions, as accepted by my examiners.

I understand that my thesis may be made electronically available to the public.

Statement of Contributions

Inter-Visit Repeatability of Retinal Blood Oximetry and Total Retinal Blood Flow under Varying Systemic Blood Gas Oxygen Saturations

Kalpana Rose; Susith I. Kulasekara; Christopher Hudson

Investigative Ophthalmology & Visual Science January 2016, Vol.57, 188-197.
doi:10.1167/iovs.15-17908

	Design	Recruitment	Data Acquisition	Analysis	Writing/ Publication
K. Rose	x	x	x	x	x
S.I. Kulasekara	x	x	x	x	
C. Hudson	x			x	x

Table detailing role of each author in this publication (x denotes significant contribution)

Abstract

Introduction: Radiation retinopathy (RR) is a chronic progressive vasculopathy developing secondary to the impact of ionizing radiation to the retina. RR develops post radiation therapy using radioactive plaque to treat intraocular tumors. It is not possible to predict which patients will develop RR. Changes in retinal blood oxygen saturation and blood flow could predict the future onset of RR, thereby facilitating the use of treatment such as intra-vitreal anti-vascular endothelial growth factor (VEGF).

Methods: Chapter 3 and 4: Total retinal blood flow (TRBF) and retinal blood oxygen saturation (SO_2) was non-invasively measured in eleven healthy human volunteers using a novel and exact provocation technique (RespirAct) that allows the precise control of the end-tidal partial pressure of oxygen ($P_{ET}O_2$). Between-visits repeatability and within-visit variability of TRBF and SO_2 measurements were assessed. Inner retinal oxygen delivery and consumption was calculated using Fick's principle during stages of normoxia, hypoxia and hyperoxia. Chapter 5 and 6: Seventeen patients diagnosed with unilateral choroidal melanoma (CM) and eight patients who had developed unilateral ischemic RR were recruited from *Ocular Oncology Clinic* in the *Princess Margaret Hospital, Toronto, Canada* i.e. the only center all over Canada to treat CM patients with radiation therapy. The subjects underwent measurement of TRBF using a prototype methodology based upon Doppler Spectral Domain Optical Coherence Tomography (SD-OCT) and retinal vessel SO_2 using a prototype Hyperspectral Retinal Camera (HRC), following pupil dilation with 1% tropicamide. In CM patients, the retinal hemodynamic parameters were studied in both eyes, before, 3months and 6months post ^{125}Iodine plaque brachytherapy treatment. For

RR patients, the measurements were taken once in both eyes after confirming the ischemic changes by wide-field fluorescein angiography.

Results: Chapter 3 and 4: When the arterial $P_{ET}O_2$ (end-tidal partial pressure of oxygen) was increased from baseline ($P_{ET}O_{2=}$100mmHg) to 200 and 300mmHg, the TRBF significantly reduced (p=0.020) from 44.60 µL/min (±8.9) to 40.28 µL/min (±8.9) and 36.23 µL/min (±4.6), respectively. Retinal arteriolar SO_2 (SaO_2) did not show any significant change during $P_{ET}O_2$ of 200 and 300mmHg, compared to baseline. However, retinal venular SO_2 (SvO_2) significantly increased (p<0.000) from 57.2% (±3.9) to 61.3% (±3.6) and 62.0% (±3.4) during $P_{ET}O_2$ of 200 and 300mmHg, respectively, compared to baseline. Lowering the arterial $P_{ET}O_2$, from baseline to 80, 60 and 50mmHg, TRBF significantly increased (p=0.040) from 43.17 µL/min (±12.7) to 45.19 µL/min (±5.5), 49.71 µL/min (±13.4) and 52.89 µL/min (±10.9) with simultaneous reduction in the SaO_2 and SvO_2 from 99.3 % (± 5.8) and 56.3% (± 4.2) to 95.6% (± 5.1) and 52.5 (± 4.1), 89.6% (± 2.8) and 49.5% (± 2.9), 83.3% (± 3.9) and 45.0 % (± 6.1), respectively (p<0.000). The group mean coefficient of repeatability (COR) for the retinal blood SaO_2, SvO_2 and TRBF were 18.4% (relative to a mean effect of 104.4%), 15.2% (relative to a mean effect of 60.3%), and 21.8 µL/min (relative to a mean effect of 44.72 µL/min). The overall coefficient of variability (COV) for SaO_2, SvO_2 and TRBF measurements were 4.7% and 6.9%, and, 15.1% respectively. The inner retinal oxygen extraction was calculated as 3.64 mLO_2/min/100g tissue in humans. Chapter 5: The average TRBF in the eye with RR was significantly lower compared to the fellow eye (33.48 ± 12.73 µL/min vs 50.37 ± 15.26 µL/min; p = 0.013). The SaO_2 and SvO_2 was higher in the retinopathy eye compared to the fellow eye (101.11 ± 4.26%, vs 94.45 ± 5.79%; p=0.008) and (62.96 ± 11.05% vs 51.24 ± 6.88%, p=0.051), respectively. Chapter 6: Out

of 17 CM patients recruited, 2 patient data was excluded due to poor image quality, and 3 others were lost to follow-up. During the six month follow up period, one person developed RR. The SaO_2 measurement was found to be significantly increased (p=0.026) from 94.4 % ($\pm$7.9) to 98.9% ($\pm$8.8) and 100.6 % ($\pm$6.4), respectively during 3 and 6 month follow up post ^{125}Iodine plaque brachytherapy compared to before treatment.

Conclusions: Chapter 3: Our study demonstrated significant changes in retinal blood SO_2 and TRBF during systemic changes in arterial $P_{ET}O_2$. The variability in TRBF measurements may reflect the impact of subjective assessment in venous area estimation as well as Doppler signal strength differences between visits. One needs to note that, a common clinical test such as visual acuity measurement also has a reported variability of up to ±0.15 logMAR (or $\pm$ 8 logMAR letters), relative to a mean effect of 0.017 logMAR ($\pm$ 4.2 letters), yet it is still being utilized as a useful clinical tool. The Doppler SD-OCT and HRC offer a quantifiable and repeatable technique of assessing retinal hemodynamics. Minimizing subjectivity in terms of blood flow analysis as well as correcting imperfections in the optics design of the HRC could possibly improve the repeatability of TRBF and retinal blood SO_2, respectively. Chapter 4: Oxygen extracted from the inner retinal vessels remains unchanged during safe levels of systemic hypoxia and hyperoxia. Chapter 5: The effect of ionizing radiation has an impact on the TRBF and retinal blood SO_2, clinically presenting similar to a rapidly developing diabetic retinopathy. The results show an altered retinal vascular physiology in patients with radiation related retinopathy. Chapter 6: ^{125}Iodine brachytherapy significantly increases the retinal arteriolar blood SO_2, suggesting improved retinal tissue perfusion in the treated eye. It is interesting to note that one patient developed RR in this six month period. About a 20% increase in retinal arteriolar and venular

blood oxygen saturation was observed in this patient, 6 month post brachytherapy compared to pre-treatment value. In order to predict who will develop RR following brachytherapy, it is important to follow up rest of the eleven subjects to measure SO_2 and TRBF during 12 and 18 month period or until they develop retinopathy. This will be a future work of interest, to recruit even large number of CM patients in a longitudinal approach. Only then a pattern or model for predicting RR in terms of SO_2 or TRBF measurements could be established. The study examines the early effects of brachytherapy on retinal hemodynamics.

Acknowledgements

First and foremost I thank God for who gives me strength and ability to pursue my dreams. I sincerely thank Dr. Chris Hudson for being my mentor, well-wisher and supervisor during the past 7 years. His advice, support and motivation helped me to achieve higher as a graduate student. It's my honor and privilege to work with him.

I would like to extend my gratitude to my advisory committee members including Dr. Trefford Simpson, Dr. Elizabeth Irving and Dr. Michael Brent for their advice and encouragement. I thank Susith Kulasekara for introducing me to the Ocular Oncology team of Princess Margaret Hospital (PMH), Toronto, Canada; from where I found an opportunity to build my PhD work.

I owe my deepest gratitude to Dr. Hatem Krema for accommodating me as a part of PMH team in recruiting choroidal melanoma patients. I am indebted to thank each and every staff of ocular oncology unit, PMH including Jan Empringham, Andrea Harris, Harini Thevarajah, Dr. Althomari, Dr. Lauri De Nicola, Dr. Priya Durairaj, Dr. Wantanee Dangboon, and Dr. Yael Chavez.

I thank Ontario Research Fund – Research Excellence award for the financial support. I extend my thanks to Jean-Philippe Sylvestre and Reza Jafari of Optina Diagnostics for helping out with oximetry software installation. I would like to thank Michal Vymyslicky, Susith Kulasekara and Ricky Cheng from Hudson lab for their friendlier support. I thank Dr. Sunita Shankar and Janet Wong for their administrative support. Special thanks to Stephanie Forsyth and Krista Parsons for their help. My gratitude extends to our summer Research Assistants, Bryan Wong and Andrew Beck for their valuable input in literature search and Introduction chapter of this thesis.

My gratitude extends to all fellow graduate students for their support and especially to those who participated in my study.

Finally I would like to thank my family and friends for their extended support and love. I cannot find words to thank my beloved Aunt Sarah and Uncle Suri for their emotional support and encouragement. I thank all my friends in Canada and Abroad for their motivation. Last but not the least; I thank my Dad, Mom, Brothers, Sisters, Husband and my Son for being there for me and believing in me.

Dedication

This thesis is dedicated to my beloved Parents Sasikala Rose and Krishnaswamy Rose; my loving Husband Prem and Son Praveen.

Table of Contents

List of Figures

List of Tables

List of Abbreviations

AMD	Age Related Macular Degeneration
CRA	Central Retinal Artery
CRV	Central Retinal Vein
COR	Coefficient of Repeatability
COV	Coefficient of Variability
CBF	Choroidal blood flow
CM	Choroidal Melanoma
DOCTORC	Doppler Optical Coherence Tomography of Retinal Circulation
DO_2	Inner retinal oxygen delivery
DD	Disc Diameter
DNA	Deoxyribonucleic acid
HRC	Hyperspectral Retinal Camera
Hb	Hemoglobin
HbO_2	Oxyhemoglobin
LDV	Laser Doppler velocimetry
ODR	Optical Density Ratio
OCT	Optical Coherence Tomography
OEF	Oxygen Extraction Fraction
PaO_2	Partial pressure of arterial concentration of oxygen
$PaCO_2$	Partial pressure of arterial concentration of carbon dioxide
$P_{ET}O_2$	End-tidal partial pressure of oxygen
$P_{ET}CO_2$	End-tidal partial pressure of carbon dioxide
PO_2	Partial Pressure of Oxygen
RBF	Retinal Blood Flow
RR	Radiation Retinopathy
SO_2	Oxygen Saturation
SaO_2	Oxygen saturation of the arteriolar blood
SvO_2	Oxygen saturation of the venular blood
SD-/- FD OCT	Spectral Domain - / - Fourier Domain Optical Coherence Tomography
TRBF	Total Retinal Blood Flow
VO_2	Inner retinal oxygen consumption
VEGF	Vascular Endothelial Growth Factor

Chapter 1 **Introduction**

1.1 The retinal vasculature: Blood supply and drainage

The central retinal artery (CRA), a branch of ophthalmic artery, enters the eye via optic nerve head and supplies the inner retina. The CRA then gives rise to four main branches: The superior, inferior, temporal and nasal retinal arterioles and these arterioles supply each quadrant of the retina.[1] Retinal arterioles usually have a capillary-free zone running parallel to the course of the vessel where the oxygen content of the tissue is thought to be higher due to free diffusion. Whereas, venules are surrounded by slightly less pronounced oxygen enriched zone compared to arterioles.[2]

The retinal capillaries are most dense in the center of the retina and eventually taper in density towards the periphery and around the perifoveal area, which surrounds the foveal avascular zone.[3] The blood from retinal capillaries is drained via the retinal venules into the central retinal vein (CRV). Upon exiting the optic nerve, the CRV drains into either the ophthalmic vein or directly into the cavernous sinus (Figure 1.1).[1,4]

1.2 Structure and arrangement of retinal vessels

The retinal vessels are arranged in a way that the major retinal artery and vein remain within the retinal nerve fiber layer and ganglion cell layer, whereas the arterioles and venules extend deeply to form the major capillary network. These networks thin as they extend themselves towards retinal periphery.[3]

The walls of the major retinal arterioles are made up of five to seven layers of smooth muscle cells, which control the contraction and relaxation of vascular lumen. The smooth muscle cells are surrounded by a basal lamina containing collagen, which anchors the blood vessel to

the surrounding tissue. The endothelial cells lie between the smooth muscle layer and circulating blood.[5] After branching, the number of layers that comprise the vessels diminishes into just one or two in the peripheral retina.[2]

The anatomical arrangement of the retinal circulation has very important clinical implications. Due to the high metabolic demand, uninterrupted blood supply from both the choroidal and inner retinal circulation is essential; loss of either of those could impact the retinal function substantially. Also, the proximity of arterioles and venules itself might affect one another, especially at the arterio-venous crossing points.[4]

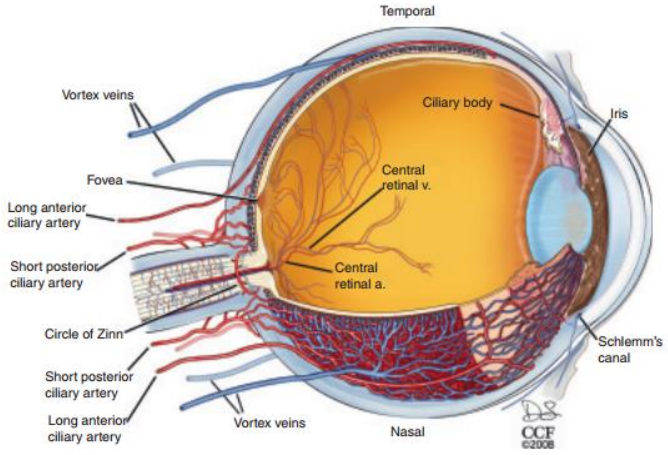

Figure 1.1 A cutaway drawing of the human eye showing the major blood vessels supplying the retina, choroid and anterior segment. Drawing by Dave Schumick. Reprinted with permission from *Encyclopedia of the eye* (Anand-apte 2010), Elsevier Books.

1.3 Autoregulation

Retinal vessels lack neural innervation. However, the blood flow is effectively regulated through various neurogenic, hormonal, metabolic and myogenic-driven feedback mechanisms. It is mostly the metabolic and myogenic mechanisms that regulate the inner retinal blood flow.[6]

1.3.1 Myogenic autoregulation

The ability of a tissue to maintain blood flow at a constant level despite changes in perfusion pressure is known as myogenic autoregulation.[7] Experimenters previously demonstrated this type of autoregulation by increasing and decreasing the perfusion pressure to study retinal vascular resistance. These studies illustrate that the retinal vessels are capable of regulating the blood flow over a substantial range of intraocular pressure and systemic blood pressure.[8,9] Myogenic autoregulation happens when vascular endothelial cells stretch or compress due to the changes in transmural pressure causing the vascular smooth muscle cells to depolarize or hyperpolarize resulting in constriction or dilation of vessels.[10,11]

1.3.2 Vascular reactivity and metabolic autoregulation

The regulation of blood flow through the action of local factors, such as changes in arterial blood gases, modulate the vessel tone through release of vasoactive factors by the vascular endothelium and/or surrounding neural tissue; this is referred as metabolic autoregulation.[11] The term 'metabolic autoregulation' can alternatively be referred to as 'vascular reactivity'. Vascular reactivity is the magnitude of change in hemodynamics to stimuli such as oxygen (O_2), carbon dioxide (CO_2), light and glucose.

As arterial blood gas concentration varies, the retinal circulation adapts to neutralize the change in the local environment by releasing endothelial-mediated factors to provide a constant supply of O_2.[12] These factors either relax the vascular tone or constrict it. Nitric oxide and prostacyclin are two of the vasorelaxing factors, whereas endothelin-1, angiotensin II, thromboxane-A_2 and prostaglandin H_2 are some of the vasoconstricting factors.

Extracellular lactate leads to the contraction or relaxation of the vessel wall according to the local tissue needs.[11,13,14]

1.3.2.1 Manipulation of blood gases: RespirAct

Provocations with various mixtures of O_2 and CO_2 have been used to investigate retinal vascular reactivity in humans and in animals. By administering safe levels of O_2 or CO_2, there will be changes in the arterial partial pressure of oxygen (PaO_2) and arterial partial pressure of carbon dioxide ($PaCO_2$), respectively. Hyperoxia is an increase in arterial partial pressure of oxygen from baseline homeostatic levels. Studies have shown that retinal vessels react to hyperoxia by local constriction of arterioles, venules and capillaries; thereby reducing the retinal blood flow (RBF).[132,133] On the other hand, hypoxia leads to an increase in RBF by decreasing the PaO_2. Independently controlling both PaO_2 and $PaCO_2$ is almost unlikely by other studies, where a 100% O_2 is administered or ~>90% O_2 and ~5% CO_2 is coadministerd, without clamping the $PaCO_2$ for hyperoxic provocation.[132,134,135] This might further reduce the $PaCO_2$ concentration, which might impact the measured variables.[136]

The novel computer-controlled prospective gas targeting system (RespirAct, Thornhill, Toronto, Canada) used in our lab has overcome the above mentioned limitation by minimizing alterations by independently maintaining $PaCO_2$ during changes of PaO_2 or vice versa. It comprises a fresh gas reservoir and an expiratory gas reservoir. Each reservoir is connected to a face mask with separate one-way valves. The face mask covers the mouth and nose of the subject. In turn, the two reservoirs are inter-connected using a positive end-expiratory pressure (PEEP) valve which allows subjects to breathe exhaled gas (i.e. rebreathe CO_2-enriched gas) when the fresh gas reservoir is depleted (Figure 1.2).[137,138] The subject's

minute CO_2 production and O_2 consumption, gas flow and composition entering the sequential gas delivery circuit (Hi-Ox^{80}, Viasys Healthcare, Yorba Linda, CA) was attained using an automated gas flow controller which is connected to a computer.

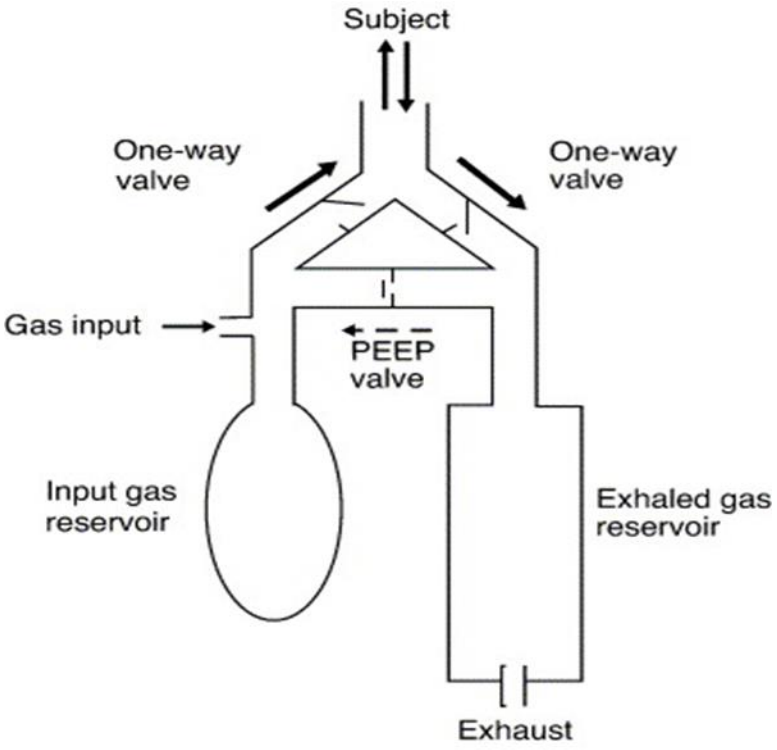

Figure 1.2 Schematic of a sequential rebreathing system. Reprinted with permission from *Microvasc Res.* 2005 May; 69(3): 149-155.

1.3.3 Impaired vascular response in retinal vascular diseases

Diseases affecting the retinal circulation also alter vasoregulation in humans. In diabetic retinopathy, structural alterations to the capillaries, increased permeability of vessel wall, and growth of new fragile blood vessels are some of the clinical features suggesting alterations in microcirculation. However, due to the progressive and long course of the disease, several undetectable vascular and neural damages might subtly occur before the clinical signs are revealed.

Impaired vascular reactivity in response to hyperoxia (i.e. increased blood gas oxygen concentration)[15,16] and flicker have been reported in diabetic retinopathy. Several animal and human studies report reduced vasodilatory response prior to the appearance of overt clinical retinopathy.[17,18] In sight-threatening disease such as glaucoma, vascular dysregulation has been reported as an important factor contributing to the pathophysiology.[19,20] It is the combination of biochemical, hemodynamic and hormonal factors that could possibly initiate the alteration in blood flow regulation before the prominent clinical signs develop.[21,22]

1.4 Vascular network of the choroid

The choroid is posterior part of the middle tunic of the eye, located in between the retina and sclera. The choroidal circulation nourishes the iris, ciliary body, and outer retinal layers including the retinal pigment epithelium and photoreceptors. The choroid receives 80% of all ocular blood, with the remaining 15% going to the iris/ciliary body and 5% to the inner retina.[4]

The choroid receives its blood supply via the ophthalmic artery from the long and several short posterior ciliary arteries (around the optic nerve head), with the short posterior ciliary arteries, supplying the posterior choroid and the long posterior ciliary arteries supplying the anterior choroid and the iris and ciliary body (Figure 1.1). The vascular layers of the choroid are divided into Haller and Sattler layers, consisting large and small arterioles and venules, respectively. The choriocapillaries form a dense network of highly anastomosed capillaries, located posterior to Bruch's membrane.[2,4] Blood from the choroid drains through the vortex veins into the ophthalmic vein.[1]

Choroidal vessels are fenestrated, unlike those in the retina (Figure 1.3). The fenestrations make them highly permeable to proteins, contributing to high oncotic pressure, which facilitates the movement of fluids in both directions between the retina and choroid. Also, sympathetic innervation controls the blood flow and other physiological functions of the choroid. The most important function of the choroid is to provide blood carrying oxygen and nutrients to the outer retina. The choroidal blood flow is the highest per unit time and weight of any other tissue. The flow is maximal at the fovea and close to the optic disc.[4]

The melanocytes present in the choroid impart a darker pigmentation[23,24] in primates. The choroid is also thought to act as a heat sink thereby preventing heat damage to the tissues.

The smooth muscle cells that line the vessels of the choroid are innervated by both divisions of the autonomic nervous system.[24] These nerve fibers form dense plexuses around the vessels. Axon terminals are also found throughout the stroma that terminate on non-vascular smooth muscle, intrinsic choroidal neurons, and possibly other cell types. There are also primary afferent sensory fibers that project to the trigeminal ganglion through the ophthalmic nerve. In mammals, the pterygopalatine ganglion is the origin of the main parasympathetic input to the choroid.[24]

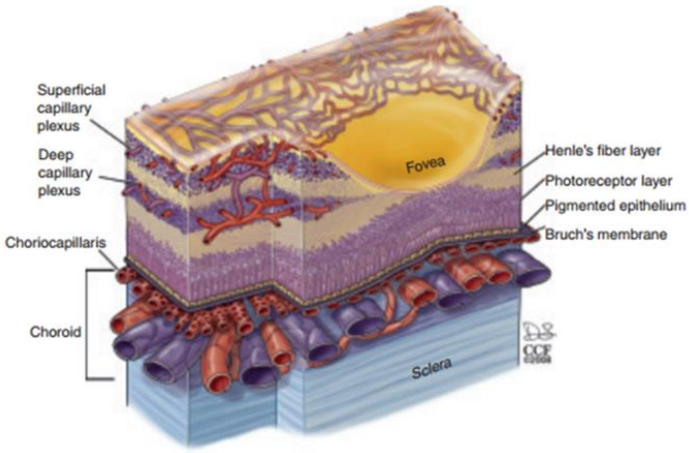

Figure 1.3 A diagram showing details of the retinal and choroidal vasculature and changes that occur at the level of the human fovea. Drawing by Dave Schumick. Reprinted with permission from *Encyclopedia of the eye* (Anand-apte 2010), Elsevier Books.

1.5 Comparative physiology and regulation of retinal and choroidal perfusion

Both the choroid and the retina are vital in supplying the metabolic needs of the eye. However, these two structures have very different hemodynamic properties. The retina has a much lower blood flow but a higher level of O_2 extraction compared to the choroid.[2] The choroid has strong central sympathetic control mechanisms and has less autoregulation capacity. The retina on the other hand, lacks sympathetic innervation and thus is controlled solely by autoregulation instead.[4] Autoregulation in the retina is effective within a wide range of perfusion pressures.[2] The retina also has mechanisms for the local modulation, or fine tuning, of retinal blood flow but the data is limited. In contrast to the retina, circulation in the choroid is controlled by extrinsic autonomic innervation. Sympathetic afferent nerves release noradrenaline which binds to alpha 1-adrenoreceptors on vascular smooth muscle cells ultimately decreasing choroidal blood flow. Conversely, parasympathetic efferent nerves release nitric oxide which causes an increase in choroidal blood flow. The choroid also

receives innervation from trigeminal sensory fibers which contain calcitonin gene-related peptide. Experiments suggest a myogenic and/or neuronal contribution to choroidal blood flow regulation during changes in perfusion pressure but data is limited. Studies have shown that when dark-adapted eyes were exposed to room light, choroidal blood flow increased. These changes in blood flow were reported in both the stimulated and the contralateral eye indicating that the choroidal response is under neuronal control. These changes in choroidal hemodynamics that occur during light and dark adaptation could contribute to passive dissipation of heat induced by light, suggesting that the choroid is important for the maintenance of stable temperatures in the outer retinal layers.[2]

Several studies have reported the precise response of retinal vasculature to changes in the blood gas concentration[25,26] as well as to light-dark transitions.[12,27] In contrast to retinal blood flow regulation, the choroid shows less hemodynamic response to flicker stimulation and light stimulation.[24]

1.6 Quantification of retinal and choroidal blood flow

The eye provides a direct opportunity to non-invasively observe the retinal circulation, unlike any other organ in the body. Taking advantage of this, several techniques have been established to study retinal microvasculature. Unlike retina, the choroidal vascular bed is not readily visible for evaluation due to the complexity and variability in terms of its distribution. Instead, high resolution broad bandwidth light sources are being utilized for choroidal imaging. Several studies have reported impaired blood flow to play a key role in the pathogenesis of retinal vascular pathologies such as diabetic retinopathy,[15,21,28] age related macular degeneration (AMD)[30,31] and glaucoma.[19,29] The technical advancement has evolved

recently with several non-invasive techniques to reliably and conveniently quantitate the "blood flow", which may become an important outcome measure and potentially a biomarker toward understanding the vascular pathophysiology.

1.6.1 General hemodynamic principles underling blood flow measurement

Early in 19th century, Poiseuille's law explained that the flow of fluid through rigid tubes is governed by the pressure gradient and resistance to flow. Accordingly, blood flow (Q) is directly proportional to the perfusion pressure (ΔP) and inversely proportional to the vascular resistance (R).

$$Q = \frac{\Delta P}{R} \quad \text{(1.1)}$$

The difference between arterial and venous pressure is known as perfusion pressure. Whereas resistance (R) of flow is defined by the following equation

$$R = \frac{8L\eta}{\pi r^4} \quad \text{(1.2)}$$

Where, L is the length of the vessel, η is the fluid viscosity and r is the radius of the vessel. Rewriting Poiseuille's equation will inter-connect all the blood flow parameters as follows.

$$Q = \frac{\Delta P \pi r^4}{8\eta L} \quad \text{(1.3)}$$

The equation shows that, compared to vessel length and viscosity of fluid, small changes in radius could trigger significantly larger changes in flow to the tissue, because flow is related to the fourth power of radius.[32] Though Poiseuille's law primarily explains the flow of fluid through rigid tubes, blood flow through a vessel is different because of the elastic property of the vessel wall. Also, the blood might not always obey Newtonian characteristics since it is viscous.

The retinal arteriolar and venular walls have the ability to adjust their caliber, i.e. contract or relax causing larger changes in the flow, therefore referred to as "resistance vessels". Whereas, the capillaries are small enough to allow a single row of red blood cells to pass through them, in order to make sure necessary metabolic exchange takes place for proper tissue function, the capillaries are called "exchange vessels".

1.6.2 Retinal blood flow

1.6.2.1 Estimation from retinal vessel diameter

Retinal blood flow is directly proportional to the square root of vessel diameter.[33] It is interesting to know how the researchers from past have made an effort to measure retinal diameter, a surrogate for blood flow. An ophthalmoscope was in fact the first instrument used to assess the overall retinal health as well as to study the retinal vessel caliber.[34] The invention of fundus photography later provided a direct measure of retinal vessel diameter.[35] High resolution and magnified (35x) fundus images were projected onto a translucent screen to get a measure of retinal vessel diameter. However, the larger size of the vessel has restricted the measurable diameter to 0.5 to 1.5 disc diameter (DD) from the optic disc margin.[36]

The retinal vessel analyzer was developed approximately 20 years ago to measure blood vessel diameter under varying brightness profile, i.e. retinal blood vessel is imaged between 420-620nm light. The difference in the absorption characteristic of erythrocytes compared to the background (which reflects the light) fundus is what is used to measure the vessel diameter.[37] Diameter measurements alone do not provide a direct estimate of the blood flow,

instead combined blood cell velocity measurement using laser Doppler velocimetry would be more meaningful.

1.6.2.2 Laser Doppler techniques

The "Doppler" principle was discovered by Christian Doppler in 1842, following which a multitude of applications were proposed based on the Doppler shift theory to determine the velocity of moving objects.[38] One significant application in science, which is utilized thus far, is measuring the moving red blood cell velocity.

1.6.2.2.1 Laser Doppler Velocimetry (LDV)

Light of a known frequency (f) reflected by the blood vessel wall remains the same unlike those reflected by the moving red blood cells, which are shown to exhibit a shift in frequency (Δf). [39] The difference in frequencies of reflected light is used to calculate the red blood cell velocity (Figure 1.4). This phenomenon is used in all the Doppler techniques mentioned below.

In LDV, the absolute velocity is measured by finding both the angle between the incident light and the blood vessel as well as the reflected light and the blood vessel. The photodetector present detects the maximum frequency shift from the center of the blood vessel. A fast Fourier transform is then used to obtain the Doppler shifted power spectrum (DSPS). The cut-off frequency of the DSPS demonstrates the maximum frequency shift, which is used to calculate the centerline blood velocity.[39]

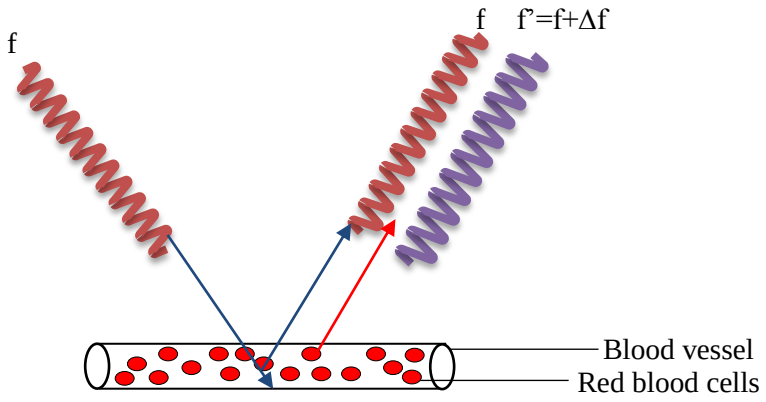

Figure 1.4 Diagrammatic illustration of "The Doppler effect" phenomenon.

1.6.2.2.2 Bidirectional Laser Doppler Velocimetry (BLDV)

Unlike LDV, the BLDV is unique in the sense that it is able to measure the absolute velocity by utilizing two photo-detectors of fixed angular separation for velocity measurements.[39] The Canon laser blood flowmeter (CLBF) utilizes BLDV technique to quantitate absolute flow velocity by simultaneous measurement of blood velocity and vessel diameter. The CLBF is a fundus-camera type device with two photo-detectors and two lasers. A red diode laser is used to measure absolute velocity and a green rectangular helium-neon laser measures vessel diameter. The light scattered by the red blood cells at the site of measurement is detected simultaneously via two photodetectors separated by a known, fixed angle. Therefore two Doppler shifted frequencies are measured. The differences in the two values are used to calculate the centerline velocity of red blood cells in absolute units.[40] In addition to the assumption that the flow within a vessel of interest is '*laminar*' in nature. The CLBF is also limited to acquire measurements from retinal vessels of diameter greater than 60µm.

1.6.2.2.3 Scanning Laser Doppler Flowmetry (SLDF)

Bonner and Nossal[41] in 1981 introduced a technique based on light scattering properties of tissue containing moving red blood cells, to measure the volumetric blood flow in the retinal and choroidal vasculature. Though the technique uses the principle of "Doppler shift", the laser light is not focused on the major retinal vessel; instead the flow is measured from the optic nerve head away from the large vessels. Therefore, SLDF only measures the relative mean velocity and volume of blood flow in arbitrary units. The major limitation is that the obtained signal from the sampled tissue could be from both retinal and choroidal vasculature, unlike LDV where the signal is strictly from RBC's within retinal blood vessel.[20,42]

Confocal scanning laser tomography later incorporated SLDF in the form of the Heidelberg Retinal Flowmeter (HRF), to quantitate optic nerve head and retinal capillary blood flow. The word "Tomography" refers to imaging by sections, deep into the tissue through the use of near-infrared light. The technical detail of HRF is described elsewhere.[43,44] Briefly, the retinal tissue is sampled at a rate of 4000Hz using a 790nm laser source. Fast Fourier transformation of recorded Doppler shifted frequencies yields the relative capillary flow from a 10 pixel x 10 pixel region of tissue. A major limitation to the HRF is that the measurement of flow in arbitrary units, unlike CLBF, which measures flow in absolute units.

1.6.2.2.4 Doppler Spectral/Fourier Domain Optical Coherence Tomography (SD-/FD-OCT)

Optical Coherence Tomography (OCT) is a non-contact and non-invasive high-resolution technique for imaging of tissue structures on a micron scale. Due to its ability to provide real time cross-sectional images of tissue in situ, it functions as a type of "optical biopsy".[45] OCT generates the cross sectional images of the tissue microstructure by measuring the echo time

delay and the magnitude of the reflected light with a Michelson-type interferometer and low-coherence light.[46]

The Doppler principle was incorporated within the OCT in late 90's, in which the Doppler frequency shift was obtained by a spectrogram method, which used a fast Fourier transformation[47] for flow velocity calculation. However, this technique had limitations in terms of sensitivity and imaging speed. Later, spectrometer based Fourier domain Doppler OCT was introduced with improved imaging speed, high spatial resolution and velocity sensitivity.[48,49] Alongside the conventional OCT images, flow images were successfully generated by Doppler based OCT. In a laminar flow system, precise measurement of the flow velocity is determined using Doppler OCT. Fourier transformation of the resulting interference signal is performed to obtain flow velocities.

Doppler based OCT measures either the change in frequency to calculate the Doppler shift due to moving red blood cells, or the phase change between sequential A-scans in order to provide increased sensitivity to small flows.[50] To measure the total retinal blood flow (TRBF), the principle of Doppler effect is utilized where the frequency shift (Δf) from backscattered light is detected and simplified to:

$$\Delta f = \frac{-2nVcos\alpha}{\lambda_0} \quad \text{(1.4)}$$

Where, V is the velocity of the moving particle, θ is the angle between the OCT beam and the flow, n is the refractive index of the medium, and λ_0 is the wavelength of the incident beam.

Flow in single vein=average (V_{max}/Pi*Doppler phase shift*sin (Doppler angle))*vessel area, V_{max} is the maximum speed corresponding to Doppler phase wrapping limit. Flow from

individual retinal venules is then summed up to obtain the total volumetric blood flow at one time point using specialized software named Doppler Optical Coherence Tomography of Retinal Circulation (DOCTORC) (Figure 1.5).[48]

Studies have demonstrated the use of color Doppler OCT measurements of blood flow in the human retina *in vivo* and in real time with high data acquisition rates.[51] In order to measure flow accurately with Doppler techniques, it is also necessary to measure the geometry of the vessel and, in particular, the angle of the vessel with respect to the indent light beam, since this determines the degree of "Doppler shift".

In contrast to the conventional Doppler OCT mentioned above, the bidirectional-based Doppler FD-OCT is capable of measuring the absolute velocity independent of the Doppler angle between the incident light and the flow velocity vector. In this technique, light reflected from a blood vessel is imaged simultaneously by two spectrometers of known angular separation. Along with the vessel diameter measurements, this technique enables quantitative retinal blood flow measurement.[129] Recently introduced three beam Doppler OCT offers the advantage of a precise determination of velocity vector irrespective of vessel geometry information to acquire total retinal blood flow.[52]

SD-OCT is limited in terms of maximal velocity measurement due to imaging speed and phase averaging effects.[53] Also flow measurement is limited to the smallest vessel diameter, since capillary flow involves single red blood cell movement, rather than continuous fluid flow as occurs in major branch vessels.[54]

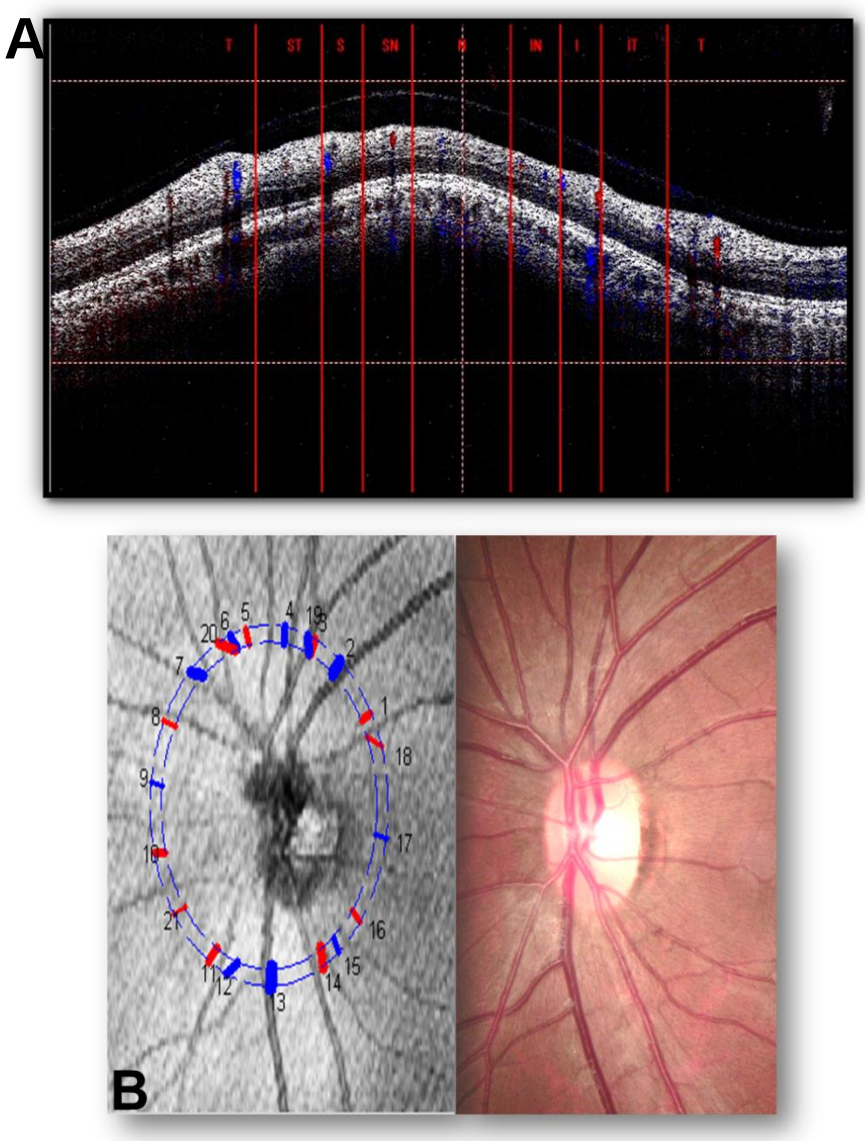

Figure 1.5 A) Screenshot of image showing the OCT beam passing through the superior nasal portion of the pupil. B) En face view of SD-OCT image with DOCTORC identified vessel location (numbers) and type (red=artery; blue=vein). Grader compares fundus photo with OCT image to confirm vessel type.

1.6.2.3 Other RBF measurement techniques

1.6.2.3.1 Measurement of leukocyte velocity

One of the oldest techniques to semi-qualitatively measure the red blood cell velocity in the retinal capillaries is *Blue field entoptic technique* suggested by Vierordt in 1860.[55] The principle relies on the psychophysical comparison of the speed of one's own leukocytes with that of the minimum and maximum speed of the simulated particles, while illuminating the retina with a 430nm light. The absorption of blue light by moving red blood cells but not by the leukocytes is the key in quantitating the retinal capillary blood flow. Though non-invasive, the technique has limited application due to its subjective way of measuring blood flow.

1.6.2.3.2 Invasive dye dilution technique

Fluorescein dye is administered intravenously to obtain a rapid sequence of photographs to visualize the time it takes for the dye to enter and clear a retinal blood vessel. This technique is known as fluorescein angiography (FA). The mean difference in passage of dye between the venous and arterial side of the blood stream is calculated as "mean circulation time".[56] Though it provides some index of retinal circulation, blood flow as such could not be quantitated using this technique. However, the technique is widely applied in clinical ophthalmology.

1.6.2.3.3 Color Doppler Imaging (CDI)

B-scan ultrasonography of tissue structure combined with Doppler shifted frequencies of moving erythrocytes evolved as CDI. In terms of blood flow measurement, CDI only provides the mean flow velocity, which is calculated from the peak systolic and end diastolic velocity.[57] However, the flow velocity beneath the Doppler threshold could not be determined due to poor Doppler angle or undetectable Doppler shifts.[42]

1.6.3 Choroidal Blood Flow (CBF)

Compared to retina, choroid has enormous blood flow (approx. 40 times greater than retinal vasculature), higher oxygen tension and most interestingly, a fenestrated, flat and wide capillary network.[58] This arrangement makes blood flow measurement technically difficult. Although the choroidal vascular bed cannot be directly visualized, several invasive and non-invasive techniques were developed to assess its circulation.[59,60,62,63,130] Invasive techniques such as direct measurement from choroidal veins, labelled microspheres,[59] and hydrogen clearance[60] are all restricted to animal studies. But, few techniques are actually carried out in human eyes.

1.6.3.1 CBF measurement in humans

Measuring the pulsatility of the blood flow was one of the earliest efforts made to study CBF. This could be due to the fact that choroid supplies the majority of the eye; therefore techniques that measures the pulsatile component of flow possibly estimate the choroidal perfusion, independent of the reterobulbar or retinal circulation.[61] Pulsatile ocular blood flow measurements using ocular blood flow tonography *per se* are however influenced by variation in ocular rigidity between individuals and by both retinal and choroidal circulations.[62] Polak and Co-workers utilized laser interferometry technique to measure the pulsations of the eye fundus to estimate the pulsatility of the blood flow. A light of wavelength 783nm is reflected both at the front side of the cornea and the retina. The changes in the interference fringes during a cardiac cycle, is observed as a distance change between cornea and retina. The maximum distance change measured is called as fundus pulsation amplitude. This technique is used to measure CBF. The CBF is measured close to the fovea, within the foveal avascular zone which is devoid of retinal circulation.[130]

The macular area of the eye is predominantly nourished by the choriocapillaries located underneath Bruch's membrane of choroid. Riva and Co-workers[63] reported the relative CBF in the foveal avascular zone, using laser Doppler flowmetry (LDF) non-invasively. LDF as explained earlier utilizes the Doppler principle to measures the red blood cell velocity. Since the fovea is devoid of retinal vessels, the achieved signal must be primarily from the choriocapillaries. However, the technique is not widely applied due to its high measurement variability.

Several imaging technique such as indocyanine green angiography,[64] laser targeted angiography,[65] have increased the understanding of choroidal circulation to the next level but the quantification of CBF using such techniques are difficult. Povazay and Co-workers[66] have proposed an ultrahigh resolution FD-OCT system which utilizes light of wavelength 1050nm to provide better visualization of choriocapillaries beneath retinal pigment epithelium. Despite the greater penetration depth and higher signal to noise ratio, the system has low sensitivity and poor image resolution.

1.6.4 Summary

Over the past few decades, the non-invasive measurement of blood flow has been a special topic of interest in retinal vascular physiology due to the fact that RBF disturbances have been reported in various retinal pathologies such as diabetic retinopathy,[15,28] AMD[30,31] and glaucoma.[19,20] The development of Doppler technology has been a major breakthrough in terms of blood flow quantification non-invasively. Several OCT techniques such as Spectral/Fourier domain, phase resolved,[49] have evolved that are promising tools to measure RBF in health and in diseased eyes.

The recently emerging optical coherence angiography (OCA) does not require dye such as fluorescein to be injected as a contrast agent into the blood stream to evaluate the motion of erythrocytes with in the vessels. Instead, a high speed FD-OCT system incorporated OCA, provides both structural and functional information by providing multiple cross-sectional images at the same location where volumetric OCA detects the relative motion of erythrocytes, in seconds, non-invasively.[42,67] Enhanced depth imaging OCT[68] and dual-beam-scan OCA[69] are built with higher sensitivity and greater penetration for enhanced visualization of choroidal vessels. However, measuring choroidal perfusion is questionable due to various anatomical and physiological variations of the choroidal vasculature such as complex arrangement of choriocapillaries, higher flow rate, and fenestrated capillaries compared to the retinal vascular bed.

1.7 Blood oxygenation measurement

Oxygen is transported to the tissues by an iron-containing protein present in the red blood cells called hemoglobin (Hb). Each Hb molecule can bind up to four molecules of O_2. Depending on the saturation or desaturation of Hb with O_2, it is referred as oxyhemoglobin (HbO_2) or deoxyhemoglobin, respectively. Measurement of oxygen saturation (SO_2) is basically defined by the percentage amount of Hb bound to the oxygen.

$$SO_2 = \frac{HbO_2}{Hb+HbO_2} \times 100 \quad \text{..... (1.5)}$$

In addition to homeostatic blood flow, the SO_2 in blood defines the metabolic state of the tissue.[20]

1.7.1 Absorption characteristics of hemoglobin

Measurement of the amount of light absorbed by a substance at a given wavelength is referred as the "extinction coefficient". The main absorption component of blood is Hb, but the oxy and deoxy hemoglobin exhibit differing molar extinction coefficients at most wavelengths (Figure 1.6). The wavelengths at which both Hb and HbO_2 exhibit similar absorption characteristics are referred as isosbestic or oxygen insensitive wavelengths, whereas, the wavelengths at which both Hb and HbO_2 exhibit different absorption characteristics are referred as oxygen sensitive or non-isosbestic wavelength.[70]

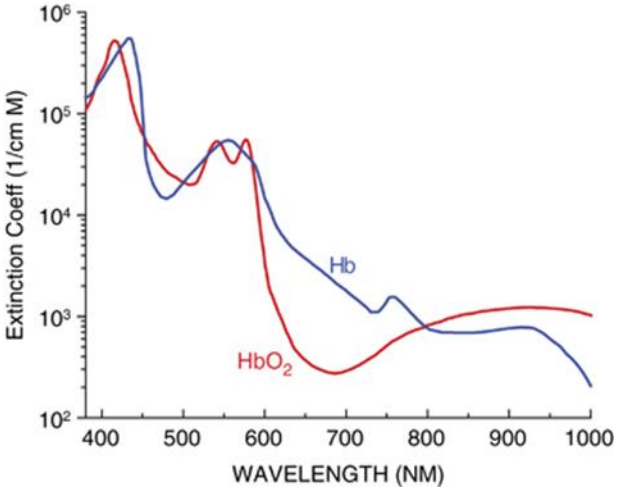

Figure 1.6 The molar extinction coefficients of deoxyhemoglobin (Hb) and oxyhemoglobin (HbO_2) as a function of wavelength. Reprinted with permission, *Eye* (2011) 25, 309-320, Nature Publishing group.

1.7.2 Retinal SO_2 measurement: Invasive techniques

Oxygen supply to the inner retina can be assessed by studying the partial pressure of oxygen (PO_2). Earlier studies report the assessment of PO_2 by inserting O_2 sensitive electrodes into the retina,[71] or through techniques such as phosphorescence quenching of palladium or ruthenium porphyrine.[72] These techniques are invasive and almost impractical to be used in human eyes.

1.7.3 Non-invasive oxygen saturation measurement

Spectrophotometric techniques are considered as one of the safest and promising tools to extract oxygen saturation in retinal blood non-invasively.[79-81,84] The different non-invasive techniques developed are discussed below.

1.7.3.1 Retinal photometric oximetry: Dual wavelength method

Measurement of oxygen saturation in blood or tissue is referred as "oximetry". In 1945, Drabkin and Co-workers[73] demonstrated the applicability of Beer-Lambert law in determining the SO_2 of blood. The Beer-Lambert law explains that for any given wavelength of light, its absorption is dependent on the extinction coefficient of the blood (ε), its concentration or hematocrit (c), and the distance (d) the light has to travel through the solution (path length):

$$I_T = I_o 10^{-\epsilon c d} \quad \text{(1.6)}$$

Where I_T is the intensity of the transmitted light through a solution and I_o is the intensity of incident light.[70]

Light absorption of a solution such as blood is given by its optical density (OD) which is given as

$$OD = -log_{10} \frac{I_T}{I_o} \quad \text{(1.7)}$$

The different absorption characteristics of oxy and deoxy hemoglobin allows the non-invasive quantification of SO_2 by spectral measurements.[74,75] The ratio of optical densities at isosbestic and non-isosbestic wavelengths gives the optical density ratio (ODR), which is given as follows

$$ODR = \frac{OD_{non-isosbestic}}{OD_{isosbestic}} \quad \text{(1.8)}$$

Although the instrument is reported to be sensitive to changes in blood oxygen saturation, various confounding factors such as the light scattering properties of red blood cells,[76] fundus pigmentation,[77] and vessel width,[74] has a significant impact on the measured SO_2. Also, the SO_2 values achieved depend on the values used for calibration of arterial and venular SO_2 i.e. 96% and 54%, respectively.[78]

1.7.3.2 Spectral Imaging

The limitations of the dual wavelength method encouraged the development of a new imaging technique utilizing spectroscopy to analyze materials by means of acquiring and identifying spectral signatures of its constituents using multiple wavelengths. The spectral signature of a molecule defines the structure of a molecule, when imaged at a series of specific wavelengths. Spectral imaging generates a number of greyscale images at various wavelengths, thereby providing both spatial and spectral information (Figure 1.7).[79]

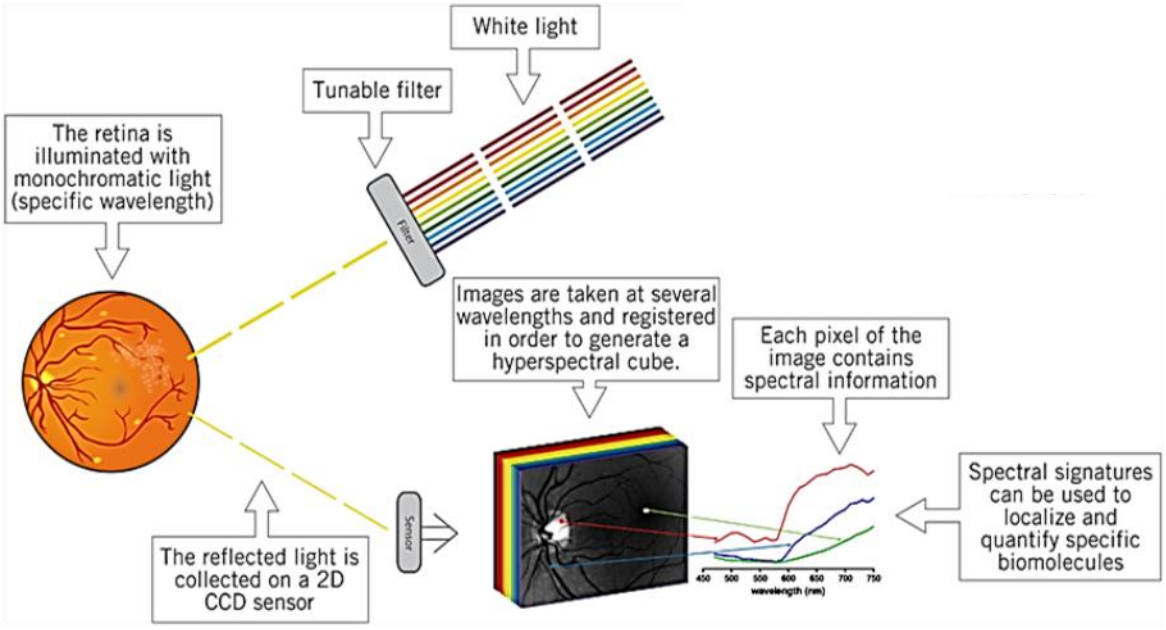

Figure 1.7 Illustrated principle of the hyperspectral imaging to generate spectral images of the retina. Reprinted with permission, *Experimental Eye Research* (2016); 146: 330-340. Elsevier.

1.7.3.3 Multispectral Vs Hyperspectral approach

A multispectral[80] approach utilizes a number of non-contiguous wavelengths at large bandwidths apart, whereas hyperspectral imaging[81] uses a large number of contiguous wavelengths at narrow bandwidths and provides higher spatial resolution. Both the approaches could provide transmission of the reflectance spectrum of each pixel within the image enabling the identification of molecules. The reflected light from the fundus is collected using a charge-coupled device and subsequently processed and analyzed to detect the substances present based on the spectral signature of each pixel. These spectral techniques are based on the principle of Beer-Lambert law and the known absorption spectra of hemoglobin to measure retinal blood SO_2.

A form of retinal oximetry using a hyperspectral retinal camera (HRC) incorporates a tunable laser source which allows the rapid access of specific wavelengths.[81,82] The HRC system records a series of time-sequential images at a sequence of wavelengths onto a 2D detector array forming a stack or cube of hyperspectral data within a few seconds. The tunable filters have no mobile parts, so the instrument is able to electronically tune into any particular wavelength. The fundus is sequentially illuminated using monochromatic light of predetermined range of wavelengths. At each wavelength, a 30° field-of-view of the posterior pole of the fundus is captured at high resolution (1.3 Megapixels). The filters are capable of delivering monochromatic light at a narrow bandwidth (FTMW = 2nm) and image acquisition occurs at a rate of 27 frames (wavelengths) per second.

A spectral data cube obtained by the HRC needs to be pre-processed before it can be analyzed. The spectral data cube is first normalized for spatial and spectral variations in light source intensity and any background 'noise' generated from the system optics is removed. Next, each image of the data cube is spatially registered with the rest of the images in the stack to correct for any motion artifacts.[81] A pre-processed data cube is then opened with an *in-house* Matlab (The Mathworks, Natick, MA) program. An automatic vessel segmentation algorithm[131] is then used to isolate the main vessel in the fundus image. The segmented vessel is further analyzed to determine the retinal blood SO_2 (Figure 1.8).

The challenges faced by these imaging techniques includes the longer acquisition time, weak fundus reflectance due to melanin pigment, and various artifacts from the imaging optics.[8]

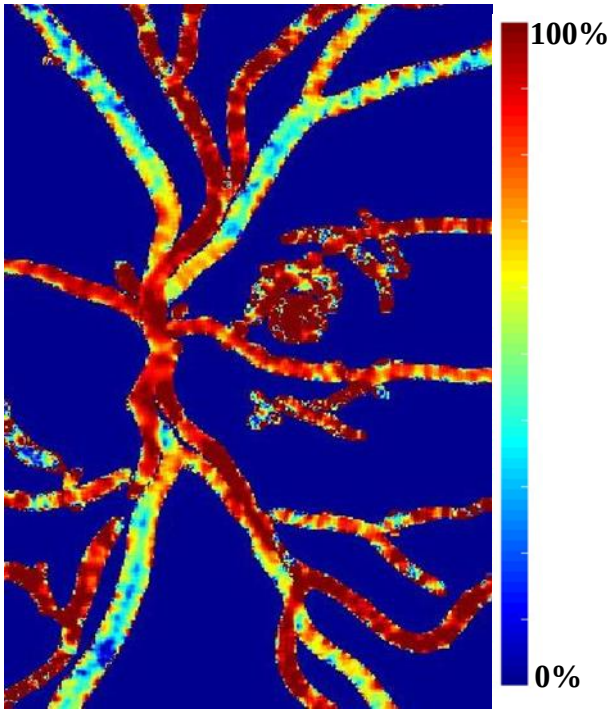

Figure 1.8 Color coded SO_2 map of retinal arterioles and venules. A scale of 0% and 100% represent percentage of oxygen saturation across the retinal vascular arcade**.**

1.7.4 Other retinal oximetry techniques

Photoelectric oximeters utilize three wavelengths (589, 569 and 586nm) to compensate for the light scattering effect of red blood cells as reported in the dual wavelength model. The optical density of the vessel at each wavelength is calculated from the estimated light transmission through the vessel using the average vessel and background fundus reflectance. The instrument is limited to measuring only a small portion of the retina.[76]

A scanning laser eye oximeter using four diode lasers emitting wavelengths centered at 629, 678, 821 and 899nm for retinal vessel oximetry was introduced.[83] The main difference compared to the three wavelength model is the use of a horizontal polarizer in the system, which compensates for the errors induced by specular reflection in the vessel wall. Hardarson and Co-workers[78] later developed a retinal oximeter which produces retinal images simultaneously at four wavelengths.

Tsuchihashi and Co-workers [84] came up with a Fourier incorporated spectral retinal imaging system comprising an interferometer coupled to a fundus camera and a digital camera, which collect the spectral cube of two dimensional retinal images. The influence of choroidal circulation on retinal tissue SO_2 calculations is a drawback of this system.

1.7.5 Choroidal oximetry

Based on the principles adapted from Hickam[85] and Beach[74] for calculating retinal SO_2, Broadfoot in 1961[86] developed a spectrophotometric choroidal oximeter to non-invasively quantify SO_2 of choroidal vessels in humans. The system had a fundus monitoring unit, light source of wavelength 650 and 805nm and an electronic system for signal processing and SO_2 calculation.[87] The oximeter could only report choroidal SO_2 of individuals with lightly pigmented fundus. Also, the reported optical density ratios of choroidal vessels were calibrated based on the previously reported retinal blood SO_2 values, which is not appropriate due to the different optical properties of the two tissues. Obviously the choroidal oximeter calls for modification and refinement to better establish a reliable choroidal SO_2 measurement in future.

1.7.6 Summary

Retinal oxygen saturation disturbances have been reported in diabetic retinopathy,[28,88,89] glaucoma[90,91] and retinal vessel occlusions.[92,93] While invasive techniques are restricted to animal studies, the development of non-invasive SO_2 measurement is a major breakthrough in terms of uplifting our understanding of retinal pathophysiology and might also help in early diagnosis. The retinal oximeters described above only quantify the SO_2 of retinal blood; however, the recently introduced metabolic hyperspectral camera could quantitate the retinal tissue SO_2.[82] It allows the derivation of oximetric maps of the fundus from capillaries and optic

nerve head tissue in humans, with a short acquisition time of 3 seconds. One potential limitation is that the reported retinal tissue SO_2 might as well be influenced from the underlying choroid which has a higher flow rate. Automation of retinal SO_2 measurement, improvements in imaging technology, eye movement tracking facility are some of the upgrading which most likely is mandatory to improve the oximeter's performance.

1.8 Inner retinal oxygen distribution

The retina is one of the highest O_2 consuming tissues in the human body. It has multiple layers with different cell types and the surrounding vascular components are spatially separated. Due to the variable degree of vascularization across the different regions of retina, a delicate balance exists between the available oxygen supply and the consumption within the retina.[94] Proper O_2 supply is vital in order to prevent the tissue from ischemic insult. Tissue hypoxia is thought to be an important factor in retinal diseases with a vascular component.[95] On the other hand excess supply might also aggravate several pathogenic factors leading to cell death.[96]

Measurement of O_2 level within the retinal layers is known to be invasive and only possible in animal studies. O_2 sensitive microelectrodes are inserted into the eye to obtain higher resolution O_2 tension measurements as a function of retinal depth. The oxygen distribution within the various retinal layers is not shown to be uniform in nature.[97] One study recently reported the dominant O_2 consuming retinal layers in rats as inner segments of the photoreceptors, the outer plexiform layer, and the inner plexiform layer.[98] Since measuring retinal tissue O_2 tension in the way mentioned above is impractical in humans, several non-invasive techniques have been developed to quantitate the amount of O_2 saturated in retinal arteriolar and venular blood to get an idea of oxygen extraction in humans.[99,100] Werkmeister and co-workers[99] recently published a

more detailed mathematical model of translating the RBF and retinal blood SO_2 values into total O_2 extraction and oxygen extraction fraction (OEF) in humans. OEF is reported to be an important biomarker to quantitatively assess the adequacy of O_2 supply for metabolism under physiological and pathological conditions.[101]

1.8.1 Inner retinal oxygen extraction

Oxygen delivery to the retina is derived from two factors, namely, RBF and O_2 content of the arterial blood. The combination of these two factors could provide insight into the inner retinal oxygen extraction. The relationship of these two factors in determining O_2 delivery and consumption of retinal tissue is given as follows.

Retinal O_2 delivery (DO_2) = Blood flow * (SaO_2*[Hb]*1.34 ml O_2/gm Hb + 0.003ml O_2/ (dLblood×mmHg)*PaO_2)

…… (1.9)

Retinal O_2 consumption (VO_2) = TRBF * (CaO_2 - CvO_2)…….…….. (1.10)

Where SaO_2 is the oxygen saturation of the retinal arteriolar blood, Hb is the hemoglobin concentration and PaO_2 is the arterial partial pressure of oxygen. Approximately > 98% of O_2 is bound to Hb in a healthy human, each gram of Hb binds to 1.34 ml of O_2. The O_2 solubility coefficient in human plasma is 0.003. The arteriovenous difference in oxygen content is given by CaO_2 - CvO_2.

The ratio of arteriovenous O_2 content difference and arterial O_2 content is given as oxygen extraction fraction.[101]

$$OEF = \frac{\mathrm{CaO2 - CvO2}}{\mathrm{CaO2}} \quad \text{(1.11)}$$

1.8.2 Summary

An alteration of retinal O_2 delivery may result from an overall increase or decrease in metabolic demand by the retinal tissue. However, in healthy retinae, the existences of regulating mechanisms control the O_2 supply and consumption by various mediating factors which are still a topic under research. These mechanisms become obvious by observing the retinal vessels under various provocative stimuli such as gas challenges, flicker, and light-dark transitions. For instance, during systemic hyperoxia, the retinal arterioles constrict to limit the blood flow in order to dampen the effect of increased oxygen consumption in the inner retina.[99,102] Also, Palkovits and co-workers[100] reported that the inner retinal O_2 consumption remains unchanged during graded hypoxia, since the retinal vessels compensate for the decrease in oxygenation by vasodilation.

1.9 RBF and SO_2 in retinal vascular diseases

A plethora of evidence suggests altered vascular regulation in diseases affecting retinal vasculature such as diabetic retinopathy, retinal occlusive diseases, AMD, and glaucoma.[28, 88-93] The transparency of the ocular media allows the direct visualization of retinal microcirculation non-invasively. Structural changes such as retinal arteriolar narrowing,[103] vessel tortuosity,[104] and a smaller arterio-venous ratio[105] have been reported in individuals with underlying systemic inflammation. Studies assessing the vascular reactivity of the retinal vessels to provocative stimuli including, hyperoxia, hypercapnia, light stimulation and changes in perfusion pressure also give meaningful insight on altered vasoregulation, which is considered as an early biomarker for diseases affecting retinal circulation. Lower blood flow[28,106] and higher SO_2[28,88,89] were earlier reported in diabetic patients with non-proliferative retinopathy, suggesting a reduced

O_2 uptake from the retina even in the early stages of the diseases. Increased venular SO_2 and lower arteriolar SO_2 was reported in patients with primary open angle glaucoma and normal tension glaucoma, respectively, compared to controls.[107,108] Another study reports a plausible relationship between reduced blood flow and visual field loss in glaucoma patients.[109] These quantitative measurements were reported to be correlated with the functional changes in progressive diseases.

The utilization of these novel tools to non-invasively quantitate RBF and SO_2 might possibly facilitate our understanding of the vascular pathophysiology as well as promote early detection and possible treatment intervention in the future.

1.10 Choroidal Melanoma (CM)

Melanoma of the choroid arises from the pigment producing cells called melanocytes. Although melanoma could arise from other part of the uveal tract, such as iris and ciliary body, choroidal melanoma alone accounts for 80% of all uveal melanoma cases. CM is known to be the most important primary intraocular tumor in adults. Individuals with light colored iris, high amount of ultraviolet exposure are at most risk of acquiring this disease.[110] In North America alone, 6 per million people or 1400 new cases of CM are diagnosed annually. The size and location of the tumor determines the type of treatment to be administered. The 5-year relative tumor related mortality for people with large choroidal melanoma of any size is almost 30%.[111]

1.10.1 Pathophysiology

CM arises from three distinct cell types known as spindle A, spindle B and epitheloid cells; of which the third type is most aggressive in nature with poor prognosis. The tumor appears as either darkly pigmented or amelanotic (Figure 1.9). As these tumors enlarge, they eventually

break through the Bruch's membrane and gives rise to a characteristic mushroom configuration. It may also evolve as diffuse, bilobular and, multilobular in shape.

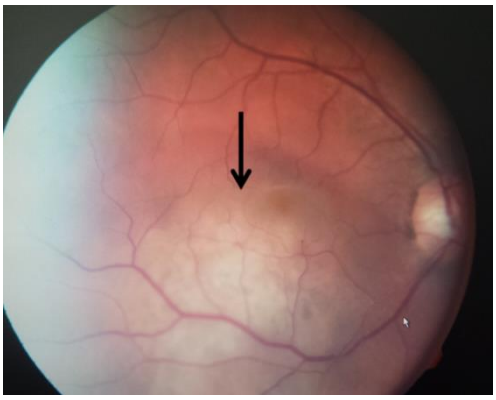

Figure 1.9 Color photograph of a dome-shaped choroidal melanoma.

As these tumors push against the retinal pigment epithelium (RPE), it deprives the outer retinal layers from normal choroidal circulation, leading to ischemia, RPE atrophy, drusen, and localized RPE detachment.[112] CM is highly metastatic in nature. Its metastatic potential depends on the histopathologic aggressiveness of the tumor cells. Due to the absence of lymphatic vessels in the eye, the common site of tumor metastasize is reported as liver.[113]

1.10.2 Treatment

Various factors such as tumor size, location, extent, patient's age and general health all play an important role in determining the treatment type needed. Some of the common treatment options are briefed below. However, tumors with large tumor base and size often require enucleation.[111]

1.10.2.1 Radiation therapy

External beam radiation therapy (EBRT) and Brachytherapy are the two main radiation treatments offered to treat CM.[114] In Brachytherapy (also known as episcleral plaque radiotherapy), radioactive seeds containing Iodine-125 or Ruthenium-106 are surgically inserted

at the tumor base using a episcleral plaque.[115,116] This plaque is then removed from the eye, once the required dose is delivered to kill the tumor cells. Compared to enucleation, brachytherapy is preferred treatment of choice for it has the possibility of salvaging the eye.

In EBRT, the radiation treatment is delivered from outside the eye. This treatment is preferred when the tumor location is close to optic nerve head, where the brachytherapy is difficult to perform.[115] Although radiation therapy is shown to be an excellent treatment for most CM patients; it comes with its own risks and side effects. Possible side effects of treatment include radiation retinopathy (RR), optic neuropathy, increased ocular pressure and poor vision.[117-119]

1.11 Effects of ionising radiation on retinal vasculature

Radiation treatment is known to be a treatment of choice for small to medium sized choroidal melanomas. Though salvaging the eye seems to be unique in this treatment, vision deterioration is often unavoidable due to developing retinopathy post treatment. RR is a vision-threatening complication after EBRT or plaque brachytherapy of the eye and surrounding tissues.[120]

Endothelial cells lining the blood vessel wall have been shown to go through radiation insult, followed by capillary occlusion.[121] The vascular pathology involved is reported as microvascular in origin including vascular occlusion, incompetence and vasoproliferation. One of the early microvascular changes observed are microaneurysms occurring singly or in small clusters,[122] followed by focal capillary occlusion. Irregular dilation of the neighboring microvasculature is also noted as an early change in retinal microvasculature. The affected vessels typically remain competent early in the course of disease.[123] Starting as a small, subtle localized retinopathic lesion, the microvasculopathy aggravates further as an increased number of microaneurysms, capillary bed collapse and development of telangiectatic-like channels. These channels are a

"hallmark" of RR and are likely due to altered local hemodynamics and radiation induced changes in the capillary wall. With higher doses of radiation, more exaggerated and diffuse patterns of capillary closure and dilatation are observed.[122,123]

RR is classified as more common non-proliferative type or severe proliferative type. Non-proliferative changes include the presence of microaneurysms, cotton-wool spots, hard exudates, hemorrhages, retinal edema and/or vascular sheathing. Proliferative retinopathy is characterized by the presence of retinal or disc neovascularization, vitreous hemorrhage and retinal detachment. These signs are typically observed in the posterior pole.

The rate of development of retinopathy can range from months to years after radiation treatment. It is almost impossible to predict who will develop RR post radiotherapy. The first signs of RR occur months to years after the exposure to radiation. Brown and Co-workers[124] reported an average of 14.6 months for RR to develop following radioactive plaque therapy. Another study reported that RR developed after a mean period of 18.7 months after external beam radiotherapy.[125] The key factors that determine the development of RR are the radiation dose, tumor size and location.[120] The Collaborative Ocular Melanoma Study (COMS) reported that RR was seen in 90.7% of eyes 8 years following Iodine-125 brachytherapy.[126] The long-term complications of RR are a consequence of the inner retinal ischemia and vascular incompetence that develops due to the changes in vasculature. In advanced RR, blindness and pain can present as a result of radiation-induced ischemia or neovascular glaucoma.[117]

1.11.1 Pathogenesis of RR

Radiation exposure damages the cells, organelles and DNA of the tumor cells. However, the surrounding healthy retinal tissue also seems to get affected indirectly. Endothelial cells are

reported to exhibit changes both structurally and functionally following radiation insult. Ionizing radiation disturbs chemical bonds in molecules, forms toxic-free radicals and damages the DNA.[127] As a result, the retinal vessels start showing similar changes as irradiated tumor vessels. Fluid and proteins leak into the retina causing edema and hard exudates. The decompensation of the retinal vessels results in microaneurysms and intraretinal microvascular abnormalities. These microaneurysms can develop into dot and bot hemorrhages. The appearance of the fundus strongly resembles that of diabetic retinopathy except that there are generally fewer microaneurysms seen with RR.[121] Later in the course of RR, the features reflect vascular occlusion at various retinal and choroidal layers. These changes present as cotton-wool spots and venous beading. Sometimes occlusion of the larger retinal vessels occur which can cause retinal arterial and vein occlusions. Proliferative RR can occur when retinal ischemia leads to neovascularization of the retina or optic disc.[125]

1.11.2 Treatment and Management

The treatment options for RR are similar to those administered to other retinopathies such as diabetic retinopathy, retinal artery and vein occlusions. Anti-Vascular Endothelial Growth Factor (VEGF) agents and intravitreal steroid injections are few of most preferred treatment choice. However, other forms of treatment such as hyperbaric oxygen treatment, and oral pentoxifylline are still under research.[128] Regardless of the type of irradiation, larger tumors make for a poorer prognosis as the amount of radiation delivered to all surrounding ocular structures is higher.

1.12 Summary

The retina is a tissue with an extremely high metabolic demand. The transparency of the tissue itself offers direct visualization of its microvasculature. Taking advantage of this, many techniques were introduced and continue to be developed to non-invasively quantitate the volume of blood/O_2 delivered to this tissue through the inner retinal vasculature. Advances in technology have allowed for non-invasive techniques of measuring blood flow and oxygen saturation in a more efficient and comfortable way compared to invasive methods.

RBF and SO_2 remain two important factors that reflect the dynamic aspects of oxygen metabolism in the retina.[80] By knowing these two parameters, net oxygen delivery to the retina could be derived non-invasively. Retinal O_2 metabolic rate is a candidate parameter to understand the functional status of the retina in health and disease. A vast majority of retinal vascular pathologies report tissue hypoxia as a disease building mechanism towards sight threatening impairment.

There are quite a few studies that report effect of ionizing radiation to the retinal vasculature. The damage to retinal vessel makes the tissue deprived of oxygen leading to ischemia. The morphological retinal changes associated with RR resemble those of diabetic retinopathy but the rate of progression is far more rapid than diabetic retinopathy. Though the radiation seems to harm the tissue in one way, it is the preferred treatment of choice for CM. Retinal SO_2 could be a useful biomarker for ischemic related retinopathies such as diabetic retinopathy and retinal vessel occlusion. This ultimately offers a potential to allow early intervention, especially at the appropriate time when needed.

By utilizing the advantages of spectral imaging techniques we are able to detect and quantify molecular spectral absorbance profiles in the retinal tissue. Oxy- and deoxy- hemoglobin are well established molecules in terms of their spectral characteristics and quantification in the retina is more relevant to understand the retinal vascular physiology in health and disease. By studying how the retinal microcirculation reacts to radiation exposure in terms of changes in oxygenation could improve our understanding of this sight-threatening vascular pathology.

Chapter 2 **Rationale**

The understanding of vascular pathophysiology underlying sight threatening ocular diseases such as diabetic retinopathy, retinal vascular occlusive diseases, AMD and glaucoma has significantly improved due to the advances in non-invasive imaging technology. Quantification of retinal blood oxygen saturation, *per se*, was once restricted in humans,[1-3] is now possible non-invasively by utilizing spectral imaging[4,5] and SD-OCT techniques.[8] The direct visualization of retinal microvasculature offers the potential for newer techniques to develop, which could eventually unveil the hemodynamic changes in retinal vascular diseases.

In contrast to flash or snap-shot hyperspectral retinal cameras, the retinal oximeter utilized in our lab constructs a spectral data cube based on non-flash ultra-high speed sequential imaging. There is evidence to suggest that using flash illumination may artificially alter the measured retinal SO_2 values.[21] On the other hand sequential imaging is more susceptible to motion artifact, however, the HRC used in our lab has a high frames per second imaging capability to minimize this effect.

Several studies in the past have reported altered RBF and SO_2 in retinal vascular diseases. Retinal blood velocity, decades back was only measured from a single retinal vessel. Together with the vessel diameter measurement, the flow was then calculated in absolute units for that particular vessel.[6,7] Whereas today, the blood flow can now be quantitated from all the retinal vessels passing in and out of the optic nerve head utilizing Doppler incorporated OCT.[8,9] This negates the limitations reported previously with other laser Doppler techniques such as laser Doppler velocimetry, color Doppler imaging and scanning laser Doppler flowmetry.[10-12]

Retinal perfusion changes in radiation induced retinopathy have not been studied as much as other retinal diseases such as diabetic retinopathy, retinal vascular diseases or glaucoma. The

primary vascular events to radiation insult are endothelial cell loss and capillary closure.[13,14] This imposes a burden on retinal metabolism due to progressive changes in retinal microvasculature. Various signs such as microaneurysms, hemorrhages, and cotton wool spots develop as a result of developing retinopathy.[15,16] It is impossible to know who will develop RR following plaque brachytherapy for CM. Studying retinal oximetry changes could predict the future onset of radiation retinopathy and would permit vasculopathy treatment such as anti-VEGF therapy and thus could salvage the eye from this sight threatening condition.

Altered RBF and oxygenation are previously reported in diabetic patients in the very early stages of retinopathy.[17-19] A possible relationship between retinal hypoxia and vascular pathogenesis has been reported in diabetic retinopathy, which further provokes neovascularization and retinal edema.[20] Similar pathogenies may be expected in RR as well, considering the fact that both the conditions show similar clinical signs, except that in RR, endothelial cells are the prime site of damage. The progression of RR is much faster than typically seen in diabetic retinopathy. Whether or not a person will develop retinopathy following brachytherapy for CM is an interesting question to answer.

2.1 General Objective

The general objective of this work is to investigate changes in retinal hemodynamic parameters such as blood flow and oxygenation, to facilitate better understanding of the vascular pathophysiology of radiation induced retinopathy.

This body of work will determine the between-visits repeatability and within-visit variability of retinal blood flow and SO_2 measurements using Doppler SD-OCT and HRC, respectively, under varying blood gas perturbations. The study will also investigate changes in retinal blood SO_2 and

TRBF in patients diagnosed with RR, post ^{125}iodine brachytherapy. The study also compares the before-after changes of these early biomarkers in CM patients who underwent plaque radiation treatment, to predict the earliest changes.

2.2 Specific Aims

1- To validate and calibrate the Doppler SD-OCT derived TRBF and HRC derived SO_2 of major retinal vessels in human volunteers using a novel and exact provocation methodology (RespirAct) that has been proven to allow the precise control of the end-tidal partial pressure of oxygen. Between visits repeatability of the TRBF and retinal blood SO_2 were also studied (Chapter 3).

2- To determine the inner retinal oxygen delivery and consumption during normoxia, hyperoxia and hypoxia in healthy humans (Chapter 4).

3- To investigate retinal blood flow and oxygen saturation changes in patients diagnosed with retinopathy following plaque radiation treatment to treat choroidal melanoma (Chapter 5).

4- To evaluate pre- and post- changes in TRBF and retinal blood SO_2, in patients who underwent ^{125}Iodine plaque brachytherapy, to treat choroidal melanoma (Chapter 6).

2.3 Hypotheses

1- Retinal blood flow and oxygen saturation measurements performed under safe levels of hypoxia and hyperoxia will be repeatable in healthy adults (Chapter 3).

2- Retinal O_2 consumption will increase and decrease during safe levels of hypoxia and hyperoxia, respectively (Chapter 4).

3- In patients diagnosed with RR, retinal blood flow and oxygen saturation will be altered in the major retinal vessels (Chapter 5).

4- Post radiation therapy, the treated eye will exhibit decreased TRBF and increased retinal blood SO_2 as a treatment response (Chapter 6).

2.4 Summary

The novel prototype instruments utilized in this study are unique in the sense that the Doppler SD-OCT is only available in two labs world-wide including our lab; and the HRC for retinal blood oximetry is not available for research elsewhere in the world except Hudson lab. These two methodologies are validated using a reliable and highly reproducible technique for the provocation and quantification of vascular reactivity of the retinal vasculature. The ability of the prototype instruments to detect changes in arterial partial pressure of oxygen was investigated in healthy human volunteers. The computer-controlled gas sequencer is unique compared to other rebreathing units utilized elsewhere, in the way it independently targets end-tidal gas concentrations, and in particular, end tidal O_2 concentrations and end-tidal CO_2 concentrations, independent of one another and also independent of minute ventilation.[22,23] The combination of computer-controlled gas sequencer that allows the implementation of precise combinations of O_2 and CO_2 concentrations as vaso-active provocative stimuli, and the quantification of retinal blood flow and oxygenation provides much reproducible data. The novel application of these established technologies in studying the retinal hemodynamic changes in radiation induced retinopathy is studied for the first time. This work also evaluates the ability of hyperspectral retinal imaging to non-invasively quantify oxygen saturation disturbances in the retinal blood post-brachytherapy for CM, prior to the development of clinically visible retinopathy. This could provide an opportunity for early intervention for developing vasculopthy using anti-VEGF agents, as well as, provide an in-sight into the pathogenesis of RR.

Chapter 3 **Inter-Visit Repeatability of Retinal Blood Oximetry and Total Retinal Blood Flow under Varying Systemic Blood Gas Oxygen Saturations**

Kalpana Rose; Susith I. Kulasekara; Christopher Hudson

Investigative Ophthalmology & Visual Science January 2016, Vol.57, 188-197.
doi:10.1167/iovs.15-17908

3.1 Introduction

The retinal blood vessels carry the necessary O_2 and other essential nutrients to the retina, in order to meet its huge metabolic demand.[1] The delivery of O_2 to the retina is determined by factors such as RBF and the arterial / arteriolar blood O_2 content. The efficient regulation of blood flow and O_2 supply is vital to the retina in order to preserve vision. Therefore, the current study focuses on measuring the amount of blood flowing through the retina and the O_2 dissolved in those blood vessels, in order to explain how the retina regulates overall blood and O_2 supply.

The retina regulates blood flow in response to the local tissue demand. Despite the absence of an intrinsic sympathetic nerve supply, RBF can be maintained constant over a wide range of perfusion pressure.[2-6] This process is termed as “autoregulation”. The smooth muscle layer and the endothelial cells lining the blood vessel wall plays a significant role in regulating the blood flow by enabling the constriction and dilation of the blood vessel, thereby decreasing and increasing the flow, respectively. The autoregulating ability of the retinal blood vessels was previously reported by many authors.[7-15] Several studies have demonstrated changes in retinal vessel diameter, velocity and flow to various provocative stimuli such as O_2, CO_2, and flicker in healthy[12,16,17] and diseased cohorts.[18-20,25]

Hypoxia, an decrease in O_2 concentration, has been shown to vasodilate the retinal vessels.[21,22] Conversely, an increase in O_2 (hyperoxia) leads to vasoconstriction.[8,13] These changes occur to maintain constant O_2 delivery and to meet every day metabolic demands of the retina. Dysregulation of retinal vasculature is considered to be a precursor of major retinal diseases.[23,24] Impaired retinal vascular reactivity has been reported in diabetic retinopathy,[18,19] glaucoma,[25] and also in smokers.[26,27]

The interest to develop imaging techniques to quantitate non-invasive RBF started in early 1970's,[28] when the first laser Doppler instrument was introduced to measure retinal red blood cell velocity. The application of Doppler technology in retinal imaging further evolved with the introduction of Canon laser blood flowmeter,[29-31] a technique that utilizes bi-directional laser Doppler velocimetry, and now as the functional extension of OCT, i.e. Doppler SD-OCT[32,33] and bi-directional laser Doppler OCT.[34] Though the blood flow measurement, *per se*, may facilitate better understanding of major retinal diseases including glaucoma, diabetic retinopathy and AMD; more meaningful conclusion could be drawn if retinal blood SO_2 could also be measured.

The introduction of spectral imaging techniques to detect and quantify molecular spectral absorbance profiles in retinal tissue is a major advancement in the field of retinal imaging. The HRC offers the potential to non-invasively quantify SO_2 disturbances in the retina. A plethora of evidence suggests retinal blood SO_2 changes in diseased eyes.[35-37] The novel application of Doppler SD-OCT and HRC might offer the potential for early intervention, and in-sight into the pathogenesis of retinal pathologies.[33,38]

In this study, the SO_2 values of major retinal vessels and the TRBF are validated and calibrated in human volunteers using a novel and exact provocation technique (RespirAct) that allows the

precise control of the $P_{ET}O_2$ to induce safe levels of hypoxia and hyperoxia. This technique uniquely targets exact $P_{ET}O_2$ and stabilizes the $P_{ET}O_2$ while maintaining isocapnia, irrespective of the individual participants' ventilatory response.[39,40] Also, the study inter-relates TRBF and retinal blood SO_2 in healthy individuals. $P_{ET}O_2$ was changed as defined by a series of step changes in inhaled O_2 and the reproducibility of SO_2 and TRBF values was assessed during normoxic conditions.

3.2 Materials and methods

3.2.1 Sample

This study was approved by the University of Waterloo Office Of Research Ethics, Waterloo, and by the University Health Network Research Ethics Board, Toronto. One eye of 11 healthy subjects, mean age 33.36 yrs, SD 6.03 yrs was recruited. All subjects had a logMAR (logarithm of minimum angle of resolution) visual acuity of 0.0, or better. All participants were young, healthy and non-smokers. Exclusion criteria included any refractive error > $\pm$ 6.00 Diopters sphere and / or $\pm$ 1.50 Diopters cylinder, intra ocular pressure > 21mm Hg, treatable respiratory disorders (e.g. asthma), systemic hypertension, cardiovascular disease, diabetes, endocrine disorders, medications with known effects on blood flow (e.g.-anti-hypertensive, medications with activity at autonomic receptors, smooth muscles, or those affects nitric oxide release.), family history of glaucoma, or a history of any ocular disease. All the participants were asked to abstain from caffeine, red meat and alcohol for 12 hours and avoid rigorous exercise about 1 hour prior to their study visit. Informed consent was obtained from each subject after a thorough explanation of the nature of the study and its possible consequences, according to the tenets of the Declaration of Helsinki.

3.2.2 Study visit

The study comprised of two visits, with two sessions each visit. During each visit, TRBF and SO_2 measurements were acquired under conditions of normoxia, hyperoxia and hypoxia. The order of hyperoxia and hypoxia was altered across two visits separated by a week interval. Each visit lasted for approximately 3 hours.

3.2.3 Instrumentation

3.2.3.1 Doppler Spectral Domain Optical Coherence Tomography (SD-OCT)

The novel prototype Doppler SD-OCT utilizes the principle of "Doppler effect" to non-invasively quantitate the TRBF. The commercially available Optovue RTVue OCT (Optovue, Inc., Fremont, CA, USA), is a spectrometer-based OCT system, consist of a super luminescent diode with a center wavelength of 841 nm and a bandwidth of 49 nm. The axial resolution is 5.6 µm in tissue and transverse resolution is 20 µm. The scan protocol for TRBF measurement consist of double circular Doppler scans in the form of two concentric rings of diameters 3.40 mm and 3.75 mm centered on the optic nerve head, transecting all branch retinal arterioles and venules.[32] A total of six scans were obtained and averaged for each ring. To measure the TRBF, the principle of Doppler effect is utilized where the frequency shift (Δf) from backscattered light is detected and simplified to:

$$\Delta f = \frac{-2nVcos\alpha}{\lambda_0} \quad \text{(3.1)}$$

Where, V is the velocity of the moving particle, θ is the angle between the OCT beam and the flow, n is the refractive index of the medium, and λ_0 is the wavelength of the incident beam.

Flow in single vein=average (Vmax/Pi*Doppler phase shift*sin (Doppler angle))*vessel area, Vmax is the maximum speed corresponding to Doppler phase wrapping limit. Flow from individual retinal venules is then summed up to obtain the total volumetric blood flow at one time point.

From the measured Doppler shift with in the vessel and Doppler angle estimation from the vessel center depth difference between two concentric rings, volumetric flow is derived using a semi-automated software (version 2.1.1.4) algorithm named DOCTORC.[41,42] The repeatability of TRBF measurements acquired using Doppler SD-OCT was reported in previous publications from our lab.[43,44]

3.2.3.2 Hyperspectral Retinal Camera (HRC)

The Hyperspectral Camera (Optina Diagnostics, Montreal, Canada) is a combination of a custom-built mydriatic fundus camera, a tunable light source, and a computer that controls image acquisition protocols, data storage and data analysis. The fundus is sequentially illuminated using monochromatic light of predetermined range of wavelengths. At each wavelength, a 30° field-of-view of the posterior pole of the fundus is captured at high resolution (1.3 Megapixels). The filters are capable of delivering monochromatic light at a narrow bandwidth (FTMW = 2nm) and image acquisition occurs at a rate of 27 frames (wavelengths) per second. This allows the instrument to generate a stack of high resolution monochromatic fundus images (spectral data cube) within few seconds.

A spectral data cube obtained by the HRC needs to be pre-processed before it can be analyzed. The spectral data cube is first normalized for spatial and spectral variations in light source intensity and any background 'noise' generated from the system optics is removed. Next, each

image of the data cube is spatially registered with the rest of the images in the stack to correct for any motion artifacts.[45] A pre-processed data cube is then opened with an *in-house* Matlab (The Mathworks, Natick, MA) program. An automatic vessel segmentation algorithm[46] is then used to isolate the main vessel in the fundus image. The segmented vessel is further analyzed to determine the SO_2 (Figure 3.1). An inferior or superior temporal arteriole and venule is chosen for retinal blood SO_2 measurements. An average of five SO_2 values were obtained along the chosen vessel location close to the optic nerve head where the vessels are relatively large and therefore less impacted by relatively small registration errors. In this study, SO_2 of a retinal blood vessel at half DD distance from the disc margin was compared at different $P_{ET}O_2$ levels; images were captured between 500 and 650 nm in 5 nm steps for each stage of gas provocation.

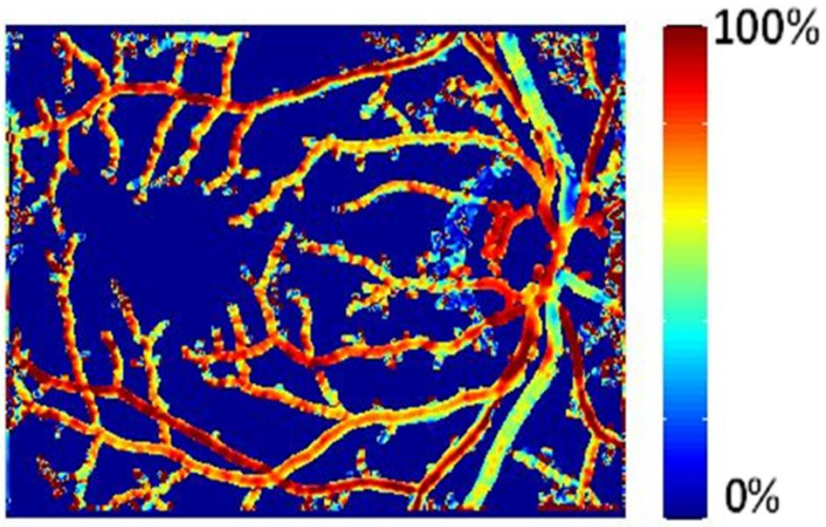

Figure 3.1 Oxygen saturation map of retinal vessels (Scale 0% -100%). Some of the vessels show implausible changes in retinal blood SO_2 along their course. These artifacts are secondary to imperfections in image registration but, they have minimal effect on the calculation of blood SO_2 because the measurements are acquired within 1DD of the optic nerve head where the vessels are relatively large and therefore impacted less by relatively small registration errors. The SO_2 measurement site was in this case on the inferior temporal arteriole and temporal to the optic nerve head.

3.2.3.3 Gas delivery system

A sequential rebreathing circuit (Hi-Ox[80], Viasys Healthcare, Yorba Linda, CA) was used to provoke isocapnic hyperoxia and hypoxia. It comprises a fresh gas reservoir and an expiratory gas reservoir. Each reservoir is connected to a face mask with separate one-way valves. The face mask covers the mouth and nose of the subject. In turn, the two reservoirs are inter-connected using a positive end-expiratory pressure valve which allows subjects to breathe exhaled gas (i.e. rebreathe CO_2-enriched gas) when the fresh gas reservoir is depleted.[39,40] The subject's minute CO_2 production and O_2 consumption, gas flow and composition entering the SGD breathing circuit was attained using an automated gas flow controller (RespirAct^{TM}, Thornhill Research, Inc., Toronto, Canada) which is connected to a computer. The RespirAct has been described in detail in previous publications.[12,25]

3.2.4 Procedures

The study is performed over two visits. At the first visit, logMAR visual acuity and intra ocular pressure (using the Goldmann Applanation Tonometer; Haag-Streit, Koniz, Switzerland) was recorded for both eyes. However, one eye was randomly selected for the study and dilated with one drop of tropicamide 1.0% ophthalmic solution (Alcon, Mississauga, Canada). Following that a 10 minute resting time was given to the participants in a sitting position under room temperature in order to stabilize cardiovascular parameters. Participants were fitted with a face mask connected distally to the RespirAct^{TM} face mask and sequential re-breathing circuit gas delivery system. At the end of this stabilization period, resting blood pressure, peripheral capillary oxygen saturation (S_pO_2), retinal blood SO_2, and TRBF measurements was taken during normoxia, hyperoxia and hypoxia using the HRC and the Doppler SD-OCT, respectively.

The order of hyperoxia and hypoxia was randomized between subjects. Pulse rate, S_PO_2 and blood pressure was monitored continuously using a rapid response critical care gas analyzer (Cardiocap 5; Datex-Ohmeda, Helsinki, Finland) and transmitted electronically to a data acquisition system (S5 Collect, Datex-Ohmeda, USA). A period of 10-12 minute was given in between the gas provocation challenges. Visit 2 was conducted on the same participants, one week after the first visit, except that the order of provocation was altered this time. A diagrammatic representation of study protocol is illustrated in figure 3.2.

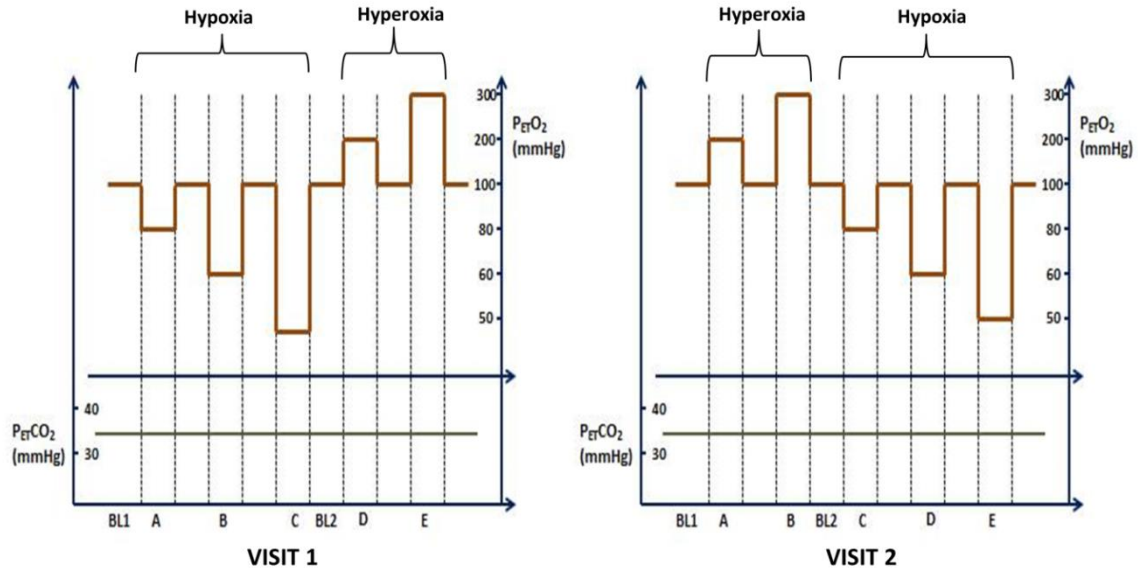

Figure 3.2 The figure demonstrates two different gas provocation protocols utilized for visits 1 and 2 under various $P_{ET}O_2$ levels (300 to 50 mmHg). Protocol 1 (left): Isocapnic hypoxia (A, B & C) followed by isocapnic hyperoxia (D & E). Protocol 2 (right): Isocapnic hyperoxia (A & B) followed by isocapnic hypoxia (C, D & E). The order of provocation was randomized between subjects. BL-baseline, $P_{ET}O_2$ - end-tidal partial pressure of oxygen, $P_{ET}CO_2$ - end-tidal partial pressure of carbon dioxide.

3.2.5 Statistical analysis

The normality of the data was ensured using Shapiro-Wilk test. The significant change in TRBF (µL/min) and SaO_2 (%) and SvO_2 (%) during various gas provocation stages were analyzed

using a repeated measures analysis of variance (reANOVA). If a significant result was achieved using reANOVA, then post hoc testing was performed using Tukey's honestly significant difference (HSD) test. The coefficient of repeatability (COR) and coefficient of variability (COV) between visits was calculated as COR: 1.96*SD of difference; COV (%): SD/Mean*100. Bland & Altman plots illustrating repeatability of measurements between visits were plotted. For correlation analysis, Pearson's correlation coefficient (r) was used. An "r" can be any value between +1 to -1. A value greater than 0 indicates a positive association between the variables, whereas, value less than 0 indicate negative association. Statistica software (StatSoft, Inc., Tulsa, OK, USA) version 12.0 was used for analyzing the data. The level of significance was set to be $p<0.05$.

3.3 Results

Eleven healthy subjects underwent retinal hemodynamic and retinal blood SO_2 measurements under conditions of normoxia, isocapnic hypoxia and isocapnic hyperoxia. The participant's mean age was 33.36 yrs ($\pm$ 6.03). For the repeatability analysis, TRBF measurements from 11 subjects was included, however, for SaO_2 measurements, data of ten subjects was included, except one, due to poor image quality.

Systemic hemodynamic parameters for all participants across two visits are shown in tables 3.1 and 3.2. Retinal hemodynamic parameters studied are given in table 3.3. During both visits, the differences in heart rate (HR) and S_pO_2 at various $P_{ET}O_2$ levels, reached statistical significance ($p<0.05$). Diastolic blood pressure only showed a significant change ($p=0.007$) during the first visit. $P_{ET}CO_2$ and systolic blood pressure were not different at the two study days.

Inter-visit repeatability and variability of TRBF/retinal blood SO_2

The Inter-visit repeatability of TRBF and SO_2 measurements were analysed and plotted using the Bland and Altman method as shown in figure 3.3. The overall COR for TRBF, SaO_2 (arteriolar blood SO_2) and SvO_2 (venular blood SO_2) measurements was 21.8 µL/min, 18.4%, and 15.2%, respectively. The overall COV for TRBF, SaO_2 and SvO_2 measurements was 15.1%, 4.7% and 6.9%, respectively (Tables 3.4 &3.5).

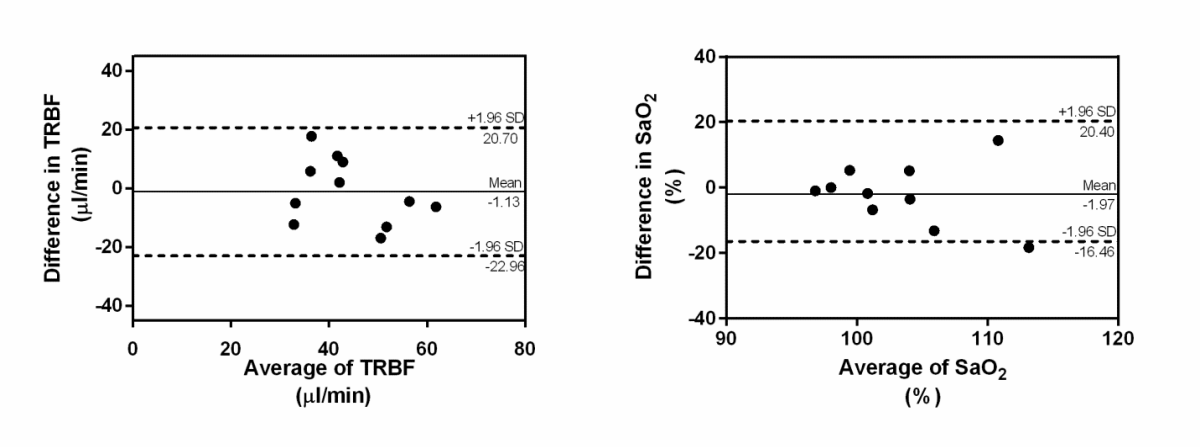

Figure 3.3 Bland and Altman plots showing difference in measurements as a function of average TRBF (left) and average SaO_2 (right) across the two visits. The dotted lines represent the limits of agreement and the center bar represents the mean of the differences between visits.

TRBF response to changes in $P_{ET}O_2$

TRBF measurements during changes in $P_{ET}O_2$ are shown in figure 3.4. There was no significant difference in baseline TRBF measurements as compared between visits. The average TRBF was 44.60 $\pm$ 8.9 µL/min during visit1. When the arterial $P_{ET}O_2$ was increased from baseline ($P_{ET}O_{2=}$100mmHg) to 200 and 300mmHg, the TRBF significantly reduced (reANOVA, p=0.020) from 44.60 µL/min ($\pm$8.9) to 40.28 µL/min ($\pm$8.9) and 36.23 µL/min ($\pm$4.6), respectively. Conversely, lowering the arterial $P_{ET}O_2$, from baseline to 80, 60 and 50mmHg, increased the TRBF significantly (reANOVA, p=0.04) from 43.17 µL/min ($\pm$12.7) to 45.19 µL/min ($\pm$5.5),

49.71 µL/min (±13.4) and 52.89 µL/min (±10.9), respectively. A post-hoc analysis for pairwise comparison was performed using Tukey's HSD test. The results show that the changes in TRBF was statistically significant only during baseline vs 300mmHg hyperoxia (p=0.010) and baseline vs 50mmHg hypoxia (p=0.040).

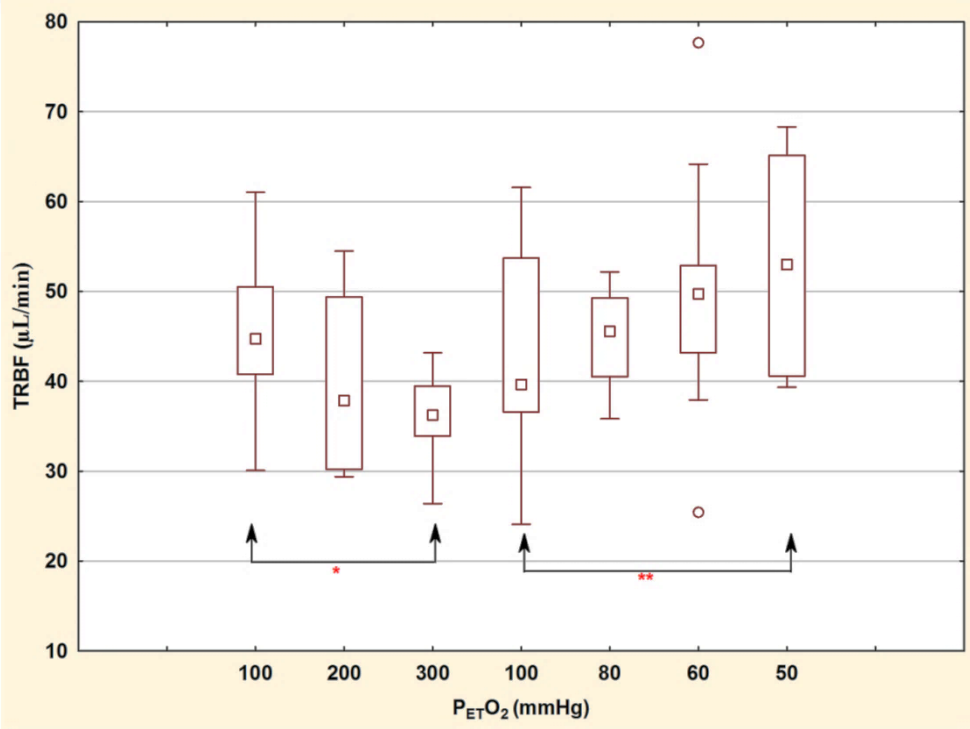

Figure 3.4 Box plots represent change in TRBF at various $P_{ET}O_2$ levels. The legend in the middle of the box represent the median value, the upper and lower extremes of the box represent 25th and 75th percentiles, the error bars represent the nonoutlier range and circle represent outliers. *p<0.05; **p<0.01.

SaO_2 and SvO_2 response during $P_{ET}O_2$ changes

Retinal blood SaO_2 and SvO_2 measurements during stable change in $P_{ET}O_2$ levels are shown in figure 3.5. Lowering the arterial $P_{ET}O_2$ from baseline (100mmHg) to 80, 60 and 50mmHg, reduced the retinal arterial and venous blood SO_2 content from 99.3 % (± 5.8) and 56.3% (± 4.2) to 95.6% (± 5.1) and 52.5 (± 4.1), 89.6% (± 2.8) and 49.5% (± 2.9), 83.3% (± 3.9) and 45.0 % (±

6.1), respectively (reANOVA, p=0.00). A Tukey's HSD test revealed a significant difference in SaO_2 and SvO_2 during baseline vs 80mmHg (p=0.018, p=0.013) baseline vs 60mmHg (p=0.000, p=0.000) and baseline vs 50mmHg (p=0.000, p=0.000). SvO_2 was significantly different during baseline vs 200mmHg (p=0.018) and baseline vs 300mmHg (p=0.006). However, no significant change in retinal blood SaO_2 occurred at 200 and 300mmHg; compared to baseline.

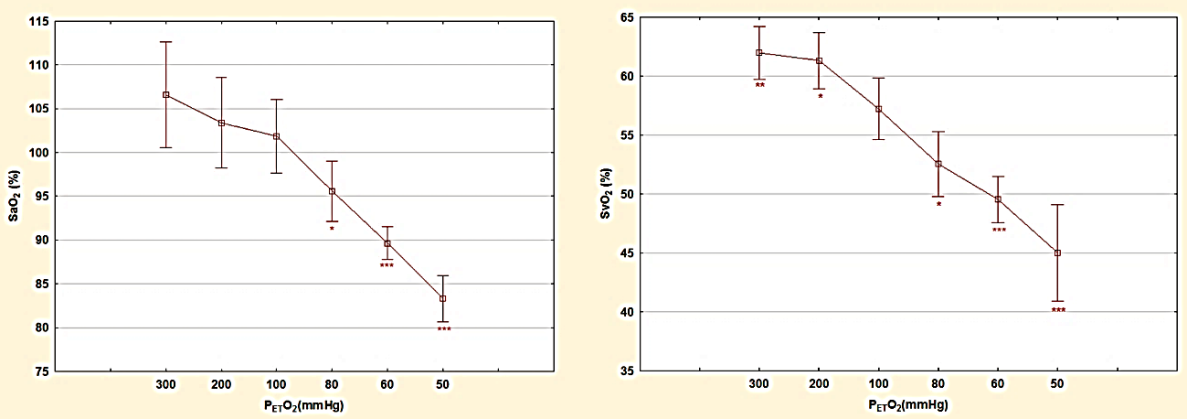

Figure 3.5 Error bars showing group mean retinal arteriolar blood SO_2 (left) and venular blood SO_2 (right) at various $P_{ET}O_2$ levels. *p<0.05; **p<0.01; ***p<0.001.

Correlation analysis of TRBF and SO_2

The relationship between dependent variables such as TRBF, venous area, SaO_2, and SvO_2, during changes in $P_{ET}O_2$ was illustrated as scatterplots in figure 3.6. The correlation analysis shows how the variables studied are associated with each other. For example, an increase in TRBF due to reduced $P_{ET}O_2$, decreases the retinal blood SaO_2 (Figure 3.6A); and SvO_2 (Figure 3.6B). The venous area changes, i.e. vasoconstriction during hyperoxia and vasodilation during hypoxia, were positively correlated with a decrease and increase in TRBF, respectively (Figure 3.6C). Using the Pearson correlation coefficient, a statistically significant relationship was found between TRBF and SaO_2 (r= -0.4, p<0.05) as well as TRBF and SvO_2 (r= -0.37, p<0.05) (Figure

3.6A & 3.6B). Also, the correlation between retinal blood flow changes and simultaneous venous area changes during stable changes in $P_{ET}O_2$ was r=0.5, p<0.05 (Figure 3.6C).

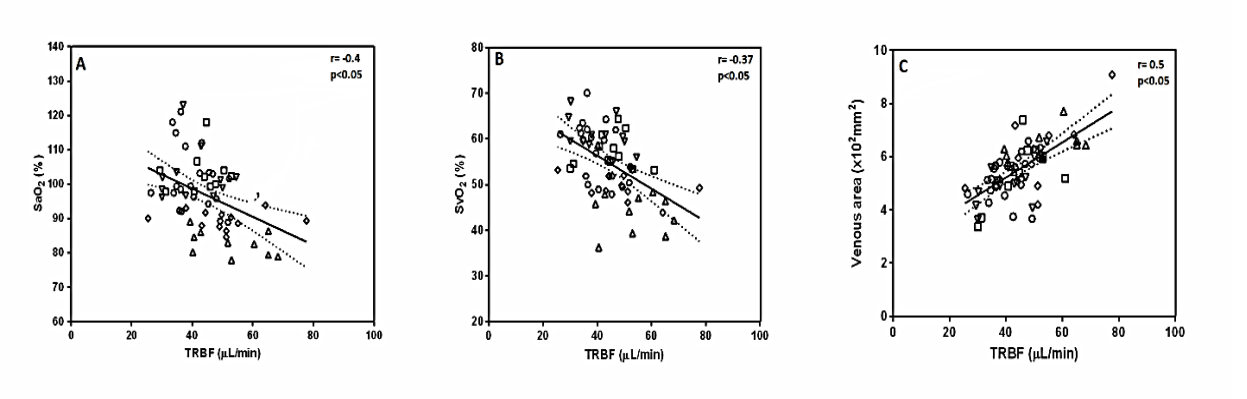

Figure 3.6 Scatterplots of A) TRBF (µL/min) against SaO_2 (%) B) TRBF (µL/min) against SvO_2 (%) C) TRBF (µL/min) against venous area ($x10^2mm^2$) during all gas provocation stages; dotted lines indicate confidence limits; different plot legend indicates various $P_{ET}O_2$ level. Squares, 300mmHg; hexagons, 200mmHg; diamonds, 100 mmHg; triangles, 80 mmHg; circles, 60 mmHg; inverted triangles, 50 mmHg.

Gas& Systemic Parameters (N=11)	$P_{ET}O_2$=300 mmHg	$P_{ET}O_2$=200 mmHg	$P_{ET}O_2$=100 mmHg	$P_{ET}O_2$=80 mmHg	$P_{ET}O_2$=60 mmHg	$P_{ET}O_2$=50 mmHg	p value (reANOVA)
Visit 1 RTVue							
$P_{ET}CO_2$ (mmHg)	32.2 ± 1.6	32.7 ± 1.2	33.5 ± 1.8	32.4 ± 1.6	32.8 ± 1.7	32.7 ± 1.5	NS
SBP (mmHg)	117.4 ± 9.6	116.6 ± 9.4	114.6 ± 10.0	118.7 ± 12.4	116.9 ± 12.3	119.7 ± 13.7	NS
DBP (mmHg)	79.5 ± 5.5	77.5 ± 6.2	76.6 ± 5.4	75.7 ± 5.4	79.2 ± 7.7	81.3 ± 7.8	p=0.007
HR (bpm)	71.3 ± 8.6	73.2 ± 6.8	75.1 ± 4.2	75.5 ± 8.6	77.0 ± 7.2	78.7 ± 11.3	p=0.019
SpO_2 (%)	99.6 ± 0.3	99.3 ± 0.4	98.2 ± 0.8	96.8 ± 1.7	89.9 ± 4.1	83.9 ± 2.9	p=0.000
Visit 1 HRC							
$P_{ET}CO_2$ (mmHg)	32.8 ± 2.0	33.0 ± 1.5	33.8 ± 2.5	32.9 ± 1.3	33.1 ± 1.6	32.8 ± 1.3	NS
SBP (mmHg)	118.3 ± 11.8	119.1 ± 12.2	116.8 ± 11.3	118.3 ± 11.3	116.9 ± 15.3	118.5 ± 14.7	NS
DBP (mmHg)	79.0 ± 7.6	78.7 ± 9.6	75.7 ± 9.7	80.6 ± 8.9	78.5 ± 9.7	77.4 ± 10.9	NS
HR (bpm)	73.4 ± 9.6	74.3 ± 10.3	78.4 ± 10.3	78.1 ± 9.4	79.4 ± 8.9	82.0 ± 9.3	p<0.001
SpO_2 (%)	99.6 ± 0.5	99.4 ± 0.4	98.1 ± 0.7	95.2 ± 2.0	87.5 ± 1.8	84.0 ± 5.4	p<0.000

Table 3.1 Group mean (±SD) for gas and cardiorespiratory parameters across various levels of $P_{ET}O_2$ during visit 1 ($P_{ET}CO_2$-partial pressure of end-tidal carbon dioxide, SBP-systolic blood pressure, DBP-diastolic blood pressure, HR-heart rate, bpm-beats per minute, $P_{ET}O_2$-partial pressure of end-tidal oxygen, S_PO_2-peripheral capillary oxygen saturation). Note: NS denotes not significant; Level of significance was set to $p<0.05$. A significant p value represents change in a given parameter over the different provocations studied.

Gas& Systemic Parameters (N=11)	$P_{ET}O_2$=300 mmHg	$P_{ET}O_2$=200 mmHg	$P_{ET}O_2$=100 mmHg	$P_{ET}O_2$=80 mmHg	$P_{ET}O_2$=60 mmHg	$P_{ET}O_2$=50 mmHg	p value (reANOVA)
Visit 2 RTVue							
$P_{ET}CO_2$ (mmHg)	33.1 ± 1.9	32.4 ± 1.5	33.3 ± 1.76	33.0 ± 1.5	33.4 ± 1.8	32.8 ± 1.5	NS
SBP (mmHg)	117.8 ± 7.6	114.0 ± 9.6	116.5 ± 8.8	114.0 ± 8.2	115.4 ± 7.5	115.2 ± 9.7	NS
DBP (mmHg)	77.3 ± 4.9	76.1 ± 6.3	75.3 ± 4.3	76.5 ± 5.1	77.4 ± 6.6	74.6 ± 6.2	NS
HR (bpm)	68.4 ± 5.6	72.9 ± 7.2	71.9 ± 7.2	79.9 ± 9.9	77.6 ± 7.3	81.8 ± 10.2	p=0.000
SpO_2 (%)	99.6 ± 0.4	99.3 ± 0.3	98.7 ± 0.8	96.2 ± 1.3	89.9 ± 2.4	84.6 ± 6.1	p=0.000
Visit 2 HRC							
$P_{ET}CO_2$ (mmHg)	32.6 ± 1.4	32.7 ± 1.5	33.1 ± 1.6	33.3 ± 1.6	33.1 ± 1.7	33.0 ± 1.6	NS
SBP (mmHg)	116.7 ± 9.1	114.3 ± 9.6	116.0 ± 11.3	113.6 ± 10.3	114.6 ± 12.1	113.8 ± 10.2	NS
DBP (mmHg)	73.8 ± 7.8	76.2 ± 6.7	75.2 ± 7.6	73.0 ± 7.5	73.5 ± 4.7	76.3 ± 7.7	NS
HR (bpm)	71.6 ± 6.4	74.0 ± 7.7	79.1 ± 8.0	76.0 ± 5.5	76.6 ± 6.4	80.1 ± 4.6	p=0.000
SpO_2 (%)	99.4 ± 0.4	99.3 ± 0.5	98.1 ± 1.0	95.9 ± 2.0	89.6 ± 3.4	82.6 ± 1.7	p=0.000

Table 3.2 Group mean (±SD) for gas and cardiorespiratory parameters across various levels of $P_{ET}O_2$ during visit 2 ($P_{ET}CO_2$-partial pressure of end-tidal carbon dioxide, SBP-systolic blood pressure, DBP-diastolic blood pressure, HR-heart rate, bpm-beats per minute, $P_{ET}O_2$-partial pressure of end-tidal oxygen, S_PO_2-peripheral capillary oxygen saturation). Note: NS denotes not significant; Level of significance was set to $p<0.05$.

Retinal Parameters (N=11)	$P_{ET}O_2$=300 mmHg	$P_{ET}O_2$=200 mmHg	$P_{ET}O_2$=100 mmHg	$P_{ET}O_2$=80 mmHg	$P_{ET}O_2$=60 mmHg	$P_{ET}O_2$=50 mmHg	p value (reANOVA)
Visit1							
TRBF (µL/min)	36.23 (4.6)*	40.28 (8.9)	43.59 (9.2)	45.19 (5.5)	49.71 (13.3)	52.89 (10.9)*	p<0.000
Venous area ($\times 10^2 mm^2$)	4.91 (0.6)	4.98 (0.8)	5.38 (1.1)	5.52 (0.8)	6.00 (1.3)	6.38 (0.6)*	p<0.000
Venous velocity (mm/s)	11.54 (1.6)	12.32 (2.2)	13.46 (2.7)	14.4 (1.8)	13.7 (3.3)	13.4 (3.6)	p=0.040
SaO_2 (%)	106.6 (9.0)	103.4 (7.7)	101.9 (6.3)	95.6 (5.1)*	89.6 (2.8)***	83.3 (3.9)***	p<0.000
SvO_2 (%)	62.0 (3.4)**	61.3 (3.6)*	57.2 (3.9)	52.5 (4.1)*	49.5 (2.9)***	45.0 (6.1)***	p<0.000
Visit 2							
TRBF (µL/min)	38.9 (10.0)	42.26 (8.2)	44.72 (12.8)	49.77 (9.7)	51.12 (10.3)	52.28 (17.7)	p<0.001
Venous area ($\times 10^2 mm^2$)	4.91 (0.6)	5.02 (0.9)	5.36 (0.8)	5.52 (0.8)	6.04 (1.3)	6.34 (0.5)**	p<0.001
Venous velocity (mm/s)	14.31 (3.1)	14.12 (2.3)	13.8 (2.4)	13.18 (1.3)	14.39 (3.0)	13.11 (2.1)	NS
SaO_2 (%) (n=10)	113.3 (13.0)	106.8 (7.7)	104.4 (7.8)	96.4 (4.5)*	91.3 (2.7)***	84.2 (4.6)***	p<0.001
SvO_2 (%) (n=10)	68.0 (7.2)*	66.8 (4.8)*	60.3 (6.8)	53.8 (5.6)*	54.6 (6.3)	46.7 (6.3)***	p<0.001

Table 3.3 Group mean (±SD) for retinal hemodynamic parameters across various levels of $P_{ET}O_2$ during visits 1 and 2 ($P_{ET}O_2$-partial pressure of end-tidal oxygen, TRBF-total retinal blood flow, SaO_2-arteriolar blood oxygen saturation, SvO_2-venular blood oxygen saturation). Note: NS denotes not significant. *p<0.05; **p<0.01; ***p<0.001vs baseline ($P_{ET}O_2$=100 mmHg).

Parameters (N=11)	Visit 1 Mean ± SD	Visit 2 Mean ± SD	COR	COV (%)	ANOVA
TRBF (µL/min)	43.59 ± 9.2	44.72 ± 12.8	21.8	15.1	NS
Venous area ($\times 10^2 mm^2$)	5.31 ± 1.1	5.36 ± 0.8	20.0	11.2	NS
Venous velocity (mm/s)	13.46 ± 2.7	13.8 ± 2.4	6.19	12.3	NS
SaO_2 (%)	101.9 ± 6.3	104.4 ± 7.8	18.4	4.7	NS
SvO_2 (%)	57.2 ± 3.9	60.3 ± 6.8	15.2	6.9	NS

Table 3.4 Baseline comparison of mean, standard deviation (SD) of blood flow and retinal blood SO_2 parameters between visits (COV-coefficient of variability, COR-coefficient of repeatability, SaO_2-arteriolar blood oxygen saturation, SvO_2-venular blood oxygen saturation, NS-not significant). COR=1.96* SD of differences; COV (%) = SD/Mean.

$P_{ET}O_2$ (mmHg)	300		200		100		80		60		50	
	COR	COV (%)	COR	COV (%)	COR	COV (%)	COR	COV (%)	COR	COV (%)	COR	COV (%)
TRBF (µL/min)	20.5	16.5	21.7	15.3	21.8	15.1	19.6	13.5	21.5	11.9	31.2	17.7
SaO_2 (%)	20.0	6.0	23.2	6.8	18.4	4.7	13.7	3.4	7.7	2.5	10.4	3.4
SvO_2 (%)	13.0	7.8	10.8	7.5	15.2	6.9	11.2	5.8	14.2	8.6	12.7	9.0

Table 3.5 COR and COV for TRBF and retinal blood SO_2 for all $P_{ET}O_2$ stages between visits (COV-coefficient of variability, COR-coefficient of repeatability, SaO_2-arteriolar blood oxygen saturation, SvO_2-venular blood oxygen saturation, TRBF-total retinal blood flow). COR=1.96* SD of differences; COV (%) = SD/Mean.

3.4 Discussion

The current study showed that the RBF and retinal blood SO_2 measurements acquired using two novel prototype instruments; the Doppler SD-OCT and the HRC, during changes in arterial O_2 tension are repeatable and consistent. The previous methods to quantitate RBF, such as the CLBF and LDV are all limited to quantitating blood flow from one vessel at a time.[34,47] Techniques like fluorescein angiography are invasive and have few associated side effects due to dye injection.[24,48] Ultrasound based color Doppler imaging only determines the blood flow velocity, however, RBF quantification is not possible due to the lack of vessel diameter measurement.[48,49] Overcoming the limitations of the above mentioned techniques, the Doppler SD-OCT could achieve TRBF from all major arterioles and venules. In this study, alongside the

TRBF measurements, retinal arteriolar and venular blood SO_2 was also achieved using the HRC. Recently, Palkovits and co-workers[21,69] have reported retinal blood SO_2 and RBF during hypoxia and hyperoxia in humans. RBF increased while retinal blood SO_2 decreased during two levels of hypoxia studied.[21] During hyperoxia, a significant decrease in RBF, vessel diameter and velocity observed as well as SO_2 increased in retinal arteries and veins by +4.4% and + 19.6%, respectively.[69] One needs to note that, in their studies, RBF measurements were achieved from one single vein as compared to TRBF reported in current study. Also, the vessel diameter and blood flow measurements were acquired using two different instruments, unlike simultaneous acquisition using Doppler SD-OCT.

The combination of computer-controlled gas sequencer along with the RBF and SO_2 measurements, allows the precise combinations of $P_{ET}O_2$, while clamping the $P_{ET}CO_2$ (i.e. to be able to achieve isocapnic hyperoxia and isocapnic hypoxia) concentrations, in turn this provides more reliable and reproducible data. The gas parameters were highly reproducible.

Studies quantitating both RBF and retinal blood SO_2 in humans are very few in literature. Most of the experiments have equipped microspheres to provide direct measurements of inner retinal O_2 tension and O_2 consumption in animals. Such techniques are more invasive and less than ideal to be used in humans.[22,50] The current study validates two novel prototype instruments to measure RBF and SO_2 non-invasively in young healthy individuals. Validation of these techniques might facilitate further understanding of retinal O_2 extraction in normal as well as in diseased eyes.

Our lab has previously reported a COR of 11% and 14% for SaO_2 and SvO_2, respectively, using hyperspectral retinal camera in six healthy subjects.[45] The current study documents COR of

18.4% and 15% for SaO_2 and SvO_2, respectively, using HRC. It is interesting to note that, the COR for SvO_2 is similar to what the previous author has reported, however, the COR of SaO_2 has a greater difference compared to the previous study. It is unclear whether this could be due to larger variability in SaO_2 measurements among individuals. In our study itself, we noticed few subjects had SaO_2 values beyond 100% during baseline conditions (i.e. normoxia), which is beyond the physiological range reported in literature.[51,52] Similar results were also published previously by many authors. Mordant and co-workers[53] reported mean SaO_2 of 104.3 % ($\pm$16.7%) in retinal arterioles using a 'snapshot' hyperspectral spectral imaging technique. Hardarson and co-workers[54] achieved SaO_2 values ranging between 93%-108% by using automated image analysis software to derive optical density ratios of arterioles.

In contrast to flash or snap-shot hyperspectral retinal cameras, the HRC constructs a spectral data cube based on sequential imaging (non-flash). There is evidence to suggest that using flash illumination may artificially alter the measured retinal SO_2 values.[55] On the other hand, sequential imaging is more susceptible to motion artifact, however, HRC's high frames per second imaging capability helps to minimize this effect.

Hammer and co-workers[56] reported average SaO_2 and SvO_2 of 98% $\pm$ 10.1% and 65% $\pm$ 11.7 %, respectively under normoxia. During 100% O_2 breathing the arterial and venous SO_2 increased by 2% and 7% respectively. Hardarson and co-workers[57] have shown that the SaO_2 increased from 96% ($\pm$ 9%) to 101% ($\pm$ 8%) during hyperoxia. In our study, the SaO_2 and SvO_2 during normoxia was 99.3% ($\pm$5.8%) and 56.3% ($\pm$4.2%). During hyperoxia ($P_{ET}O_2$=300mmHg), the retinal SaO_2 and SvO_2 increased by 4.7% and 4.8%, respectively. In contrast, during hypoxia ($P_{ET}O_2$=50mmHg) we found a reduction in SaO_2 and SvO_2 values to 16% and 11.3% compared

to baseline. The variability of SO_2 measurements reported in our study is much less compared to those reported by similar studies in literature. Figure 3.5 shows almost a "linear" trend of SaO_2 and SvO_2 in response to decrease in $P_{ET}O_2$ below 100mmHg. This trend suggests a positive relationship between the systemic changes in $P_{ET}O_2$ to that of the changes in retinal blood SO_2.

Garhofer and Co-workers[34] have reported a high inter-individual variability in TRBF (44.0 $\pm$ 13.3 μL/min) measurements using bidirectional LDV, in young healthy subjects. One needs to note here that TRBF reported is not from the simultaneous measurement of retinal blood velocity and vessel diameter, rather it is derived from one vessel at a time due to the technological limitations. In contrast to bi-directional LDV, Doppler SD-OCT utilizes "Doppler shift" principle to quantitate the red blood cell velocity from all major arterioles and venules in single point of time.[32] Venous area measurements are extracted from the acquired Doppler OCT images using a semi-automated software named DOCTORC. Although there are manual steps involved in venous area estimation using DOCTORC, few studies have actually reported the repeatability and variability of the manual grading technique, *per se*.[41-43]

A recent study from our lab have reported a COV of 7.5% and COR of 6.43 μL/min in young adults using Doppler SD-OCT.[44] Wang and co-workers[32,33] reported mean TRBF in healthy young subjects as 45.6 $\pm$ 3.8 μL/min and COV of 10.5% using a single-beam FD-OCT. Our study report a TRBF of 43.59 $\pm$ 9.2 μL/min, which is comparable to the previous studies. In our study, the reported COV and COR for TRBF during normoxia was 15.1% and 21.8 μL/min. During hyperoxia ($P_{ET}O_2$=300mmHg) TRBF is decreased by 8.37 μL/min and during hypoxia ($P_{ET}O_2$=50mmHg) TRBF increased by 9.72 μL/min compared to baseline. Due to the large variability in blood flow data (Figure 3.4), as well as smaller sample recruited, a significant

difference in TRBF was not achieved during rest of the $P_{ET}O_2$ stages (i.e. $P_{ET}O_2$ of 200,80,60 mmHg).

Hyperoxia is an increase in arterial partial pressure of oxygen from baseline homeostatic levels. Several studies have shown that retinal vessels react to hyperoxia by local constriction of arterioles, venules and to a lesser extent in capillaries; thereby reducing the RBF.[8,13,15] Recently Palkovits and co-workers[70] have reported the effect of breathing 100% oxygen on flicker-induced vasodilation in humans. In contrast to animal studies,[71] breathing oxygen was showed to increase the flicker induced retinal vasodilation in humans. In our study, we mainly emphasized on the physiological responses of retinal vasculature to hyperoxia alone without involving neuro-vascular coupling.

Studies from other labs have just used 100% O_2 or coadministerd O_2 (~>90%) and CO_2 (~5%), without clamping the PCO_2 for hyperoxic provocation.[8,10,16] This might further reduce the PCO_2 concentration, which might impact the measured variables.[58] The novel computer-controlled gas provocation technique used in the current study has overcome the above mentioned limitation by minimizing alterations to the systemic PCO_2 concentration during both hyperoxic and hypoxic provocation, thereby streamlines the retinal vascular reactivity response to O_2 only. It has been reported that endothelin-1 is known to mediate the vasoconstrictive response to hyperoxia.[59] However, animal studies have reported that, other factors such as thromboxane and 20-hydroxyeicosatetraenic acid might as well contribute to hyperoxia-induced vasoconstriction.[60] This remains to be investigated in humans.

Hypoxia leads to increase in blood flow, due to vasodilation.[21,22] The current study utilized safe levels of hypoxia to study the TRBF and SO_2 changes. In humans, lower ATP (adenosine

triphosphate) levels as well as release of the metabolite adenosine during hypoxia would lead to an increased retinal vessel diameter.[61] Few animal studies have reported other metabolic factors such as retinal lactate,[62] adenosine, retinal relaxing factor[63] and nitric oxide[64] to mediate retinal blood flow response to hypoxia.

In this study, retinal blood SO_2 is found to be significantly reduced during changes in arterial O_2 tension i.e. below 100mmHg; above which, there seems to be no significant change in retinal blood SaO_2, since the hemoglobin is almost 100% saturated. The increase in blood flow during hypoxia as shown in the present study compensates for the reduced retinal blood SO_2; thereby, demonstrating the regulation of inner retinal tissue during hypoxic environment. Our results demonstrate an inverse linear relationship between TRBF and retinal blood SO_2 in response to hypoxia as shown in Figure 3.6A & 3.6B. This finding is consistent with other cerebral[65,66] and retinal[21] studies in literature.

At the same time, decreased blood flow during hyperoxia is due to the vasoconstricting ability of retinal vessels. The higher concentration of O_2 in retina leads to an increased retinal arteriolar and venular blood SO_2. Also, the dissolved O_2 from choroid might as well increase the O_2 concentration in the retina considerably.[67,68]

There are possible limitations involved with this study. The TRBF derived using DOCTORC software needs several manual input in terms of grading, such as, defining the cross-sectional area for retinal vessels from the Doppler OCT image and assigning confidence score based on the Doppler signal. The Doppler signal achieved was not uniform among all the scans from the same subject under various $P_{ET}O_2$ levels; this might have underestimated or overestimated the blood flow and vessel area estimation. Due to the long study duration (~3 hours), subject's lack

of concentration to fixate and eye movements, image registration limitations using a manual system might have possibly influenced the quality of scans obtained or the quality of the acquired data. In Figure 3.1, the implausible changes in saturation along some of the vessels are due to artifact secondary to imperfections in image registration. This possibly could have attributed to the variability in the results. Keeping in mind that, the image acquisition and image analysis was performed by trained personnel, the influence of human error could be considered minimal. It is very difficult to conceive how the operator might bias the result given that semi-automated software is needed to translate the images into quantitative data. Retinal SO_2 was measured in a single superior or inferior temporal retinal arteriole and venule close to the optic nerve head. This approach, rather than measuring total retinal SO_2, was undertaken for a number of reasons: 1). There is a known marked regional variation in retinal SO_2 between the hemifields[72] 2). The use of summary statistics to describe "total" retinal SO_2 values will result in the loss of the technique to identify localized change. This study is first to report the TRBF and retinal blood SO_2 measurements simultaneously in healthy subjects under conditions of hypoxia and hyperoxia.

In conclusion, Doppler SD-OCT and HRC could provide reliable and reproducible TRBF and retinal blood SO_2 measurements, respectively. By using a novel gas provocation technique to manipulate safe levels of $P_{ET}O_2$, we have demonstrated that both the techniques could detect changes and showed the anticipated physiological response. In other words, increase in arterial $P_{ET}O_2$ from baseline decreases the TRBF. Conversely, decreasing the arterial $P_{ET}O_2$ from baseline increases the TRBF with simultaneous reduction in the retinal blood SO_2. Retinal blood

flow and SO_2 measurements performed under safe levels of hypoxia and hyperoxia were repeatable in healthy adults.

Chapter 4 **Inner Retinal Oxygen Delivery and Consumption during Hypoxia and Hyperoxia in Humans**

4.1 Introduction

The retina has highest metabolic demand compared to any other tissue in the human body[1] and is perfused by a vascular system with no or little redundancy, thus requiring an uninterrupted blood supply to stay healthy and to preserve vision. The retina has dual blood supply, namely, the retinal and the choroidal vasculature. The inner two-thirds of retina are supplied by the central retinal artery, whose major arteriolar branches are located in the nerve fiber layer. The outer one-third of the retina is supplied by the choroidal vessels. The retinal vasculature has a low flow and higher O_2 extraction (35-40%) compared to the choroidal system.[2] Due to its higher flow, the choroidal vessels deliver approximately 60-80% of O_2 consumed by the retina.[3]

Studies investigating inner retinal O_2 metabolism are receiving increased attention due to the relevance in understanding the pathophysiology of retinal diseases. Several studies have reported tissue hypoxia as a precursor for major retinal vascular diseases such as diabetic retinopathy,[4] AMD,[5,6] and glaucoma.[7,8]

To date, direct measurement of O_2 delivery and consumption is restricted to animal studies due to the use of invasive techniques. In animals such as rat,[9,10] pig,[3] cat,[11]and rabbit,[12] O_2 sensitive microelectrodes are inserted into the eye to measure the O_2 tension profile within retinal layers in order to derive the actual O_2 consumption rate of the retina. However, very few studies have calculated the inner retinal O_2 extraction in humans non-invasively.[13]

The current study reports inner retinal oxygen delivery (DO_2) and consumption (VO_2) in young adults. Also, the ratio of tissue oxygen supply versus demand i.e. oxygen extraction fraction

(OEF) is calculated using Fick's principle. Several cerebral studies indicate that increased OEF is associated with risk of cerebrovascular diseases.[14-17] The mention of cerebral studies is due to the reduced availability of retinal studies in literature reporting OEF in humans, as well as due to the structural and physiological similarities of the two organs.[18,19] As far as we are aware, the current study is the first to report normative data for the non-invasive estimation of inner retinal OEF in healthy individuals. However, Wanek and Co-workers have previously reported the inner retinal OEF in rats to be 0.46 under normoxia, which significantly increased to 0.67 during hypoxia.

4.2 Materials and methods

4.2.1 Subjects

This study was approved by the University of Waterloo Office of Research Ethics, Waterloo, and by the University Health Network Research Ethics Board, Toronto; all the methods were carried out in accordance with the approved guidelines of these two research ethics organizations. One eye of 11 healthy subjects, mean age 33.36 yrs, SD 6.03 yrs was recruited. All subjects had a logMAR visual acuity of 0.0, or better. All participants were young, healthy and non-smokers. Exclusion criteria included any refractive error > $\pm$ 6.00 Diopters sphere and / or $\pm$ 1.50 Diopters cylinder, intra ocular pressure > 21mm Hg, treatable respiratory disorders (e.g. asthma), systemic hypertension, cardiovascular disease, diabetes, endocrine disorders, medications with known effects on blood flow (e.g. anti-hypertensive, medications with activity at autonomic receptors, smooth muscles, or those affecting nitric oxide release), family history of glaucoma, or a history of any ocular disease. All the participants were asked to abstain from caffeine, red meat and alcohol for 12 hours and avoid rigorous exercise about 1 hour prior to their study visit. Informed

consent was obtained from each subject after a thorough explanation of the nature of the study and its possible consequences, according to the tenets of the Declaration of Helsinki.

4.2.2 Instrumentation

4.2.2.1 Total Retinal Blood Flow (TRBF) measurement

The novel prototype Doppler SD-OCT utilizes the principle of "Doppler effect" to non-invasively quantitate the TRBF. The commercially available Optovue RTVue OCT (Optovue, Inc., Fremont, CA, USA), is a spectrometer-based OCT system, consist of a super luminescent diode with a center wavelength of 841 nm and a bandwidth of 49 nm. The axial resolution is 5.6 µm in tissue and transverse resolution is 20 µm. The scan protocol for TRBF measurement consist of double circular Doppler scans in the form of two concentric rings of diameters 3.40 mm and 3.75 mm centered on the optic nerve head, transecting all branch retinal arterioles and venules.[20] A total of six scans were obtained and averaged for each ring. From the measured Doppler shift with in the vessel and Doppler angle estimation from the vessel center depth difference between two concentric rings, volumetric flow is derived using a semi-automated software (version 2.1.1.4) algorithm named DOCTORC.[21,22] The repeatability of TRBF measurements acquired using Doppler SD-OCT was reported in previous publications from our lab.[23-25]

4.2.2.2 Retinal blood SO_2 measurement

In this study, retinal blood SaO_2 and SvO_2 measurements were achieved using the HRC. The HRC (Optina Diagnostics, Montreal, Canada) is a combination of a custom-built mydriatic fundus camera, a tunable light source, and a computer that controls image acquisition protocols, data storage and data analysis. The fundus is sequentially illuminated using monochromatic light of predetermined range of wavelengths. At each wavelength, a 30° field-of-view of the posterior pole of the fundus is captured at high resolution (1.3 Megapixels). The filters are capable of delivering monochromatic light at a narrow bandwidth (FTMW = 2nm) and image acquisition occurs at a rate of 27 frames (wavelengths) per second. This allows the instrument to generate a stack of high resolution monochromatic fundus images (spectral data cube) within a few seconds. A spectral data cube obtained by the HRC was pre-processed prior to analysis. The spectral data cube was first normalized for spatial and spectral variations in light source intensity and any background 'noise' generated from the system optics was removed. Next, each image of the data cube was spatially registered with other images in the stack to correct for any motion artifacts.[26] A pre-processed data cube was then opened with an *in-house* Matlab (The Mathworks, Natick, MA) code. An automatic vessel segmentation algorithm [27] was then used to isolate the chosen vessel in the fundus image. The segmented vessel was further analyzed to determine the SO_2.

4.2.2.3 Gas provocation technique

A sequential rebreathing circuit (Hi-Ox^{80}, Viasys Healthcare, Yorba Linda, CA) was used to provoke isocapnic hyperoxia and hypoxia. It comprises a fresh gas reservoir and an expiratory gas reservoir. Each reservoir is connected to a face mask with separate one-way valves. The face mask covers the mouth and nose of the subject. In turn, the two reservoirs are inter-connected

using a PEEP valve which allows subjects to breathe exhaled gas (i.e. rebreathe CO_2-enriched gas) when the fresh gas reservoir is depleted.[28,29] The subject's minute CO_2 production and O_2 consumption, gas flow and composition entering the sequential breathing circuit was attained using an automated gas flow controller (RespirAct^{TM}, Thornhill Research, Inc., Toronto, Canada) which is connected to a computer.[7,30]

4.2.3 Experimental Protocol

The study was performed in a single visit. LogMAR visual acuity and intra ocular pressure (using the Goldmann Applanation Tonometer; Haag-Streit, Koniz, Switzerland) was recorded for both eyes. One eye was randomly selected for the study and dilated with one drop of tropicamide 1.0% ophthalmic solution (Alcon, Mississauga, Canada). Following that a 10 minute resting time, or longer if necessary, was given to the participants in a sitting position under room temperature in order to stabilize cardiovascular parameters. Participants were fitted with a face mask connected distally to the RespirAct^{TM} face mask and sequential re-breathing circuit gas delivery system. At the end of this stabilization period, resting blood pressure, S_pO_2, retinal blood SO_2, and TRBF measurements was taken during normoxia, hyperoxia and hypoxia using the HRC and the Doppler SD-OCT, respectively. Pulse rate, S_PO_2 and blood pressure was monitored continuously using a rapid response critical care gas analyzer (Cardiocap 5; Datex-Ohmeda, Helsinki, Finland) and transmitted electronically to a data acquisition system (S5 Collect, Datex-Ohmeda, USA). A period of 10-12 minute was given in between the gas provocation challenges. The order of hypoxia and hyperoxia as well as order of TRBF and SO_2 measurement was randomized between subjects (Figure 4.1).

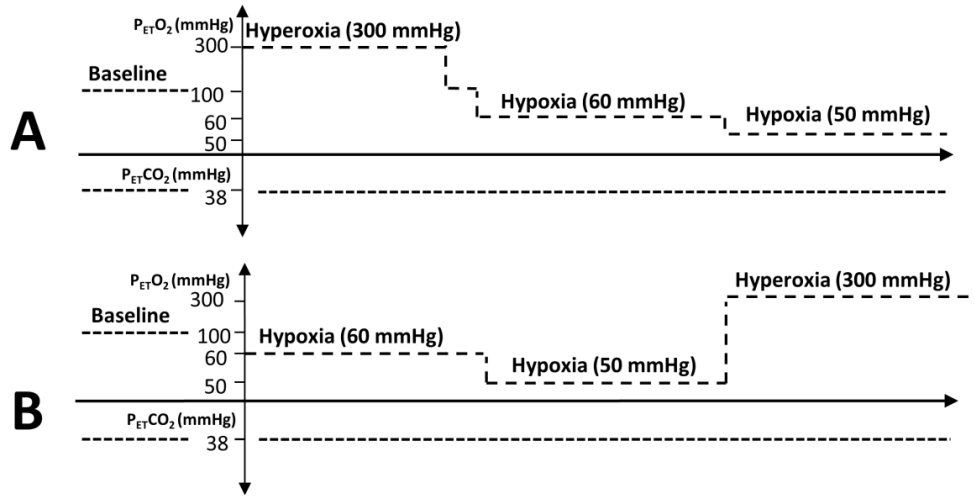

Figure 4.1 Schematic representation of the study protocol. A and B represents the two gas provocation protocols i.e. A, Hyperoxia and Hypoxia B, Hypoxia and Hyperoxia. The order of hypoxia and hyperoxia was randomized between the subjects. (Note: the $P_{ET}O_2$ scales are not linear).

4.2.4 Calculation of retinal oxygen extraction

***Inner retinal O_2 delivery*:** DO_2 is the product of TRBF and the oxygen content of the arterial blood (CaO_2) and is expressed in nL/min.

$DO_2 = TRBF * CaO_2$…….. (4.1)

***Inner retinal O_2 consumption*:** VO_2 is the product of TRBF and retinal blood arteriovenous difference in oxygen content (CaO_2 - CvO_2); where CaO_2 is the oxygen content of the arterial blood and CvO_2 is the oxygen content of the venous blood.

$VO_2 = TRBF * (CaO_2 - CvO_2)$…… (4.2)

This method of calculating oxygen consumption relies on the Fick's principle which is based on the conservation of mass. In the above equation CaO_2 is calculated as follows,

$CaO_2 = SaO_2$*[Hb]*1.34 ml O_2/gm Hb + 0.003ml O_2/ (dL blood×mmHg)*PaO_2……. (4.3)

Where SaO_2 is the oxygen saturation of the retinal arterial blood, Hb is the hemoglobin concentration and PaO_2 is the arterial partial pressure of oxygen. In this study, end-tidal partial

pressure of oxygen ($P_{ET}O_2$) measured using the sequential gas delivery system, was used as a surrogate for PaO_2. Also, hemoglobin concentration was not measured, instead considered to be an average of 15gm/dL.[31] To measure venous oxygen content the following equation was used,

$CvO_2 = SvO_2$*[Hb]*1.34 ml O_2/gm Hb + 0.003ml O_2/ (dL blood×mmHg)*PvO_2…… (4.4)

Where SvO_2 is the oxygen saturation of the retinal venular blood and PvO_2 is venous oxygen partial pressure. Since PvO_2 was not directly measured in the current study, the Hill equation and oxygen hemoglobin dissociation curve[32] was used to estimate PvO_2 from SvO_2 measurement. The Hill equation is written as follows,

$$SO_2 = \frac{K*PO_2{}^n}{1+K*PO_2{}^n} \quad \text{(4.5)}$$

***Oxygen Extraction Fraction (OEF)*:** OEF was calculated from the ratio of VO_2 to DO_2 based on Fick's principle,[33]

$$OEF = \frac{VO_2}{DO_2} \quad \text{(4.6)}$$

4.2.5 Statistical analysis

A repeated measures ANOVA was used to analyze the significant changes in retinal blood flow, retinal blood SO_2, DO_2, VO_2 and OEF during hypoxia, hyperoxia and normoxia. If a significant result was achieved using reANOVA, then post-hoc testing was performed using Tukey's HSD test. Data is presented as mean and SD. The level of significance was set to be $p<0.05$. For correlation analysis, Pearson's correlation coefficient (r) was used. Statistica software (StatSoft, Inc., Tulsa, OK, USA) version 12.0 was used for analyzing the data.

4.3 Results

Systemic physiological parameters

The systemic and gas parameters of the subjects during each breathing condition (i.e. normoxia, hyperoxia, and hypoxia) are given in table 4.1. $P_{ET}O_2$ was significantly different between the breathing conditions ($p=0.000$). Heart rate and systemic peripheral oxygen saturation (S_PO_2) was significantly decreased during hypoxia ($p<0.05$).

Inner retinal oxygen delivery, consumption and OEF

Inner retinal DO_2 and VO_2 during normoxia was 8.48 mLO_2/100g/min and 3.64 mLO_2/100g/min, respectively. DO_2 and VO_2 during all the stages of gas provocation are shown in figure 4.2. OEF during normoxia was 0.43. There was no significant difference found in DO_2, VO_2 and OEF during hyperoxia or hypoxia compared to normoxia. Correlation between systemic arterial blood SO_2 and retinal arteriolar blood SO_2 was $r=0.77$ ($p<0.05$) (Figure 4.3)

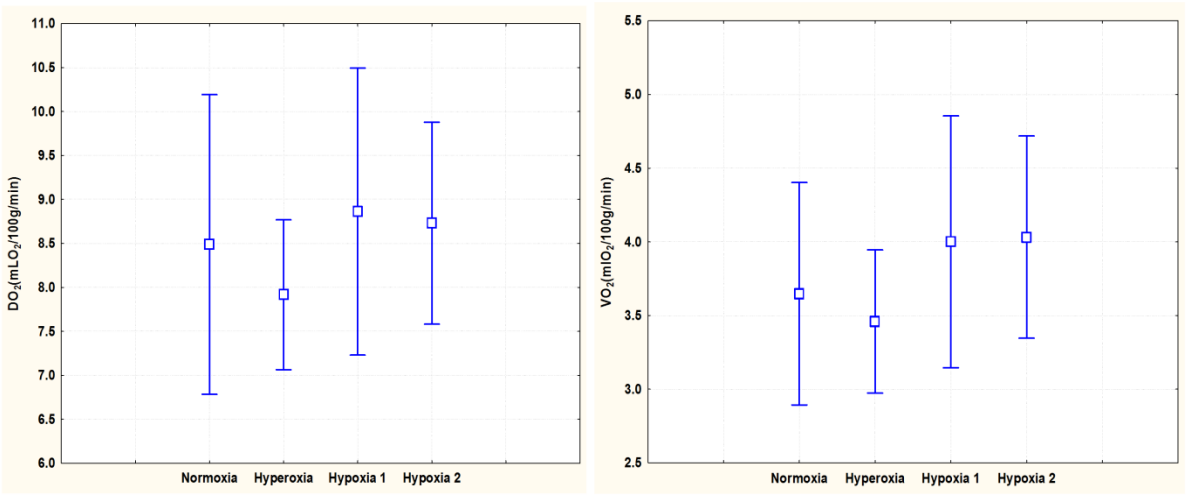

Figure 4.2 Mean DO_2 (left) and VO_2 (right) during hyperoxia and hypoxia. Box in the middle represents mean and vertical bars on either side denote 95% confidence intervals.

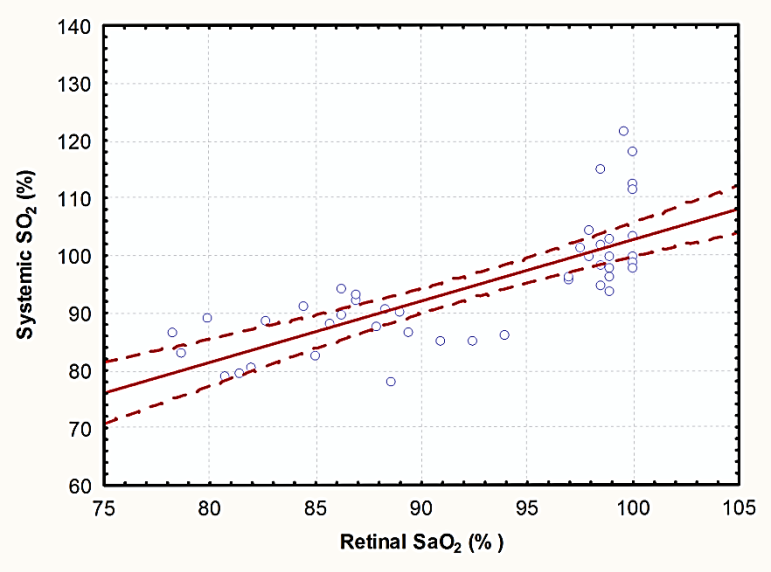

Figure 4.3 Scatterplot of systemic arterial blood SO_2 and retinal arteriolar blood SO_2 during all gas provocation stages; dotted lines indicate confidence limits.

TRBF and SO_2 during various $P_{ET}O_2$ levels

Hyperoxia ($P_{ET}O_2$=300mmHg)

During hyperoxia, TRBF decreased significantly (p=0.01) from 43.17 μL/min (±12.7) to 36.23 μL/min (±4.6). SaO_2 was not significantly different compared to baseline, however SvO_2 showed a significant increase (p=0.005) compared to baseline.

Hypoxia (Stage 1: $P_{ET}O_2$=60mmHg; Stage 2: $P_{ET}O_2$=50mmHg)

Although there is a trend for increase of TRBF during stage 1 hypoxia ($P_{ET}O_2$ = 60mmHg), the results were not statistically significant compared to baseline ($P_{ET}O_2$ = 100mmHg). However, retinal blood SaO_2 and SvO_2 decreased significantly (p<0.050) from 101.9 % (±6.3) and 57.2 % (±3.9) to 89.6 % (±2.8) and 49.5 % (±2.9), respectively. TRBF significantly increased (p< 0.008) from 43.17 μL/min (±12.7) to 52.89 μL/min (±10.9) during stage 2 hypoxia ($P_{ET}O_2$ = 50mmHg). Retinal blood SaO_2 and SvO_2 also reduced significantly (p<0.000) from 101.9 % (±6.3) and 57.2 % (±3.9) to 83.3 % (3.9) and 45.0 % (±6.1), respectively. The percentage change in TRBF, retinal blood SaO_2 and SvO_2 during various $P_{ET}O_2$ stages are shown in figures 4.4 and 4.5.

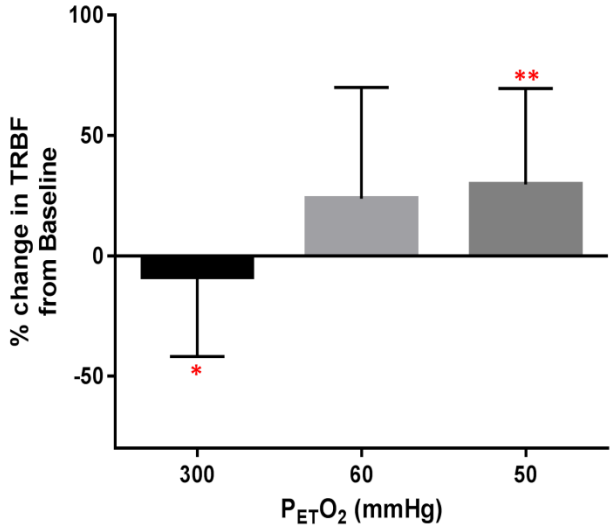

Figure 4.4 Bar graph shows percentage change from baseline in TRBF in response to hyperoxia (300mmHg) and hypoxia (60 and 50 mmHg). Level of significance was set to $p<0.05$. *$p<0.001$,**$p<0.01$.

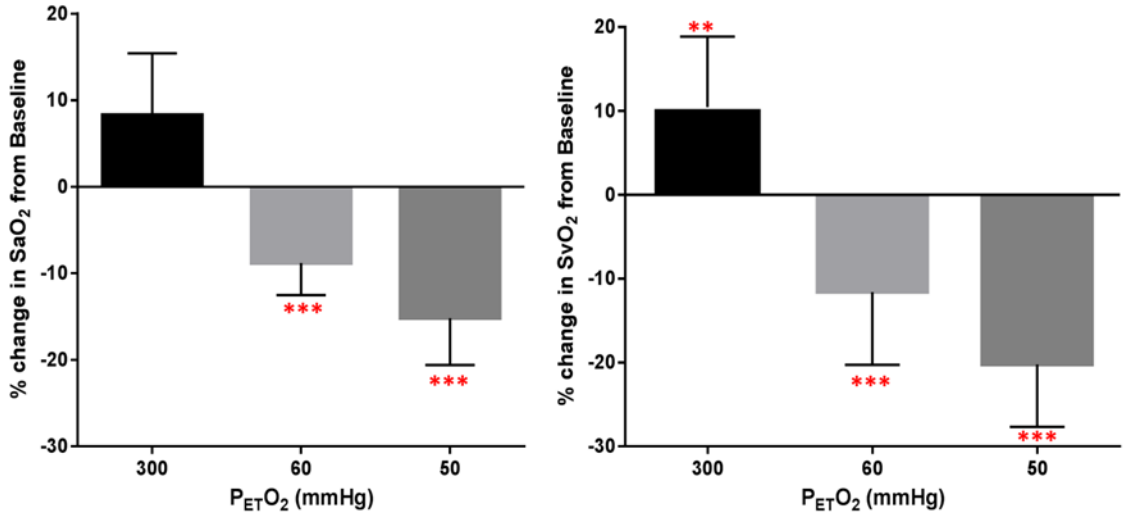

Figure 4.5 Bar graph shows percentage change from baseline in SaO_2 and SvO_2 in response to hyperoxia (300mmHg) and hypoxia (60 and 50 mmHg). Level of significance was set to $p<0.05$. **$p<0.01$, ***$p<0.05$.

4.4 Discussion

The current study estimates inner retinal convective O_2 delivery and consumption in humans partly based on a number of assumptions. During the stages of hypoxia, both DO_2 and VO_2 seem to remain relatively constant compared to normoxia as shown in figure 4.2. For most participants there is a decreasing trend in both DO_2 and VO_2 during hyperoxia as compared to normoxia, but these changes are not statistically significant. Non-significant changes in VO_2 and DO_2 indicate that the hypoxic and hyperoxic values used are well within the regulatory range of the retinal vessels. Recently, Palkovits and Co-workers[34] have also reported that, despite decrease in arteriovenous oxygen difference, the inner retinal oxygen extraction remains unaltered during two levels of graded hypoxia (12% O_2 + 88% N_2 and 15% O_2 + 88% N_2 breathing).

The adequacy of oxygen supply relative to the metabolic demand of the tissue is given as OEF.[35] Previous animal studies utilized microelectrodes[36] to measure retinal oxygen tension and consumption of the retina.[1,9,37] In this study, calculations of oxygen tension in arterioles and venules were made from Fick's principle which is based on the conservation of mass. Wanek and Co-workers[9] have demonstrated that O_2 delivery and consumption was maintained at a PaO_2 of 46mmHg relative to baseline but significantly decreases at 31mmHg PaO_2 in rat. VO_2 may become supply dependent at and below a PaO_2 asymptote of ~37 mmHg where blood flow is maximum and unable to maintain oxygen delivery with reduced PaO_2.[38] The critical DO_2 is likely near the PaO_2 asymptote, below which delivery cannot meet demand and as a consequence OEF might begin to increase.

Estimation of OEF has received significant attention in cerebral studies,[14,15,39] but has not quite been investigated in the retina due to the lack of non-invasive techniques to quantify retinal OEF.

Cerebral imaging techniques may lack the resolution required to quantify retinal O_2 extraction,[40] however, indirect estimation of the inner retinal OEF may be possible from retinal blood flow and blood oxygenation data. In the present study, RBF was measured using Doppler SD-OCT, and, retinal blood SO_2 was quantitated using the HRC. These two data were utilized to calculate OEF using Fick's principle.

A few animal studies have calculated OEF of inner retina in rat under hypoxia[9] as well as in response to light flicker.[41] The reported OEF under normoxic conditions was 0.46, which is similar to our estimation of 0.43 in humans. During hypoxia, Wanek and Co-workers[9] have reported a significant increase in OEF from 0.46 to 0.67. This trend was not observed in our study, due to relatively moderate level of hypoxia utilized. In diseases affecting the retinal metabolism, however, higher values of OEF might be expected in humans. This remains to be investigated in future studies. The significance of OEF has previously been reported in several cerebral studies, where higher OEF was considered a powerful predictor of cerebro-vascular diseases in humans.[17,42,43]

It is interesting to note that, both DO_2 and VO_2 appear to show decreasing trends during physiological perturbations of hyperoxia as shown in figure 4.2. This decreased trend in DO_2 is likely due to the overcompensation of the retinal arterioles during hyperoxia[36] but is non-significant because we used a lower hyperoxic stimulus as compared to previous studies which have generally used the inhalation of 100% O_2.[34,44,46] Caution must be used to interpret the trend that shows a decrease in VO_2 during hyperoxia because retinal arterio-venous shunt may increase SvO_2 causing an underestimation of VO_2. Furthermore, the contributions of the choroidal vasculature need to be taken into account because it may supply more oxygen to the inner retina

during hyperoxia due to the increase in the diffusive components of O_2 delivery (i.e. increased partial pressure of O_2). The choroid during hyperoxia may provide much of the O_2 uptake of the inner retina, while the retinal vasculature provides less, leading to a lower calculated VO_2 from Fick's principle of material balances.

The current study reports inner retinal DO_2 of 8.48 mLO_2/100g/min and respectively, in humans during normoxia. As a comparison, the inner retinal DO_2 of 11.8 mLO_2/100g/min[9] was estimated in rat; a DO_2 of 5.6 mLO_2/100g/min was reported in newborn lamb.[45] Similarly, inner retinal oxygen extraction i.e. VO_2 reported in our study is 3.64 mLO_2/100g/min, comparable to those found in other animals; 4.6 to 3.8 mLO_2/100g/min in pig,[3] 2.7 mLO_2/100g/min in rat[10] and 3.7 mLO_2/100g/min in cat.[11] Werkmeister and Co-workers[46] have recently reported inner retinal oxygen extraction as 1.42 mLO_2/min/100g tissue blood in humans. A inner retinal oxygen extraction of 1.42 mLO_2/min/100g tissue blood, as discussed by the authors, is lower than might be anticipated.[46] This value is almost half of what we have estimated in our study. The differences in RBF and blood O_2 measurement techniques, variation in TRBF and SO_2 analysis, as well as absence of direct measurement of certain variables in our study might also contribute to the estimated difference in O_2 extraction value between the two studies. However, the baseline TRBF value in our study is 43.17 $\pm$ 12.7 μL/min, which is comparable to 44.3 $\pm$ 9.0 μL/min, as reported by Werkmeister and Co-workers.[46]

Our data further shows that, inner retinal vessels demonstrate effective autoregulation during systemic hypoxia and hyperoxia studied i.e. TRBF significantly increased and decreased by + 29.7% and -8.7% during $P_{ET}O_2$ of 60 and 300 mmHg, respectively (Figure 4.3). Also, retinal blood SaO_2 and SvO_2 increased by +8.2% and +10.4% during hyperoxia ($P_{ET}O_2$ of 300 mmHg);

two levels of systemic hypoxia significantly reduced the retinal blood SaO_2 by -8% and -15% with a simultaneous reduction in SvO_2 by -11% and -20%, during $P_{ET}O_2$ of 60 and 50 mmHg, respectively (Figure 4.4).

Limitations of the study include absence of direct measurement of certain variables. Alveolar oxygen tension (PaO_2) was not measured; instead, $P_{ET}O_2$ was considered as a surrogate for PaO_2. However, previous studies report that $P_{ET}O_2$ is a surrogate of the PaO_2.[47] Hemoglobin concentration and pH of the blood was not measured directly, instead, assumed to be 15 gm/dL and 7.4, respectively. Venous oxygen content (PvO_2) was evaluated from arterial and venous partial pressure. The hemoglobin oxygen dissociation curve and the Hill equation were used to estimate PaO_2 and PvO_2 values from SaO_2 and SvO_2, respectively. A recent paper has quantitated the relationship between SaO_2 and PaO_2 using the Hill equation.[32] Although the current study reports the simultaneous measurement of both TRBF and retinal blood SO_2, two different techniques were used, so the measurement location of each parameter (i.e. TRBF and retinal SaO_2 and SvO_2) might differ slightly. Therefore future Doppler OCT instrument with in-built oximetry for oxygen saturation measurement would be a major advancement.[48,49]

The current study establishes baseline values of inner retinal oxygen extraction in healthy individuals during physiological perturbations of hyperoxia and hypoxia. Future studies will investigate the changes in these parameters in diseased eyes. The study concludes that despite the presence of changes in retinal blood flow and retinal blood SO_2, during mild-moderate physiological perturbations of hypoxia and hyperoxia, inner retinal oxygen delivery and consumption was not significantly changed. Whether this remains true during severe hypoxic or

hyperoxic perturbation, as well as during the event of various retinal vascular pathologies needs further investigation.

Gas& Systemic Parameters (N=11)	Normoxia $P_{ET}O_2$=100 mmHg	Hyperoxia $P_{ET}O_2$=300 mmHg	Hypoxia Stage 1 $P_{ET}O_2$=60 mmHg	Hypoxia Stage 2 $P_{ET}O_2$=50 mmHg	p value (reANOVA)
RTVue					
$P_{ET}CO_2$ (mmHg)	33.3 ± 1.76	33.1 ± 1.9	33.4 ± 1.8	32.8 ± 1.5	NS
$P_{ET}O_2$ (mmHg)	99.9 ± 4.3	303.7 ± 2.9	59.0 ± 1.4	49.6 ± 2.1	p=0.000
SBP (mmHg)	116.5 ± 8.8	117.8 ± 7.6	115.4 ± 7.5	115.2 ± 9.7	NS
DBP (mmHg)	75.3 ± 4.3	77.3 ± 4.9	77.4 ± 6.6	74.6 ± 6.2	NS
HR (bpm)	71.9 ± 7.2	68.4 ± 5.6	77.6 ± 7.3	81.8 ± 10.2	p=0.000
SpO_2 (%)	98.7 ± 0.8	99.6 ± 0.4	89.9 ± 2.4	84.6 ± 6.1	p=0.000
HRC					
$P_{ET}CO_2$ (mmHg)	33.1 ± 1.6	32.6 ± 1.4	33.1 ± 1.7	33.0 ± 1.6	NS
$P_{ET}O_2$ (mmHg)	100.0 ± 1.6	301.9 ± 2.3	60.3 ± 1.4	50.2 ± 1.1	p=0.000
SBP (mmHg)	116.0 ± 11.3	116.7 ± 9.1	114.6 ± 12.1	113.8 ± 10.2	NS
DBP (mmHg)	75.2 ± 7.6	73.8 ± 7.8	73.5 ± 4.7	76.3 ± 7.7	NS
HR (bpm)	79.1 ± 8.0	71.6 ± 6.4	76.6 ± 6.4	80.1 ± 4.6	p=0.000
SpO_2 (%)	98.1 ± 1.0	99.4 ± 0.4	89.6 ± 3.4	82.6 ± 1.7	p<0.000

Table 4.1 Group mean (±SD) for gas and cardiorespiratory parameters across various levels of $P_{ET}O_2$. ($P_{ET}CO_2$-partial pressure of end-tidal carbon dioxide, SBP-systolic blood pressure, DBP-diastolic blood pressure, HR-heart rate, bpm-beats per minute, $P_{ET}O_2$-partial pressure of end-tidal oxygen, S_PO_2-peripheral capillary oxygen saturation). Note: NS denotes not significant; Level of significance was set to $p<0.05$.

	Normoxia ($P_{ET}O_2$=100mmHg)	**Hyperoxia ($P_{ET}O_2$=300mmHg)**	**Hypoxia1 ($P_{ET}O_2$=60mmHg)**	**Hypoxia2 ($P_{ET}O_2$=50mmHg)**	**p value (reANOVA)**
DO_2 (mLO_2/100g/min)	8.48 ± 2.5	7.91 ± 1.2	8.86 ± 2.4	8.73 ± 1.7	NS
VO_2 (mLO_2/100g/min)	3.64 ± 1.1	3.45 ± 0.7	4.0 ± 1.2	4.03 ± 1.0	NS
OEF	0.43	0.43	0.44	0.45	NS

Table 4.2 Inner retinal DO_2, VO_2 and OEF during normoxia, hyperoxia and hypoxia.

Chapter 5 **Retinal Perfusion Changes in Radiation Retinopathy Post-brachytherapy for Choroidal Melanoma**

5.1 Introduction

Radiation retinopathy (RR) is a chronic progressive vasculopthy developing secondary to the impact of ionizing radiation to the retina.[1] First described in 1933, the common retinopathic findings include hemorrhages, microaneurysms, cotton-wool spots, hard exudates, and retinal edema.[1,2] Although progressive ischemia and proliferative changes mimics that of a fast developing diabetic retinopathy, their etiologies are different. RR develops post radiation therapy using radioactive plaque to treat intraocular tumors[3,4] or external beam radiotherapy for head and neck cancers.[5]

Plaque brachytherapy is the most popular treatment option for small to medium sized choroidal melanomas,[3,6,7] with the larger tumors often managed by enucleation.[8] Radioactive seeds containing ^{125}Iodine are placed within a gold-shielded episcleral plaque, which then are surgically inserted at the tumor base. Though the plaque is removed from the eye within few days of insertion, the radiation dose delivered to the kill the tumor seems to have a significant impact on the surrounding healthy retinal tissues, especially blood vessels, which later manifest as progressive vasculoapathy.[3] Pre-existing diabetes, hypertension, young age, and proximity of irradiated area to macula or optic nerve head all pose risk factors for retinopathy to develop in the irradiated eye.[3,9]

The primary vascular event following radiation therapy is reported as endothelial cell loss followed by vascular occlusion and capillary drop out, which ultimately leads to vascular incompetence and retinal ischemia.[10] The radiation significantly alters the structural and

functional aspects of the retinal microvasculature due to compromised blood-retinal barrier.[11] This process, however, could take up to months to years to develop as clinically visible retinopathy. It is not always predictable to discern those patients who develop RR. The available treatment options to this sight threatening condition are similar to those offered to other retinopathies, such as intravitreal anti- VEGF and intravitreal steroid agents.[12,13]

Studies in the past have reported tissue hypoxia as a blinding mechanism underlying retinal vascular diseases such as diabetic retinopathy,[14,15,16] central retinal artery and vein occlusion,[17,18] and glaucoma.[19,20,21] Non-invasive spectral imaging of retinal blood vessels at wavelengths between 500-620nm is utilized in retinal oximetry by incorporating the differences in the spectral absorption characteristic of oxygenated and deoxygenated hemoglobin.[22] Color coded maps of the retinal vascular tree provide qualitative and quantitative assessment of arteriolar and venular blood oxygen saturation.

In our laboratory, Doppler SD-OCT and HRC are used to provide the non-invasive measurement of TRBF and SO_2, respectively. The repeatability of these two techniques were previously analyzed under varying blood gas challenges and the results were published elsewhere.[23,24] Diabetic patients with early retinopathy who were previously evaluated using these two techniques showed lower TRBF and increased arteriolar and venular SO_2.[14,25] Also, retinal oximetry using HRC showed higher venular SO_2 in patients with primary open angle glaucoma compared to controls.[19] The results from our lab using these novel techniques are in general agreement with those reported by other investigators.[15,16,20] The current study, for the first time, reports the retinal oxygenation and blood flow changes in early non-proliferative radiation retinopathy post ^{125}Iodine brachytherapy.

5.2 Materials and methods

5.2.1 Sample

This study was approved by the University of Waterloo Office of Research Ethics, Waterloo, and by the University Health Network Research Ethics Board, Toronto. RR patients were recruited from the *Ocular Oncology Clinic* located at *Princess Margaret Hospital*, Toronto, Canada. Eight patients diagnosed with unilateral radiation related retinopathy (ischemic changes) as confirmed by wide-field fluorescein angiography in one eye (mean age 55.75yrs, SD 12.58 yrs) was recruited. All subjects were free from media opacity, diabetes, glaucoma, and other retinal or choroidal vascular disease. Exclusion criteria included intra-ocular pressure >21mmHg, history of ocular surgery, medications with known effects on blood flow except routine anti-hypertensive medication (no change in prescription at least during past 6 months), history of cardiovascular diseases, stroke, myocardial infarction, diabetes, endocrine disorders, smoking, additional retinal diseases other than RR, previous trans-pupillary thermotherapy or external beam radiotherapy to either eye. Informed consent was obtained from each subject after a thorough explanation of the nature of the study and its possible consequences, according to the tenets of the Declaration of Helsinki.

5.2.2 Study visit

The study comprised a single visit, during which TRBF and SO_2 measurements were taken one after the other in both eyes. The order of instrumentation was systematically varied between subjects.

5.2.3 Instrumentation

5.2.3.1 Doppler SD-OCT, RTVue

The Doppler SD-OCT (RTVue; Optovue, Inc., Fremont, CA, USA) is a novel prototype instrument with an inbuilt spectrometer that transmits wavelength of 841nm and a bandwidth of 49nm. The axial and temporal resolutions are 5.6 µm and 20 µm, respectively in tissue. Double circular scans centered on the optic nerve head measure red blood cell velocity over a consecutive 2-second interval. About 3000 A-lines are sampled for each circular scan located at radii of 3.4mm and 3.75mm centered on the optic nerve head.[26] The phase differences between the sequential A-lines are used to obtain the Doppler frequency shift (Δf) of retinal blood cells, which can be derived as

$$\Delta f = -2nV\cos\alpha/\lambda_0 \quad (5.1)$$

where n is the refractive index of the medium, V is the velocity of the flow, α is the angle between the flow and incident beam and λ_0 is the center wavelength of the light.[27]

A total of six scans were acquired for the TRBF measurements, where the blood vessels were identified as arterioles and venules based on the Doppler signal from the OCT images. Vessel area estimation was performed using a semi-automated software (version 2.1.1.4) named DOCTORC. A computer caliper was used to determine the cross sectional diameter of each retinal vessel within the Doppler OCT image.[28,29] The estimated retinal vessel area along with the measured flow velocity gives the volumetric rate of blood flow for a given vessel in the scan. TRBF was calculated by summing the flow from all valid venules with detectable Doppler signal.[30,31]

5.2.3.2 Hyperspectral Retinal Camera

In this study, retinal blood SaO_2 and SvO_2 measurements were achieved using the HRC. The HRC (Optina Diagnostics, Montreal, Canada) is a prototype system comprising of a tunable laser source and custom made fundus camera. These two units are in turn connected to a computer that controls the image acquisition protocols, data storage and analysis. The inbuilt calibration system ensures the reproducibility of acquired spectral images at various ranges of pre-determined wavelengths. The inbuilt filters enable the acquisition of high resolution monochromatic fundus images, due to its capability of delivering monochromatic light at a narrow bandwidth of 2nm. A stack of data cubes containing spectral images are then generated within few seconds for the quantification of retinal blood SO_2. The chosen wavelengths for retinal vessel oximetry are between 520nm-620nm at 5nm steps. Following the spectral image acquisition, the data cubes are then normalized and registered using PHySpec software (Photon etc, Montreal, QC, Canada). The technical details of normalization and registration are published previously elsewhere.[22] An *in-house* Matlab (The Mathworks, Natick, MA) program is then used to open a pre-processed data cube in order to extract oxygen saturation data from retinal blood vessels. A single arteriole and venule is chosen along the superior or inferior temporal vessel arcade close to the optic nerve head for retinal blood SO_2 measurement. The chosen vessel is then isolated from rest of the fundus image using an automatic vessel segmentation algorithm[32] and the segmented vessel is analyzed further to derive the oxygen saturation along the retinal blood vessel.

5.2.4 Procedures

During the subjects visit, logMAR visual acuity and intra ocular pressure (using the Goldmann Applanation Tonometer; Haag-Streit, Koniz, Switzerland) was recorded for both eyes. After making sure the blood pressure and pulse rate (Omron®) are within normal limits, both eyes were dilated with one drop of tropicamide 1.0% ophthalmic solution (Alcon, Mississauga, Canada). Upon pupil dilation, both eyes were imaged using Doppler SD-OCT and HRC. The order of instrumentation was systematically varied between subjects.

5.2.5 Statistical analysis

Statistica software (StatSoft, Inc., Tulsa, OK, USA) version 13.0 was used for analyzing the data. Two-tailed paired t-test was used to compare the results of the retinopathy eye and fellow eye. The level of significance was set to be $p<0.05$.

5.3 Results

A total of 8 patients diagnosed with RR in one eye were recruited for the study. The mean age was 55.75yrs, SD 12.58 yrs. All the study subjects were females. The average time since ^{125}Iodine brachytherapy treatment to the onset of retinopathy was 2.82 yrs, SD 1.29 yrs. LogMAR visual acuity in the eye with retinopathy was significantly lower compared to the fellow eye (0.63 ± 0.36 vs 0.04 ± 0.06, $p=0.002$). The average systolic and diastolic blood pressures of subjects were 132 ± 15.72 mmHg and 86.25 ± 9.52 mmHg, respectively. The mean heart rate was 73.12 ± 15.04 beats/minute.

Retinal Hemodynamic measurements

The subject's retinal hemodynamic parameters are given in Table 5.1. TRBF in the eye with retinopathy was 33.48 $\pm$ 12.73 µL/min, significantly lower compared to 50.37 $\pm$ 15.26 µL/min in the fellow eye (n=8, p=0.013) as shown in figure 5.1. The venous area and venous velocity in the RR eye were found to be not significantly different compared to the fellow eye, 4.27 $\pm$ 1.46 ($X10^2mm^2$) vs 5.41 $\pm$ 1.27 ($X10^2mm^2$) and 13.16 $\pm$ 3.69 mm/sec vs 17.04 $\pm$ 7.98 mm/sec, respectively. Retinal SaO_2 was found to be significantly (p=0.008) increased in the retinopathy eye (101.11 $\pm$ 4.26%) compared to the fellow eye (94.45 $\pm$ 5.79%). Retinal SvO_2 was found to be marginally higher in the affected eye (62.96 $\pm$ 11.05%) compared to the fellow eye (51.24 $\pm$ 6.88%, p=0.051). Figure 5.2 shows the retinal blood SaO_2 and SvO_2 in retinopathy eye and fellow eye.

	RR eye	Fellow eye	p value (paired t test)
Vision (logMAR)	0.63 ± .36	0.04 ± .06	p=0.002
TRBF (µL/min)	33.48 ± 12.73	50.37 ± 15.26	p=0.013
Venous area ($X10^2mm^2$)	4.27 ± 1.46	5.41 ± 1.27	NS
Venous Velocity (mm/sec)	13.16 ± 3.69	17.04 ± 7.98	NS
SaO_2 (%)	101.11 ± 4.26	94.45 ± 5.79	p=0.008
SvO_2 (%)	62.96 ± 11.05	51.24 ± 6.88	p=0.051
A-V diff (%)	38.14 ± 10.9	43.21 ± 8.82	NS

Table 5.1 Comparison of vision and retinal hemodynamic parameters between radiation retinopathy eye and fellow eye. Paired t-test was used for statistical comparison. Level of significance was set to $p<0.05$.

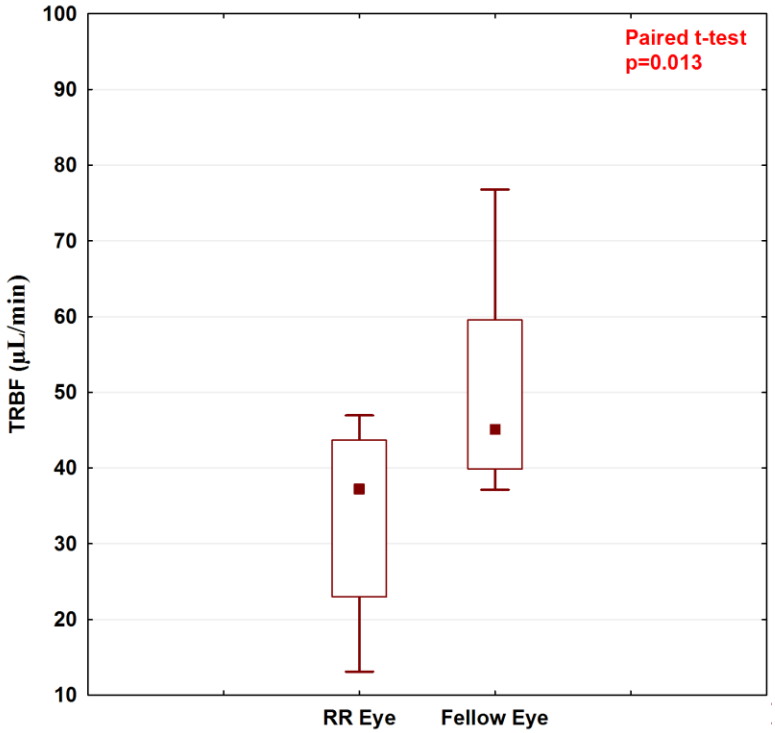

Figure 5.1 Box plots showing total retinal blood flow (TRBF) of the RR eye vs Fellow eye. The legend in the middle of the box represent median, the upper and lower extremes of the box represent 25th and 75th percentiles. Error bars on either side represent nonoutlier range.

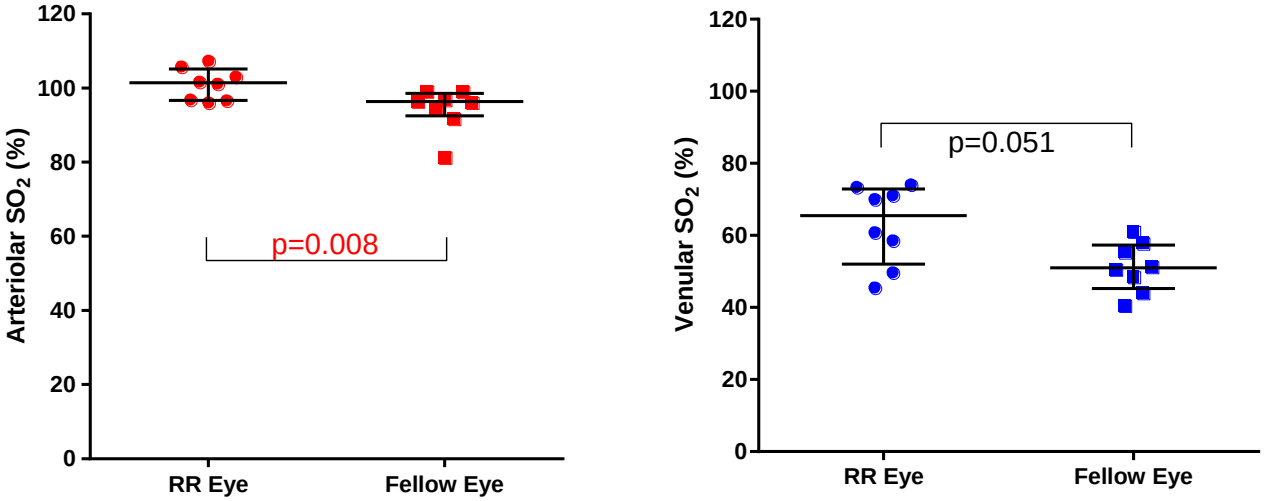

Figure 5.2 Retinal oxygen saturation of arterioles (red) and venules (blue) in eye with retinopathy and fellow eye. Each dot represent mean oxygen saturation (%) along inferior or superior temporal retinal vessel located within 1 disc diameter of the optic nerve head. The horizontal line represents median and error bars on either side represent interquartile range.

5.4 Discussion

A plethora of studies report altered retinal hemodynamics in patients developing retinopathy due to various diseases such as diabetes,[14-16,33] hypertension,[34,35], retinal artery and vein occlusions.[17,18,36] However, the current study is first to report retinal blood flow and SO_2 changes in radiation induced retinopathy from plaque brachytherapy treatment for choroidal melanoma.

Ionizing radiation has been reported to damage endothelial cells, cell membranes, organelles, and DNA.[10,37,38] Histologically, retinal blood vessels have also been shown to exhibit similar changes as seen in irradiated tumor vessels.[39] Radiation damage to blood vessels result in the form of intra retinal vascular leakage and edema due to vascular incompetence. The vulnerable vessels exhibit capillary wall narrowing and capillary drop out, thus causing localized ischemia and infarction.[2,10,11]

Vascular endothelial cells are most vulnerable to radiation damage by losing their integrity of intercellular tight junctions, making the blood vessels more permeable to macro molecules and leakage of protein and fluids into the tissue.[10] Free radical damage due to radiation is accentuated by the higher O_2 tension at the arteriolar side of the retinal microvasculature and also due to the direct exposure of endothelial cells to the ionizing radiation. The developing retinopathy exhibits an early quiet phase of microvascular changes followed by an unpredictable and variable latent period.[10,40,41]

The incidence of developing retinopathy following brachytherapy varies between studies. Two studies have reported a 2 year and 5 year incidence of retinopathy following ^{125}Iodine brachytherapy as 30%[3] and 52%,[42] respectively. However, the incidence of RR is higher in

patients with diabetes.[3,43] The advanced stages of retinopathy due to radiation damage can be painful as a result of ocular ischemia or neovascular glaucoma.[11,44]

The current study reports increased retinal blood oxygenation and reduced blood flow in the eye developing RR. The decreased TRBF in RR could be from less demand by the tissue itself due to cell death or degeneration process as a result of radiation insult. This ultimately reduces O_2 demand and therefore lower flow. Also, the blood vessel wall thickening secondary to the deposition of fibrillary or hyaline material, post radiation could have narrowed the vessel lumen, thus allowing less blood to flow through the blood vessels. Roth and Co-Workers[41] have previously reported decrease in retinal vessel diameter 30 days post radiation in experimentally irradiated hamsters. Our study shows a non-significant trend for reduced venous area in the eye with retinopathy compared to the fellow eye (4.27 ± 1.46 X$10^2 mm^2$ vs 5.41 ± 1.27 X$10^2 mm^2$).

Substantial changes in retinal microcirculation could lead to compromised O_2 distribution. In this study, retinal blood SO_2 is found higher in the eye with retinopathy compared to fellow eye. Decreased O_2 demand due to cell necrosis results in a proportionate decrease in O_2 consumption, which explains the higher SO_2 in retinal vessels. Another explanation for the altered O_2 distribution could be due that the capillaries have already lost their endothelial cells secondary to the radiation effect and this is thought to eventually collapse and occlude the vessel, while others vessels might dilate and appear telangiectatic.[2,10,11] These dilated capillaries are thought to quickly shunt the blood bypassing the retinal arterioles and venules, thus leaving the tissue deprived of O_2, leading to ischemia.

Data pertaining to retinal blood flow and oxygenation in RR patients is very limited. More than a decade ago, two experimental animal studies reported the results of early (30 days) and late (180

days) ionizing radiation effects on the retinal circulation in the absence of retinopathy. Red blood cell velocity was reduced and vessel diameter was decreased following early radiation exposure in hamsters;[41] the later study reported increased red blood cell velocity and increased capillary blood flow, as a late effect to the irradiated hamster retina.[40]

Higginson and Co-workers[5] reported altered retinal blood SO_2 prior to any clinically visible retinopathy in patients who were treated with external beam radiotherapy for head and neck cancer. Also, they reported high within eye variability of SO_2 measurements in nine irradiated patients compared to the controls. Our study shows increased retinal blood SO_2 in patients who have already developed retinopathy post plaque brachytherapy for choroidal melanoma. The venular SO_2 of the eye with retinopathy seem to show higher variability (62.96% $\pm$ 11.05%) compared to the fellow eye (51.24% $\pm$ 6.88%). One needs to be cautious in comparing the results between these two studies, since the radiation treatment type and the disease for which the patients were treated in the two studies are entirely different.

Lack of a control group for comparison and smaller sample are possible limitations of this study. However, the data is first to report retinal hemodynamic changes in RR. The instruments used to measure retinal SO_2 and blood flow are previously reported to be repeatable under various gas provocation challenges.[23,24] The pathophysiology behind radiation induced retinopathy is studied to be microvascular in origin,[2,10,45] however, the evidence is limited. Future work is to predict these ischemic changes at an early stage using current technologies, which might benefit the patient by availing current treatment options, such as intravitreal anti-VEGF, and to salvage the eye from this sight threatening vasculopathy.

Chapter 6 **Increased Retinal Blood Oxygen Saturation Post Plaque Brachytherapy for Choroidal Melanoma**

6.1 Introduction

Choroidal Melanoma (CM) is the most common primary malignant tumor of the adult eye,[9] and carries an overall mortality rate of 50% in developed countries.[7] Reports predict that about six out of each million people will be diagnosed with CM in North America each year.[27] Hispanics and Asians are thought to have a small but intermediate risk of acquiring CM compared to whites and blacks.[20,26]

Primary CM arises from the melanocytes within the choroid. Three distinct cell types are found to be involved in the pathophysiology. They are spindle A, spindle B, and epitheloid cell types; of which the epitheloid cell type is more aggressive in behavior and carries a poor prognosis.[14] Malignant choroidal melanomas can metastasize to other parts of the body, with a survival rate of only 13%.[8] Diagnosis of CM is based on the presence of characteristic clinical features such as tumor thickness, sub-retinal fluid accumulation and orange pigmentation over the tumor.

Brachytherapy using radioactive plaques is considered as one of the most popular and preferred treatment of choice to treat CM.[18,19] Although radiotherapy controls the tumor growth, the impact of ionizing radiation on the surrounding retinal vasculature was not understood until retinopathic changes emerged in the treated eye.[28] The morphological retinal changes associated with RR resemble those of diabetic retinopathy but the rate of progression is far more rapid than diabetic retinopathy. Slowly proliferating tissues such as vascular endothelium, start manifesting radiation damage at a later stage. This predisposes changes in functional parameters of retinal microvasculature such as blood flow, velocity and vessel diameter.[21,24]

The effects of ionizing radiation on retinal vascular physiology are not well reported in literature. Our lab offers the facility to utilize two novel prototype instruments, i.e. the HRC and the Doppler incorporated SD-OCT to quantitate retinal blood SO_2 and TRBF, respectively. These non-invasive tools may provide improved methods of predicting those who develop retinopathy following plaque brachytherapy, as well as to better understand the pathophysiology of RR.

6.2 Materials and methods

6.2.1 Sample

This study was approved by the University of Waterloo Office of Research Ethics, Waterloo, and by the University Health Network Research Ethics Board, Toronto. CM patients were recruited from the *Ocular Oncology Clinic located at Princess Margaret Hospital*, Toronto, Canada. Seventeen patients diagnosed with unilateral CM (mean age 50.58yrs, SD 13.9yrs) were recruited. The subjects were free from media opacity, diabetes, glaucoma or any other retinal or choroidal disease except CM. Exclusion criteria included history of ocular surgery, intra-ocular pressure >21mmHg, medications with known effects on blood flow except routine anti-hypertensive medication (no change in prescription at least during past 6 months), history of cardiovascular diseases, stroke, myocardial infarction, diabetes, endocrine disorders, smoking, and previous trans-pupillary thermotherapy or external beam radiotherapy to either eye. Informed consent was obtained from each subject after a thorough explanation of the nature of the study and its possible consequences, according to the tenets of the Declaration of Helsinki.

6.2.2 Study visit

The study was conducted in three visits. At the first visit, i.e. pre-treatment, TRBF and retinal blood SO_2 was measured in both eyes. During visits 2 and 3, i.e. 3months and 6months post ^{125}Iodine plaque brachytherapy, the measurements of TRBF and retinal blood SO_2 were taken only from the treated eye.

6.2.3 Instrumentation

6.2.3.1 Doppler SD-OCT

The Doppler technology incorporated SD-OCT (Optovue Inc. Freemont, CA, USA) enables the simultaneous measurement of absolute retinal blood velocity and venous area to derive TRBF, non-invasively. The movement of red blood cells with in a blood vessel creates a "Doppler shift" within the reflected SD-OCT A-scan. The magnitude of Doppler shift depends upon the angle between the moving red blood cells and the reflected beam. A morphometric based algorithm named DOCTORC is utilized to determine the angle between the scanning laser beam and blood flow vector in order to measure absolute velocity.[29,30] The velocity values are integrated from each blood vessel around the optic nerve head to determine the TRBF of the inner retina.

The Optovue SD-OCT comprises a superluminescent diode, operating at a wavelength of 841nm and a bandwidth of 49nm. It has axial resolution of 5.6 μm and transverse resolution of 20 μm. The SD-OCT utilizes a Fourier transformation of the reflected signal spectrum for faster image acquisition. The interference pattern from the backscattered light is detected by a 1024-pixel high speed line-scan camera. Transformation of the spectral interference pattern gives a complex function of phase and amplitude. The phase difference between the sequential A-scans

determines the Doppler shift within the blood vessel. The technique is described extensively in various papers.[29,32-34]

For TRBF measurements, four pairs of double circular scans that are approximately 3.40mm and 3.75mm in diameter are taken over approximately two cardiac cycles for each measurement.[30,34] The scans are centered on the optic nerve head. The angle between the incident beam and the velocity direction of the blood, as well as the Doppler shifted frequency is used to determine the retinal blood velocity as given in the following equation

$$\Delta f = \frac{2Vn\cos\theta}{\lambda} \quad \text{(6.1)}$$

where, V is the velocity of the moving particle, θ is the angle between the OCT beam and the flow, n is the refractive index of the medium, and λ is the wavelength of the incident beam.

The double circular scans enable the absolute blood velocity measurement through each and every vessel around the optic nerve head from the 3D OCT image. Semi-automated software named DOCTORC then allows for the identification of vessel type and location, to determine the venous area by subjective grading based on Doppler signal strength (Figure 6.1). Once the individual venous area is estimated, the flow from all the venules around the optic nerve head is then summed up to calculate the TRBF.

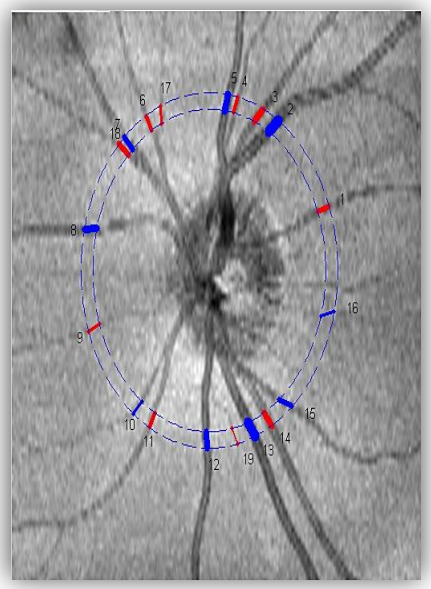

Figure 6.1 En face view of Doppler SD-OCT image with DOCTORC software identified vessel location (numbers) and type (red=artery; blue=vein).

6.2.3.2 Hyperspectral Retinal Camera

Hyperspectral retinal imaging determines the spectral absorption characteristics for a wide range of wavelengths ranging from 420 to 1000nm. It allows the two dimensional imaging for each specific wavelength to derive a measured data set called "image cube", in which the third dimension represent the spectral absorbance value as a function of wavelength. The molecular content within the image is further determined based upon the spectral absorption spectra of well-established molecule such as hemoglobin.

The instrument has an inbuilt mydriatic fundus camera and a tunable laser source (TLS).The TLS allows the rapid transmission of wavelength between 420 to 1000nm at a bandwidth of 2nm. The imaging Bragg Tunable Filter (i-BTF) technology (Photon etc), incorporated within the super-continuum light source allows for the precise and accurate wavelength selection

(<1nm). An in-built spectral power meter controls the temporary light fluctuations to enable uninterrupted image acquisition. The unique "non-flash" camera enables the high definition spectral imaging along 30 degree field of view. The TLS is controlled by software named PHySpec^{TM} (PHySpec^{TM}, Optina, QC, Canada) for image acquisition and image post-processing. For retinal imaging, the chosen wavelength range from 520nm to 620nm. The time taken to generate a hyperspectral data cube i.e. a stack of 21 monochromatic fundus images was 80ms.[22] The acquired stack of data cubes are then loaded into the PHySpec^{TM} software for normalization and registration of images. The normalization generally corrects for image artifacts, while the registration corrects for eye movements and deformations due to imaging optics. After ensuring that the poor quality images are removed from further analysis, the remaining data cubes are then pre-processed using *in-house* Matlab software (The Mathworks, Natick, MA). An automated vessel segmentation algorithm is used to isolate the retinal vessels from the fundus background.[25] A major superior or inferior temporal vessel is chosen within 1 disc diameter of the optic nerve head for the SO_2 measurement. The percentage of SO_2 within the chosen vessel is automatically extracted from the optical density ratios using the well-established Hardarson's two-wavelength model.[12] The Matlab software displays the color coded map of retinal arterioles and venules, where the colors represent the oxygen saturation within the retinal vessels.

6.2.4 Procedures

The CM patients scheduled to undergo ^{125}Iodine plaque brachytherapy were recruited from the *Ocular Oncology Clinic located at Princess Margaret Hospital*, Toronto, Canada. After making sure the subjects fit within the study inclusion criteria, the subjects were scheduled for visit 1, i.e. a day before ^{125}Iodine plaque brachytherapy treatment. During visit 1, subject's cardiovascular

parameters such as blood pressure and heart rate were measured (Omron®). Following which, vision and intraocular pressure were recorded in both eyes, and then the pupils were dilated with one drop of tropicamide 1.0% ophthalmic solution (Alcon, Mississauga, Canada). Upon pupil dilation, both eyes were imaged using Doppler SD-OCT and HRC. The order of instrumentation was systematically varied between subjects. The patients were then scheduled for visits 2 and 3, i.e. 3months and 6 months post treatment. During visits 2 and 3, only the treated eye was imaged using Doppler SD-OCT and HRC following pupil dilation.

6.2.5 Statistical analysis

Statistica software (StatSoft, Inc., Tulsa, OK, USA) version 13.0 was used for analyzing the data. Paired t-test was used to compare the results of the untreated CM eye and fellow eye. A repeated measure ANOVA was used to compare the results between visits1 to 3 i.e. before, 3month and 6 month post brachytherapy in the CM eye.

6.3 Results

A total of seventeen CM patients were recruited for the study. The mean age was 50.5 yrs, SD 14.8 yrs (12 Males, 5 Females). Out of 17 CM patients recruited, 2 patient data was excluded due to poor image quality, and 3 others were lost to follow-up. Rest of the twelve subjects were followed up before, 3mth and 6 month post brachytherapy. The systemic and ocular characteristics of the CM patients during all the three visits are listed in table 6.1.

	Visit 1	Visit 2	Visit 3	p Value, reANOVA
SBP (mmHg)	136.25 ± 23.7	133.41 ± 24.0	128.5 ± 20.8	NS
DBP (mmHg)	79.58 ± 21.6	77.75 ± 16.8	80.91 ± 13.4	NS
HR (beats/min)	75.25 ± 10.1	72.58 ± 13.8	76.12 ± 12.7	NS
LogMAR VA	0.31 ± 0.3	0.40 ± 0.3	0.44 ± 0.4	NS
Tumor Height (mm)	2.61 ± 1.3	2.60 ± 1.4	2.20 ± 1.4	p=0.020

Table 6.1 Group mean (±SD) for systemic and ocular characteristics across visits in CM patients. SBP-systolic blood pressure; DBP-diastolic blood pressure; HR-heart rate; VA-visual acuity; NS-not significant. Level of significance was set to $p<0.05$.

Untreated CM eye vs Fellow eye

During visit 1, retinal hemodynamic parameters studied were not found to be significantly different in the untreated CM eye compared to the fellow eye (Table 6.2). A paired t- test was used to analyse the data. However, visual acuity was found to be significantly lower in the untreated CM eye compared to the fellow eye ($p=0.01$, Figure 6.2). Also, it was found that the smaller the tumor distance from the foveal avascular zone, the worse the visual acuity ($r=-0.5$, $p<0.05$) (Figure 6.3).

	CM Eye	Fellow eye	p value, Paired t test
SaO_2 (%)	93.87 ± 8.1	93.80 ± 8.4	NS
SvO_2 (%)	51.81 ± 6.8	51.99 ± 8.6	NS
TRBF (µL/min)	44.66 ± 15.6	40.1 ± 12.8	NS
Venous area ($\times 10^2 mm^2$)	5.5 ± 1.3	4.9 ± 0.9	NS
Venous velocity (mm/s)	13.76 ± 5.2	14.7 ± 6.1	NS

Table 6.2 Comparison of retinal hemodynamic parameters between untreated CM eye and fellow eye (n=15). Paired t-test was used for statistical comparison. Level of significance was set to $p<0.05$.

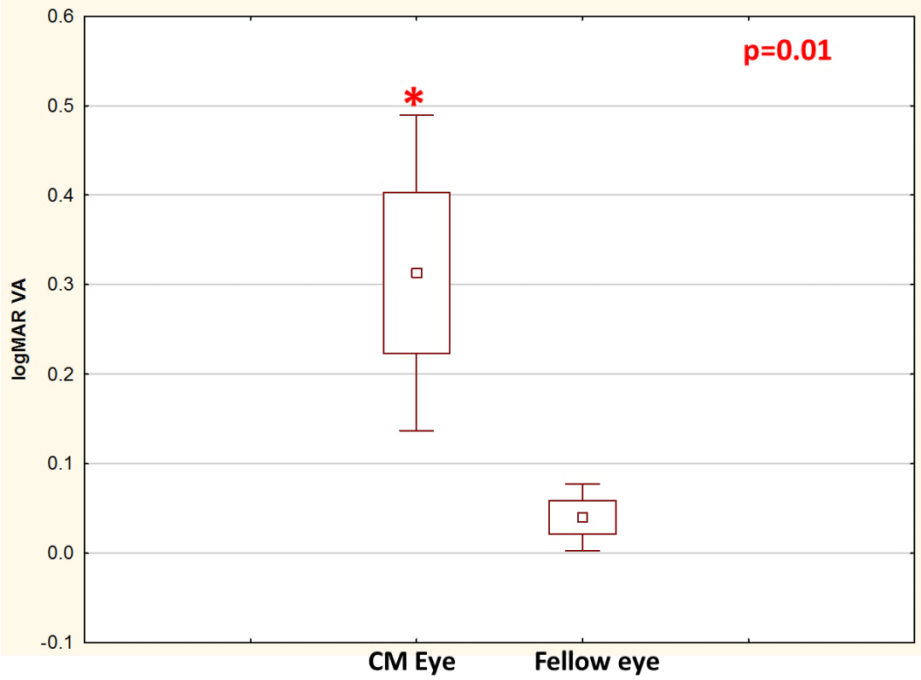

Figure 6.2 Box plots represent visual acuity in CM eye vs Fellow eye. . The legend in the middle of the box represents the mean; the upper and lower extremes of the box represent 25th and 75th percentiles. Error bars represent the nonoutlier range.

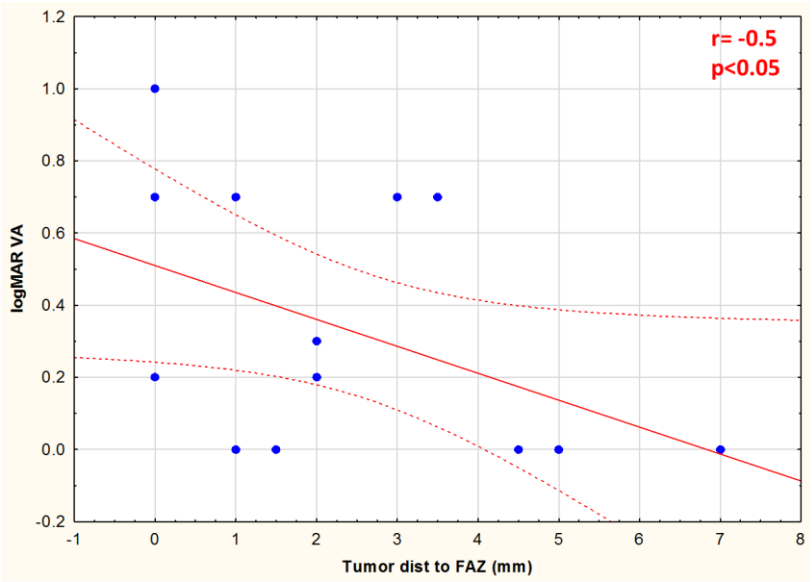

Figure 6.3 Scatterplot of logMAR visual acuity to tumor distance from the foveal avascular zone.

Retinal hemodynamic parameters pre- and post-brachytherapy

The subject's retinal hemodynamic parameters during visits 1 to 3 are given in table 6.3. Retinal arteriolar SaO_2 significantly increased (reANOVA, p=0.026) from 94.4 % ($\pm$7.9) to 98.9% ($\pm$8.8) and 100.6 % ($\pm$6.4), respectively during 3 and 6 month follow up post ^{125}Iodine plaque brachytherapy compared to before treatment (Figure 6.4). A post-hoc analysis for pairwise comparison was performed using Tukey's HSD test. The results show that SaO_2 was significantly increased only during 6month post treatment compared to pre-treatment (p=0.024). Regression plots for retinal SO_2 measurements for each patient across all three visits are shown in figure 6.5. However, all the parameters including SvO_2, TRBF, venous area, and venous velocity did not show a significant change across the visits (Table 6.3). The CM tumor height

was significantly reduced (reANOVA, p=0.020) 6 month post treatment compared to pre-treatment (Figure 6.6).

	Visit 1	Visit 2	Visit 3	p Value, reANOVA
SaO_2 (%)	94.11 ± 7.8	98.93 ± 8.8	100.6 ± 6.4	p=0.026
SvO_2 (%)	52.53 ± 7.3	52.37 ± 9.1	55.19 ± 9.9	NS
TRBF (µL/min)	43.00 ± 16.8	40.44 ± 9.2	46.57 ± 15.03	NS
Venous area ($\times 10^2 mm^2$)	5.84 ± 1.3	5.29 ± 0.8	5.14 ± 0.9	NS
Venous velocity (mm/s)	12.29 ± 4.0	12.8 ± 2.8	15.4 ± 5.6	NS

Table 6.3 Group mean (±SD) for retinal hemodynamic parameters across study visits in CM patients. SaO_2-arteriolar blood oxygen saturation; SvO_2-venular blood oxygen saturation; TRBF-total retinal blood flow; NS-not significant. Level of significance was set to $p<0.05$.

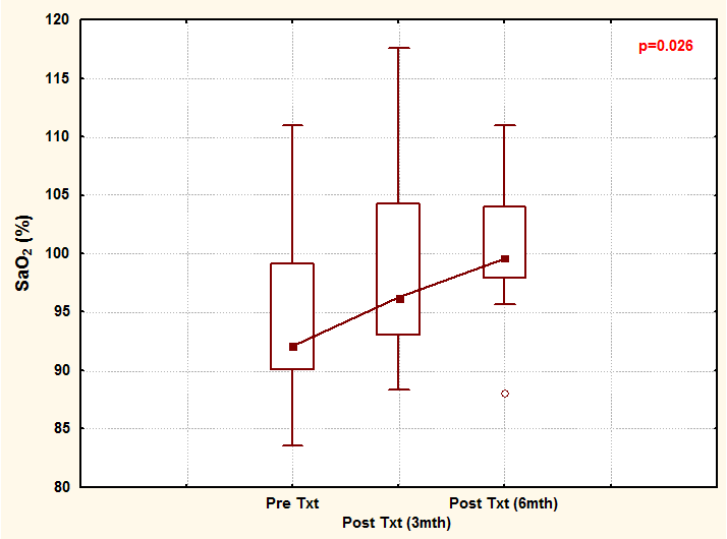

Figure 6.4 Box plots represent change in SaO_2 across visits. The legend in the middle of the box represents the median; the upper and lower extremes of the box represent 25th and 75th percentiles. Error bars represent the nonoutlier range. Circle represents outlier.

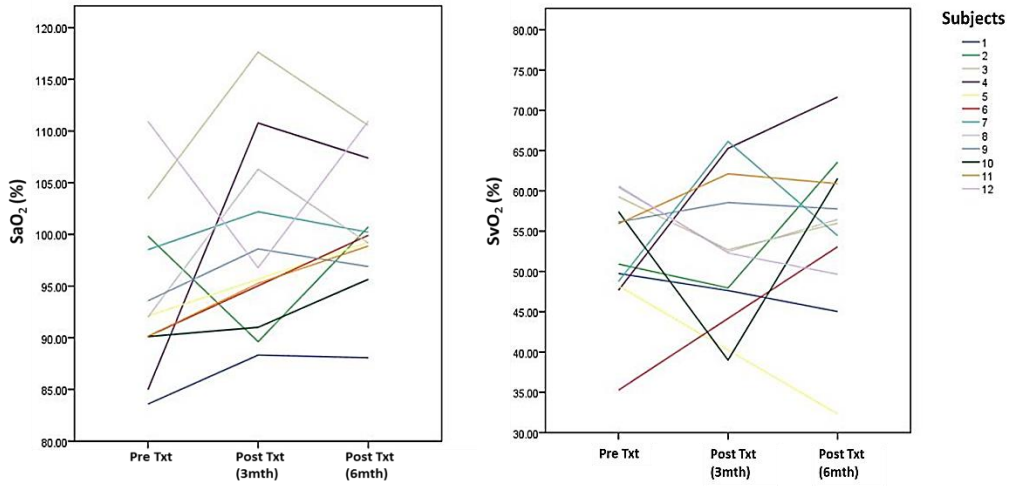

Figure 6.5 Changes in retinal SaO_2 (left) and SvO_2 (right) across visits in all the twelve CM subjects.

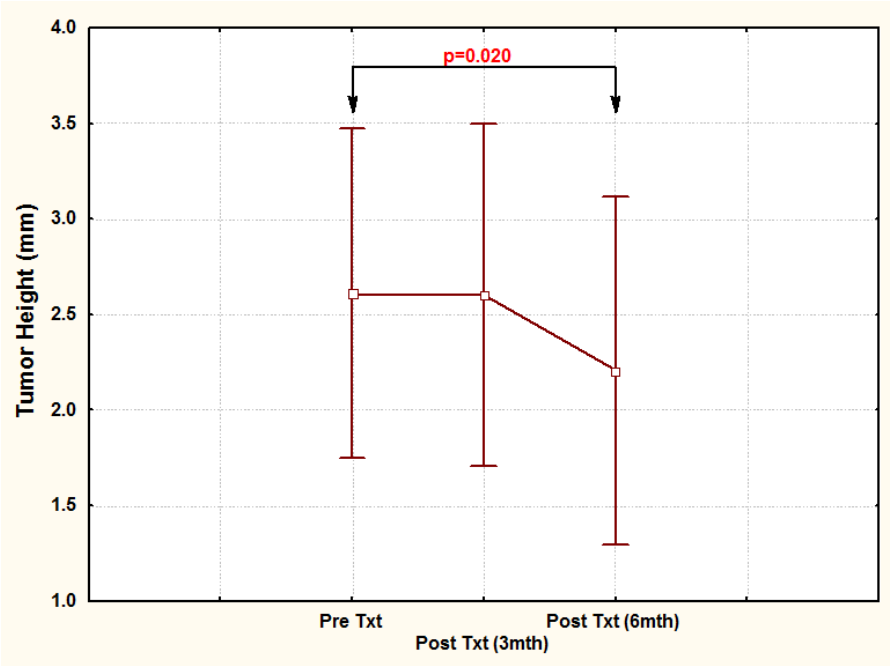

Figure 6.6 Group mean and error bars (±95% Confidence Intervals) showing changes in choroidal melanoma tumor height pre- and post- ^{125}Iodine brachytherapy.

6.4 Discussion

Brachytherapy using radioisotopes is one of the preferred treatments of choice to treat CM, due to its potential to preserve vison and salvage the eye, compared to other management options such as proton beam radiotherapy, helium ion therapy, stereotactic brachytherapy and enucleation.[5,19,17,37] ^{125}Iodine brachytherapy emits relatively low energy photons, due to which radiation related complications are expected to be low. However, the treatment is known to be associated with complications such as keratitis, radiation cataract, neovascular glaucoma, retinopathy and optic neuropathy.[35]

RR presents with microaneurysms, telangiectases, hard exudates, cotton wool spots, neovascularization and macular edema. Retinal capillary incompetence and closure are the earliest microvasculopathic changes reported.[2,6] Radiation exposure to the surrounding healthy retinal vasculature other than tumor, leads to preferential loss of endothelial cells of the inner blood vessel lining and pericytes surrounding the blood vessels. The direct exposure of radiation to the endothelial cells initiates high ambient oxygen and iron from blood as a result of free radical reaction due to ionizing radiation.[3] The more severe form of retinopathy is characterized by the presence of neovascularization, vitreous hemorrhage, macular edema and tractional retinal detachment, secondary to retinal ischemia. The mean time to onset of proliferative RR following plaque brachytherapy was reported as 32 months, with younger age, pre-existing diabetes, closer tumor distance to fovea and optic nerve head having a higher predictability of proliferative RR.[4]

Currently, the earliest these retinopathic changes could be identified is from fluorescein angiography; however, since the early signs are rarely symptomatic, the condition is mostly

diagnosed only during a routine follow-up visit. The present study reports earliest changes in retinal blood SO_2, for the first time, in patients treated with ^{125}Iodine plaque brachytherapy.

The effect of single high doses of radiation on cerebral vasculature is manifested as significant reductions in regional cerebral blood flow and vessel length density, 3 weeks post treatment in rat retinae.[1] Resch and Co-workers[23] studied choroidal perfusion in eyes with untreated CM, and found no significant change in blood flow parameters between affected eye and unaffected contralateral eyes. In contrast, another study reports higher pulsatile ocular blood flow in eyes with untreated CM.[36] The central retinal artery blood velocity of the treated CM eye was found significantly reduced 6month, 12month and 24month post stereotactic radiotherapy.[31] In our study, neither the blood velocity nor the flow was found significantly different pre- and post-treatment. In interpreting the results from these various studies, one needs to be cautious that the radiation dose and treatment type is entirely different between studies. Previous authors state that the untreated eye with CM may be expected to exhibit poor retinal perfusion in two ways, i.e. in untreated eyes due to "steal effect" of the blood towards the tumor and post-radiation, as secondary consequence to radiation effect.[31] However, this result was not observed in the present work.

Reduced red blood cell velocity and decreased vessel diameter was found in experimentally irradiated hamsters 30 days post radiation.[24] Whereas, retinal blood velocity and capillary flow increased in the same animals 180 days post radiation exposure.[21] These two studies report the early and late effects of ionizing radiation, indicating a slow and progressive impact of ionizing radiation on retinal hemodynamics. In the present study, although the blood flow seems to be increased from 43µL/min to 46.57 µL/min and blood velocity increased from 12.29 mm/s to

15.4mm/s, six month post brachytherapy, the results did not reach statistical significance. The radiation dose used in the animal study and our study is different.

Out of the twelve CM patients, one developed retinopathy during 6th month follow-up. It is interesting to note that this subject had a steep increase in both SaO_2 and SvO_2 (approx. 20%) from a pre-treatment value of 84.9% and 47.6% to 107.3% and 71.6%, respectively, six month post brachytherapy (Subject 4 in Figure 6.5). Also, the same patient showed significant increase in TRBF from 52.9 µL/min (pre-treatment) to 64.8 µL/min (6month post treatment). This patient scenario is only used as an example to discuss but not to extrapolate this patient's result in rest of the CM patients.

Previous studies have reported that increased retinal SvO_2 indicates reduced oxygen release to the tissue in the capillary bed, which could result in tissue hypoxia.[10,11,13] The reduced oxygen extraction could be due to the various retinal microvascular changes such as capillary occlusion and formation of telangiectasiac vessels. The current study reports increased retinal arteriolar SO_2 3month and 6month post brachytherapy. The absence of any previous studies reporting retinal blood SO_2 in CM eyes post brachytherapy makes it difficult to compare the current results with that in literature.

An increase in retinal arteriolar blood SO_2 could be attributed to the improved retinal perfusion as a treatment response to brachytherapy. In another way, the radiation destroys the tumor cells, so the so called "steal effect" of the tumor is expected to not exist, thus retinal tissue perfusion increases post brachytherapy. In the long run, we might expect the same increasing trend in both the retinal arteriolar and venular blood SO_2, due to the fact that capillaries might slowly (over years with peak effect about 3 years post treatment) lose their endothelial cells and pericytes and

occlude secondary to the effects of radiation. Decreased O_2 demand due to cell necrosis results in a proportionate decrease in oxygen consumption, which might cause higher SO_2 in retinal vessels especially in venules, despite underlying ischemic insult. The radiation dose, proximity of the tumor to foveal avascular zone, young age and pre-existing diabetes are some of the determinants for the time of onset, rate of progression and severity of retinopathy.[16] The unique clinical pattern and unpredictable latency of radiation retinopathy is related to the life cycle of the retinal vascular endothelial cell.[2,3]

One of the major limitations of the current work is the small number of subjects followed-up. This could be avoided in future studies by recruiting a higher volume of patients. A retrospective chart review will be conducted in the patients recruited so far to follow-up on the retinopathic changes. Predicting who will develop RR from the retinal blood SO_2 changes require more patient data in order to reach a conclusive result. This will be addressed in future work.

Chapter 7 **General Discussion**

The retinal tissue offers unique opportunity to directly observe its microvasculature non-invasively. This has led to the development various non-invasive techniques to quantify retinal blood flow. Previous measurement techniques such as blue field entoptic technique, retinal vessel analyzer, gave only a surrogate measure of flow. The introduction of Doppler techniques to measure red blood cell velocity within retinal vessels has revolutionized the field of objective retinal hemodynamic assessment. Doppler incorporated OCT offers the volumetric measure of TRBF at a single point in time. This technique surpasses the limitations of other previously introduced laser Doppler techniques such as Canon laser blood flowmeter which could measure blood flow from a single vessel at any one point in time.[1-3]

Though the repeatability and variability parameters still need to be improved for the Doppler Spectral Domain OCT (SD-OCT) technology to be utilized in a clinical setting, it remains to be the only prototype currently available, that is capable of measuring TRBF in a single measurement. Chapter 3 details the repeatability and variability of Doppler SD-OCT under varying systemic oxygen concentrations. Overall, the coefficient of repeatability tends to be moderately high relative to a mean effect; however, the Doppler SD-OCT gave consistent and reliable measurements of blood flow during systemic changes in $P_{ET}O_2$ in normal healthy individuals.

Retinal blood supply is tightly regulated under various hemodynamic considerations.[4] Changes in light stimulation, blood gas concentration, intra ocular pressure, and systemic blood pressure are all have known to reciprocate changes in blood flow and vascular resistance.[5-8] Impairment

of retinal vascular reactivity *per se* has been reported in retinal vascular diseases such as diabetic retinopathy, glaucoma, and even in young healthy smokers.[9-12]

In chapter 3, the novel gas provocation utilized, allows the precise combinations of $P_{ET}O_2$, while clamping the $P_{ET}CO_2$, or vice versa, provides reliable and reproducible measure of vascular reactivity. Previous techniques were unable to independently control $P_{ET}O_2$ and $P_{ET}CO_2$;[13,14] but instead used 100% O_2 or coadministerd O_2 (~>90%) and CO_2 (~5%), without clamping the $P_{ET}CO_2$.[15,16] This could impact the results of the measured retinal vascular response.[22] The automated gas flow controller detailed in chapter 3, controls the subject's minute CO_2 production and O_2 consumption, gas flow and composition entering the sequential gas delivery circuit. This standardized gas provocation technique is utilized to calibrate the Doppler based retinal blood flow measurements using SD-OCT and HRC derived retinal arteriolar and venular blood SO_2 measurements. The calibration of gas provocation unit is undertaken once a day using reference gases of known combinations of O_2, CO_2, and N_2 (Nitrogen).

Measurement of retinal blood SO_2 was once possible only by using invasive techniques such as oxygen sensitive microelectrodes to study the oxygen tension of the inner retina.[17-19] In contrast, the recently introduced spectral imaging technology represents a substantial advance in terms of non-invasive assessment of retinal blood SO_2. The HRC is a non-invasive prototype system which allows the measurement of retinal arteriolar and venular blood SO_2. Compared to the "snap-shot" systems, which could bleach the retinal photo pigments, the HRC has a "non-flash" camera, which makes it unique compared to other oximetry techniques available elsewhere. As is common in other retinal oximetry techniques, some arteriolar blood SO_2 values were above

100%, which is beyond the physiological range. At this point, it is unsure whether this could be due to the error in terms of SO_2 calculation itself or secondary to poorly registered images. However, the images included for the analyses in this thesis were carefully selected and examined before calculating SO_2.

The variability reported (chapter 3) for both the prototype techniques of Doppler SD-OCT and HRC, could be attributed to the subjectivity in terms of blood flow analysis and Doppler signal differences between visits as well as few imperfections in the optics design of the HRC, respectively. Improving such aspects could greatly reduce the variability and improve the repeatability of these two novel techniques to be utilized clinically.

By measuring the retinal blood flow and blood SO_2, in chapter 4, inner retinal oxygen extraction was calculated using Fick's principle which is the product of TRBF and arterial-venous oxygen content difference (CaO_2-CvO_2). Measurement of retinal O_2 extraction could bring forth a clearer understanding of the retinal health in disease. However, these measurements were not made simultaneously at the same vessel, same location and at the same time, instead measurements were acquired sequentially. Future OCT technology with in-built Doppler blood flow and retinal oximetry methodologies[20,21] would be a major advancement.

We decided to apply these novel methods in the CM patients undergoing brachytherapy treatment because RR is one of the common sight-threatening complications following radiation treatment such as brachytherapy for CM. Also, it is interesting that the RR presents clinically similar to a fast developing diabetic retinopathy. Whether or not ionizing radiation impacts the retinal vasculature remains to be an interesting question to answer.

Therefore, in chapter 5 I investigated the impact of brachytherapy on retinal blood flow and oxygen saturation. RR patients were recruited from the Ocular Oncology Clinic located at Princess Margaret Hospital, Toronto, Canada. In this study, reduced TRBF and increased retinal blood SO_2 was found in the eye with RR compared to the fellow eye. The reported higher retinal blood SO_2 in the retinopathy eye could be secondary to decreased oxygen demand due to cell necrosis. The decreased TRBF in RR could be from less demand by the tissue itself due to cell death or degeneration process as a result of radiation insult. These results indicate an altered retinal vascular physiology in patients with radiation related retinopathy. Lack of a control group for comparison and a small sample size are possible limitations of this study. However, the data is first to report changes in retinal blood SO_2 in radiation induced retinopathy and this sample of patients with RR is the largest prospective group that we are aware of in the literature.

Chapter 6 detailed the changes in retinal blood SO_2 in CM patients before and after brachytherapy treatment. The ultimate aim is to derive a model to predict retinopathy form the changes in retinal oximetry, which seem to be a precursor to tissue hypoxia in diseases such as diabetic retinopathy. It is interesting to note that the RR clinically presents similar to a rapidly developing diabetic retinopathy.

CM patients were recruited from the Ocular Oncology Clinic located at Princess Margaret Hospital, Toronto, Canada. This remains to be the only center in Canada to treat CM patients using plaque brachytherapy. The study reports increased retinal arteriolar blood SO_2 post ^{125}Iodine brachytherapy for CM. Predicting who will develop radiation retinopathy from the retinal blood SO_2 changes observed requires a longer follow-up period in order to reach a conclusive result. This work is in progress.

7.1 Future direction

Improvement of the Doppler SD-OCT and HRC technologies is needed in order to reduce the variability, which could make these prototype techniques less demanding clinically. In terms of the HRC, the imperfectible optics design of the retinal camera causes a number of image artifacts that cannot be completely corrected in image processing steps, which excludes such images. The automation of blood flow analysis and a faster scan rate would also reduce the variability. The Doppler SD-OCT is reported to have a coefficient of variability of 15.1% in young healthy participants. The repeatability could be worse in elderly population, where maintaining steady fixation and controlling eye movement could be more challenging. The retinal blood SO_2 reported in this study is from one single arteriole and venule, whereas, deriving the SO_2 for the whole of the vascular tree would be undoubtedly beneficial.

Longitudinal studies that could track changes in retinal blood SO_2 are important to better understand the impact of ionizing radiation in the progression of RR. A larger sample must be recruited since these patients experience significant psychological trauma as a result of the diagnosis, and therefore are easily lost to follow-up. Along with the retinal SO_2 measurement it would be worthwhile to investigate the level of inflammatory biomarkers such as VEGF at different stages of progression of radiation retinopathy to better understand the pathogenesis behind the latency and variability in developing retinopathy.

In summary, the variability and repeatability of two novel prototype techniques of Doppler SD-OCT and HRC are reported under varying blood gas perturbations using standardized gas provocation methodology.

These two protype techniques are further utilized in the assessment of retinal perfusion changes in RR for the first time, where the ionizing radiation used to treat CM seems to have an impact on retinal vascular physiology.

The effect of brachytherapy treatment on retinal vasculature is studied longitudinally, except that the results of the initial six months post treatment are presented in this work. Interestingly, retinal blood SO_2 increases significantly post brachytherapy in CM patients. Further follow-up to predict who will develop RR will be continued in future work.

Letters of Copyright Permission

NATURE PUBLISHING GROUP LICENSE

TERMS AND CONDITIONS

This Agreement between Kalpana Rose ("You") and Nature Publishing Group ("Nature Publishing Group") consists of your license details and the terms and conditions provided by Nature Publishing Group and Copyright Clearance Center.

License Number

3897670165973

License date

Jun 28, 2016

Licensed Content Publisher

Nature Publishing Group

Licensed Content Publication

Eye

Licensed Content Title

Spectral imaging of the retina

Licensed Content Author

D J Mordant, I Al-Abboud, G Muyo, A Gorman, A Sallam et al.

Licensed Content Date

Mar 10, 2011

Licensed Content Volume Number

25

Licensed Content Issue Number

3

Type of Use

reuse in a dissertation / thesis

Requestor type

academic/educational

Format

electronic

Portion

figures/tables/illustrations

Number of figures/tables/illustrations

1

High-res required

no

Figures

The molar extinction coefficients of deoxyhaemoglobin (Hb) and oxyhaemoglobin (HbO2) derivatives as a function of wavelength.

Author of this NPG article

no

Your reference number

Title of your thesis / dissertation

RETINAL PERFUSION CHANGES IN CHOROIDAL MELANOMA POST BRACHYTHERAPY

Expected completion date

Jun 2017

Estimated size (number of pages)

200

Requestor Location

Kalpana Rose

200 University avenue east

Waterloo, ON N2L3G1

Canada

Attn: Kalpana Rose

Billing Type

Invoice

Billing Address

Kalpana Rose
200 University avenue east
Waterloo, ON N2L3G1
Canada
Attn: Kalpana Rose
Total
0.00 USD
Terms and Conditions
Terms and Conditions for Permissions
Nature Publishing Group hereby grants you a non-exclusive license to reproduce this material for this purpose, and for no other use, subject to the conditions below:

1. NPG warrants that it has, to the best of its knowledge, the rights to license reuse of this material. However, you should ensure that the material you are requesting is original to Nature Publishing Group and does not carry the copyright of another entity (as credited in the published version). If the credit line on any part of the material you have requested indicates that it was reprinted or adapted by NPG with permission from another source, then you should also seek permission from that source to reuse the material.

2. Permission granted free of charge for material in print is also usually granted for any electronic version of that work, provided that the material is incidental to the work as a whole and that the electronic version is essentially equivalent to, or substitutes for, the print version. Where print permission has been granted for a fee, separate permission must be obtained for any additional, electronic re-use (unless, as in the case of a full paper, this has already been accounted for during your initial request in the calculation of a print run).NB: In all cases, web-based use of full-text articles must be authorized separately through the 'Use on a Web Site' option when requesting permission.

3. Permission granted for a first edition does not apply to second and subsequent editions and for editions in other languages (except for signatories to the STM Permissions

Guidelines, or where the first edition permission was granted for free).

4. Nature Publishing Group's permission must be acknowledged next to the figure, table or abstract in print. In electronic form, this acknowledgement must be visible at the same time as the figure/table/abstract, and must be hyperlinked to the journal's homepage.

5. The credit line should read:
   Reprinted by permission from Macmillan Publishers Ltd: [JOURNAL NAME] (reference citation), copyright (year of publication)
   For AOP papers, the credit line should read:
   Reprinted by permission from Macmillan Publishers Ltd: [JOURNAL NAME], advance online publication, day month year (doi: 10.1038/sj.[JOURNAL ACRONYM].XXXXX)

   Note: For republication from the *British Journal of Cancer*, the following credit lines apply.
   Reprinted by permission from Macmillan Publishers Ltd on behalf of Cancer Research UK: [JOURNAL NAME] (reference citation), copyright (year of publication)For AOP papers, the credit line should read:
   Reprinted by permission from Macmillan Publishers Ltd on behalf of Cancer Research UK: [JOURNAL NAME], advance online publication, day month year (doi: 10.1038/sj.[JOURNAL ACRONYM].XXXXX)
6. Adaptations of single figures do not require NPG approval. However, the adaptation should be credited as follows:
   Adapted by permission from Macmillan Publishers Ltd: [JOURNAL NAME] (reference citation), copyright (year of publication)
   Note: For adaptation from the *British Journal of Cancer*, the following credit line applies.
   Adapted by permission from Macmillan Publishers Ltd on behalf of Cancer Research

UK: [JOURNAL NAME] (reference citation), copyright (year of publication)

7. Translations of 401 words up to a whole article require NPG approval. Please visit http://www.macmillanmedicalcommunications.com for more information.Translations of up to a 400 words do not require NPG approval. The translation should be credited as follows:

   Translated by permission from Macmillan Publishers Ltd: [JOURNAL NAME] (reference citation), copyright (year of publication).

   Note: For translation from the *British Journal of Cancer*, the following credit line applies.

   Translated by permission from Macmillan Publishers Ltd on behalf of Cancer Research UK: [JOURNAL NAME] (reference citation), copyright (year of publication)

We are certain that all parties will benefit from this agreement and wish you the best in the use of this material. Thank you.

Special Terms:

v1.1

Questions? customercare@copyright.com or +1-855-239-3415 (toll free in the US) or +1-978-646-2777.

ELSEVIER LICENSE

TERMS AND CONDITIONS

This Agreement between Kalpana Rose ("You") and Elsevier ("Elsevier") consists of your license details and the terms and conditions provided by Elsevier and Copyright Clearance Center.

License Number	3898810021130
License date	Jun 30, 2016
Licensed Content Publisher	Elsevier
Licensed Content Publication	Experimental Eye Research
Licensed Content Title	Preliminary investigation of multispectral retinal tissue oximetry mapping using a hyperspectral retinal camera
Licensed Content Author	Michèle Desjardins,Jean-Philippe Sylvestre,Reza Jafari,Susith Kulasekara,Kalpana Rose,Rachel Trussart,Jean Daniel Arbour,Chris Hudson,Frédéric Lesage
Licensed Content Date	May 2016
Licensed Content Volume Number	146
Licensed Content Issue Number	n/a
Licensed Content Pages	11
Start Page	330
End Page	340
Type of Use	reuse in a thesis/dissertation
Intended publisher of new work	other

Portion	figures/tables/illustrations
Number of figures/tables/illustrations	1
Format	electronic
Are you the author of this Elsevier article?	Yes
Will you be translating?	No
Order reference number	
Original figure numbers	Figure 1
Title of your thesis/dissertation	RETINAL PERFUSION CHANGES IN CHOROIDAL MELANOMA POST BRACHYTHERAPY
Expected completion date	Jun 2017
Estimated size (number of pages)	200
Elsevier VAT number	GB 494 6272 12
Requestor Location	Kalpana Rose 200 University avenue east Waterloo, ON N2L3G1 Canada Attn: Kalpana Rose
Total	0.00 USD

Terms and Conditions

INTRODUCTION

1. The publisher for this copyrighted material is Elsevier. By clicking "accept" in connection with completing this licensing transaction, you agree that the following terms

and conditions apply to this transaction (along with the Billing and Payment terms and conditions established by Copyright Clearance Center, Inc. ("CCC"), at the time that you opened your Rightslink account and that are available at any time at http://myaccount.copyright.com).

GENERAL TERMS

2. Elsevier hereby grants you permission to reproduce the aforementioned material subject to the terms and conditions indicated.

3. Acknowledgement: If any part of the material to be used (for example, figures) has appeared in our publication with credit or acknowledgement to another source, permission must also be sought from that source. If such permission is not obtained then that material may not be included in your publication/copies. Suitable acknowledgement to the source must be made, either as a footnote or in a reference list at the end of your publication, as follows:

"Reprinted from Publication title, Vol /edition number, Author(s), Title of article / title of chapter, Pages No., Copyright (Year), with permission from Elsevier [OR APPLICABLE SOCIETY COPYRIGHT OWNER]." Also Lancet special credit - "Reprinted from The Lancet, Vol. number, Author(s), Title of article, Pages No., Copyright (Year), with permission from Elsevier."

4. Reproduction of this material is confined to the purpose and/or media for which permission is hereby given.

5. Altering/Modifying Material: Not Permitted. However figures and illustrations may be altered/adapted minimally to serve your work. Any other abbreviations, additions, deletions and/or any other alterations shall be made only with prior written authorization of Elsevier Ltd. (Please contact Elsevier at permissions@elsevier.com)

6. If the permission fee for the requested use of our material is waived in this instance, please be advised that your future requests for Elsevier materials may attract a fee.

7. Reservation of Rights: Publisher reserves all rights not specifically granted in the combination of (i) the license details provided by you and accepted in the course of this licensing transaction, (ii) these terms and conditions and (iii) CCC's Billing and Payment

terms and conditions.

8. License Contingent Upon Payment: While you may exercise the rights licensed immediately upon issuance of the license at the end of the licensing process for the transaction, provided that you have disclosed complete and accurate details of your proposed use, no license is finally effective unless and until full payment is received from you (either by publisher or by CCC) as provided in CCC's Billing and Payment terms and conditions. If full payment is not received on a timely basis, then any license preliminarily granted shall be deemed automatically revoked and shall be void as if never granted. Further, in the event that you breach any of these terms and conditions or any of CCC's Billing and Payment terms and conditions, the license is automatically revoked and shall be void as if never granted. Use of materials as described in a revoked license, as well as any use of the materials beyond the scope of an unrevoked license, may constitute copyright infringement and publisher reserves the right to take any and all action to protect its copyright in the materials.

9. Warranties: Publisher makes no representations or warranties with respect to the licensed material.

10. Indemnity: You hereby indemnify and agree to hold harmless publisher and CCC, and their respective officers, directors, employees and agents, from and against any and all claims arising out of your use of the licensed material other than as specifically authorized pursuant to this license.

11. No Transfer of License: This license is personal to you and may not be sublicensed, assigned, or transferred by you to any other person without publisher's written permission.

12. No Amendment Except in Writing: This license may not be amended except in a writing signed by both parties (or, in the case of publisher, by CCC on publisher's behalf).

13. Objection to Contrary Terms: Publisher hereby objects to any terms contained in any purchase order, acknowledgment, check endorsement or other writing prepared by you, which terms are inconsistent with these terms and conditions or CCC's Billing and Payment terms and conditions. These terms and conditions, together with CCC's Billing and Payment terms and conditions (which are incorporated herein), comprise the entire

agreement between you and publisher (and CCC) concerning this licensing transaction. In the event of any conflict between your obligations established by these terms and conditions and those established by CCC's Billing and Payment terms and conditions, these terms and conditions shall control.

14. Revocation: Elsevier or Copyright Clearance Center may deny the permissions described in this License at their sole discretion, for any reason or no reason, with a full refund payable to you. Notice of such denial will be made using the contact information provided by you. Failure to receive such notice will not alter or invalidate the denial. In no event will Elsevier or Copyright Clearance Center be responsible or liable for any costs, expenses or damage incurred by you as a result of a denial of your permission request, other than a refund of the amount(s) paid by you to Elsevier and/or Copyright Clearance Center for denied permissions.

LIMITED LICENSE

The following terms and conditions apply only to specific license types:

15. **Translation**: This permission is granted for non-exclusive world **English** rights only unless your license was granted for translation rights. If you licensed translation rights you may only translate this content into the languages you requested. A professional translator must perform all translations and reproduce the content word for word preserving the integrity of the article.

16. **Posting licensed content on any Website**: The following terms and conditions apply as follows: Licensing material from an Elsevier journal: All content posted to the web site must maintain the copyright information line on the bottom of each image; A hyper-text must be included to the Homepage of the journal from which you are licensing at http://www.sciencedirect.com/science/journal/xxxxx or the Elsevier homepage for books at http://www.elsevier.com; Central Storage: This license does not include permission for a scanned version of the material to be stored in a central repository such as that provided by Heron/XanEdu.

Licensing material from an Elsevier book: A hyper-text link must be included to the Elsevier homepage at http://www.elsevier.com . All content posted to the web site must

maintain the copyright information line on the bottom of each image.

Posting licensed content on Electronic reserve: In addition to the above the following clauses are applicable: The web site must be password-protected and made available only to bona fide students registered on a relevant course. This permission is granted for 1 year only. You may obtain a new license for future website posting.

17. **For journal authors:** the following clauses are applicable in addition to the above:

Preprints:

A preprint is an author's own write-up of research results and analysis, it has not been peer-reviewed, nor has it had any other value added to it by a publisher (such as formatting, copyright, technical enhancement etc.).

Authors can share their preprints anywhere at any time. Preprints should not be added to or enhanced in any way in order to appear more like, or to substitute for, the final versions of articles however authors can update their preprints on arXiv or RePEc with their Accepted Author Manuscript (see below).

If accepted for publication, we encourage authors to link from the preprint to their formal publication via its DOI. Millions of researchers have access to the formal publications on ScienceDirect, and so links will help users to find, access, cite and use the best available version. Please note that Cell Press, The Lancet and some society-owned have different preprint policies. Information on these policies is available on the journal homepage.

Accepted Author Manuscripts: An accepted author manuscript is the manuscript of an article that has been accepted for publication and which typically includes author-incorporated changes suggested during submission, peer review and editor-author communications.

Authors can share their accepted author manuscript:

- - immediately
    - via their non-commercial person homepage or blog
    - by updating a preprint in arXiv or RePEc with the accepted manuscript
    - via their research institute or institutional repository for internal institutional

uses or as part of an invitation-only research collaboration work-group
    - directly by providing copies to their students or to research collaborators for their personal use
    - for private scholarly sharing as part of an invitation-only work group on commercial sites with which Elsevier has an agreement
- after the embargo period
    - via non-commercial hosting platforms such as their institutional repository
    - via commercial sites with which Elsevier has an agreement

In all cases accepted manuscripts should:

- link to the formal publication via its DOI
- bear a CC-BY-NC-ND license - this is easy to do
- if aggregated with other manuscripts, for example in a repository or other site, be shared in alignment with our hosting policy not be added to or enhanced in any way to appear more like, or to substitute for, the published journal article.

Published journal article (JPA): A published journal article (PJA) is the definitive final record of published research that appears or will appear in the journal and embodies all value-adding publishing activities including peer review co-ordination, copy-editing, formatting, (if relevant) pagination and online enrichment.

Policies for sharing publishing journal articles differ for subscription and gold open access articles:

Subscription Articles: If you are an author, please share a link to your article rather than the full-text. Millions of researchers have access to the formal publications on ScienceDirect, and so links will help your users to find, access, cite, and use the best available version.

Theses and dissertations which contain embedded PJAs as part of the formal submission can be posted publicly by the awarding institution with DOI links back to the formal publications on ScienceDirect.

If you are affiliated with a library that subscribes to ScienceDirect you have additional private sharing rights for others' research accessed under that agreement. This includes use

for classroom teaching and internal training at the institution (including use in course packs and courseware programs), and inclusion of the article for grant funding purposes.

Gold Open Access Articles: May be shared according to the author-selected end-user license and should contain a CrossMark logo, the end user license, and a DOI link to the formal publication on ScienceDirect.

Please refer to Elsevier's posting policy for further information.

18. **For book authors** the following clauses are applicable in addition to the above: Authors are permitted to place a brief summary of their work online only. You are not allowed to download and post the published electronic version of your chapter, nor may you scan the printed edition to create an electronic version. **Posting to a repository:** Authors are permitted to post a summary of their chapter only in their institution's repository.

19. **Thesis/Dissertation**: If your license is for use in a thesis/dissertation your thesis may be submitted to your institution in either print or electronic form. Should your thesis be published commercially, please reapply for permission. These requirements include permission for the Library and Archives of Canada to supply single copies, on demand, of the complete thesis and include permission for Proquest/UMI to supply single copies, on demand, of the complete thesis. Should your thesis be published commercially, please reapply for permission. Theses and dissertations which contain embedded PJAs as part of the formal submission can be posted publicly by the awarding institution with DOI links back to the formal publications on ScienceDirect.

Elsevier Open Access Terms and Conditions

You can publish open access with Elsevier in hundreds of open access journals or in nearly 2000 established subscription journals that support open access publishing. Permitted third party re-use of these open access articles is defined by the author's choice of Creative Commons user license. See our open access license policy for more information.

Terms & Conditions applicable to all Open Access articles published with Elsevier:

Any reuse of the article must not represent the author as endorsing the adaptation of the

ELSEVIER LICENSE
TERMS AND CONDITIONS

This Agreement between Kalpana Rose ("You") and Elsevier ("Elsevier") consists of your license details and the terms and conditions provided by Elsevier and Copyright Clearance Center.

License Number	4006121235325
License date	Dec 11, 2016
Licensed Content Publisher	Elsevier
Licensed Content Publication	Elsevier Books
Licensed Content Title	Encyclopedia of the Eye
Licensed Content Author	B. Anand-Apte,J.G. Hollyfield
Licensed Content Date	2010
Licensed Content Pages	7
Start Page	9
End Page	15
Type of Use	reuse in a thesis/dissertation
Portion	figures/tables/illustrations
Number of figures/tables/illustrations	2
Format	electronic
Are you the author of this Elsevier chapter?	No

Will you be translating?	No
Order reference number	
Original figure numbers	Figure 1, Figure 3
Title of your thesis/dissertation	RETINAL PERFUSION CHANGES IN CHOROIDAL MELANOMA POST BRACHYTHERAPY
Expected completion date	Jun 2017
Estimated size (number of pages)	200
Elsevier VAT number	GB 494 6272 12
Requestor Location	Kalpana Rose 200 University avenue east Waterloo, ON N2L3G1 Canada Attn: Kalpana Rose
Total	0.00 USD

Terms and Conditions

INTRODUCTION

1. The publisher for this copyrighted material is Elsevier. By clicking "accept" in connection with completing this licensing transaction, you agree that the following terms and conditions apply to this transaction (along with the Billing and Payment terms and conditions established by Copyright Clearance Center, Inc. ("CCC"), at the time that you opened your Rightslink account and that are available at any time at http://myaccount.copyright.com).

GENERAL TERMS

2. Elsevier hereby grants you permission to reproduce the aforementioned material subject

to the terms and conditions indicated.

3. Acknowledgement: If any part of the material to be used (for example, figures) has appeared in our publication with credit or acknowledgement to another source, permission must also be sought from that source. If such permission is not obtained then that material may not be included in your publication/copies. Suitable acknowledgement to the source must be made, either as a footnote or in a reference list at the end of your publication, as follows:

"Reprinted from Publication title, Vol /edition number, Author(s), Title of article / title of chapter, Pages No., Copyright (Year), with permission from Elsevier [OR APPLICABLE SOCIETY COPYRIGHT OWNER]." Also Lancet special credit - "Reprinted from The Lancet, Vol. number, Author(s), Title of article, Pages No., Copyright (Year), with permission from Elsevier."

4. Reproduction of this material is confined to the purpose and/or media for which permission is hereby given.

5. Altering/Modifying Material: Not Permitted. However figures and illustrations may be altered/adapted minimally to serve your work. Any other abbreviations, additions, deletions and/or any other alterations shall be made only with prior written authorization of Elsevier Ltd. (Please contact Elsevier at permissions@elsevier.com). No modifications can be made to any Lancet figures/tables and they must be reproduced in full.

6. If the permission fee for the requested use of our material is waived in this instance, please be advised that your future requests for Elsevier materials may attract a fee.

7. Reservation of Rights: Publisher reserves all rights not specifically granted in the combination of (i) the license details provided by you and accepted in the course of this licensing transaction, (ii) these terms and conditions and (iii) CCC's Billing and Payment terms and conditions.

8. License Contingent Upon Payment: While you may exercise the rights licensed immediately upon issuance of the license at the end of the licensing process for the transaction, provided that you have disclosed complete and accurate details of your proposed use, no license is finally effective unless and until full payment is received from

you (either by publisher or by CCC) as provided in CCC's Billing and Payment terms and conditions. If full payment is not received on a timely basis, then any license preliminarily granted shall be deemed automatically revoked and shall be void as if never granted. Further, in the event that you breach any of these terms and conditions or any of CCC's Billing and Payment terms and conditions, the license is automatically revoked and shall be void as if never granted. Use of materials as described in a revoked license, as well as any use of the materials beyond the scope of an unrevoked license, may constitute copyright infringement and publisher reserves the right to take any and all action to protect its copyright in the materials.

9. Warranties: Publisher makes no representations or warranties with respect to the licensed material.

10. Indemnity: You hereby indemnify and agree to hold harmless publisher and CCC, and their respective officers, directors, employees and agents, from and against any and all claims arising out of your use of the licensed material other than as specifically authorized pursuant to this license.

11. No Transfer of License: This license is personal to you and may not be sublicensed, assigned, or transferred by you to any other person without publisher's written permission.

12. No Amendment Except in Writing: This license may not be amended except in a writing signed by both parties (or, in the case of publisher, by CCC on publisher's behalf).

13. Objection to Contrary Terms: Publisher hereby objects to any terms contained in any purchase order, acknowledgment, check endorsement or other writing prepared by you, which terms are inconsistent with these terms and conditions or CCC's Billing and Payment terms and conditions. These terms and conditions, together with CCC's Billing and Payment terms and conditions (which are incorporated herein), comprise the entire agreement between you and publisher (and CCC) concerning this licensing transaction. In the event of any conflict between your obligations established by these terms and conditions and those established by CCC's Billing and Payment terms and conditions, these terms and conditions shall control.

14. Revocation: Elsevier or Copyright Clearance Center may deny the permissions

described in this License at their sole discretion, for any reason or no reason, with a full refund payable to you. Notice of such denial will be made using the contact information provided by you. Failure to receive such notice will not alter or invalidate the denial. In no event will Elsevier or Copyright Clearance Center be responsible or liable for any costs, expenses or damage incurred by you as a result of a denial of your permission request, other than a refund of the amount(s) paid by you to Elsevier and/or Copyright Clearance Center for denied permissions.

LIMITED LICENSE

The following terms and conditions apply only to specific license types:

15. **Translation**: This permission is granted for non-exclusive world **English** rights only unless your license was granted for translation rights. If you licensed translation rights you may only translate this content into the languages you requested. A professional translator must perform all translations and reproduce the content word for word preserving the integrity of the article.

16. **Posting licensed content on any Website**: The following terms and conditions apply as follows: Licensing material from an Elsevier journal: All content posted to the web site must maintain the copyright information line on the bottom of each image; A hyper-text must be included to the Homepage of the journal from which you are licensing at http://www.sciencedirect.com/science/journal/xxxxx or the Elsevier homepage for books at http://www.elsevier.com; Central Storage: This license does not include permission for a scanned version of the material to be stored in a central repository such as that provided by Heron/XanEdu.

Licensing material from an Elsevier book: A hyper-text link must be included to the Elsevier homepage at http://www.elsevier.com . All content posted to the web site must maintain the copyright information line on the bottom of each image.

Posting licensed content on Electronic reserve: In addition to the above the following clauses are applicable: The web site must be password-protected and made available only to bona fide students registered on a relevant course. This permission is granted for 1 year

only. You may obtain a new license for future website posting.

17. **For journal authors:** the following clauses are applicable in addition to the above:

Preprints:

A preprint is an author's own write-up of research results and analysis, it has not been peer-reviewed, nor has it had any other value added to it by a publisher (such as formatting, copyright, technical enhancement etc.).

Authors can share their preprints anywhere at any time. Preprints should not be added to or enhanced in any way in order to appear more like, or to substitute for, the final versions of articles however authors can update their preprints on arXiv or RePEc with their Accepted Author Manuscript (see below).

If accepted for publication, we encourage authors to link from the preprint to their formal publication via its DOI. Millions of researchers have access to the formal publications on ScienceDirect, and so links will help users to find, access, cite and use the best available version. Please note that Cell Press, The Lancet and some society-owned have different preprint policies. Information on these policies is available on the journal homepage.

Accepted Author Manuscripts: An accepted author manuscript is the manuscript of an article that has been accepted for publication and which typically includes author-incorporated changes suggested during submission, peer review and editor-author communications.

Authors can share their accepted author manuscript:

- - immediately
    - via their non-commercial person homepage or blog
    - by updating a preprint in arXiv or RePEc with the accepted manuscript
    - via their research institute or institutional repository for internal institutional uses or as part of an invitation-only research collaboration work-group
    - directly by providing copies to their students or to research collaborators for their personal use
    - for private scholarly sharing as part of an invitation-only work group on

commercial sites with which Elsevier has an agreement

- - after the embargo period
    - via non-commercial hosting platforms such as their institutional repository
    - via commercial sites with which Elsevier has an agreement

In all cases accepted manuscripts should:

- - link to the formal publication via its DOI
- - bear a CC-BY-NC-ND license - this is easy to do
- - if aggregated with other manuscripts, for example in a repository or other site, be shared in alignment with our hosting policy not be added to or enhanced in any way to appear more like, or to substitute for, the published journal article.

Published journal article (JPA): A published journal article (PJA) is the definitive final record of published research that appears or will appear in the journal and embodies all value-adding publishing activities including peer review co-ordination, copy-editing, formatting, (if relevant) pagination and online enrichment.

Policies for sharing publishing journal articles differ for subscription and gold open access articles:

Subscription Articles: If you are an author, please share a link to your article rather than the full-text. Millions of researchers have access to the formal publications on ScienceDirect, and so links will help your users to find, access, cite, and use the best available version.

Theses and dissertations which contain embedded PJAs as part of the formal submission can be posted publicly by the awarding institution with DOI links back to the formal publications on ScienceDirect.

If you are affiliated with a library that subscribes to ScienceDirect you have additional private sharing rights for others' research accessed under that agreement. This includes use for classroom teaching and internal training at the institution (including use in course packs and courseware programs), and inclusion of the article for grant funding purposes.

Gold Open Access Articles: May be shared according to the author-selected end-user license and should contain a CrossMark logo, the end user license, and a DOI link to the

formal publication on ScienceDirect.

Please refer to Elsevier's posting policy for further information.

18. **For book authors** the following clauses are applicable in addition to the above: Authors are permitted to place a brief summary of their work online only. You are not allowed to download and post the published electronic version of your chapter, nor may you scan the printed edition to create an electronic version. **Posting to a repository:** Authors are permitted to post a summary of their chapter only in their institution's repository.

19. **Thesis/Dissertation**: If your license is for use in a thesis/dissertation your thesis may be submitted to your institution in either print or electronic form. Should your thesis be published commercially, please reapply for permission. These requirements include permission for the Library and Archives of Canada to supply single copies, on demand, of the complete thesis and include permission for Proquest/UMI to supply single copies, on demand, of the complete thesis. Should your thesis be published commercially, please reapply for permission. Theses and dissertations which contain embedded PJAs as part of the formal submission can be posted publicly by the awarding institution with DOI links back to the formal publications on ScienceDirect.

Elsevier Open Access Terms and Conditions

You can publish open access with Elsevier in hundreds of open access journals or in nearly 2000 established subscription journals that support open access publishing. Permitted third party re-use of these open access articles is defined by the author's choice of Creative Commons user license. See our open access license policy for more information.

Terms & Conditions applicable to all Open Access articles published with Elsevier:

Any reuse of the article must not represent the author as endorsing the adaptation of the article nor should the article be modified in such a way as to damage the author's honour or reputation. If any changes have been made, such changes must be clearly indicated. The author(s) must be appropriately credited and we ask that you include the end user

permission from Elsevier and will be subject to a fee.

Commercial reuse includes:

- - Associating advertising with the full text of the Article
- - Charging fees for document delivery or access
- - Article aggregation
- - Systematic distribution via e-mail lists or share buttons

Posting or linking by commercial companies for use by customers of those companies.

20. **Other Conditions**:

v1.9

Questions? customercare@copyright.com or +1-855-239-3415 (toll free in the US) or +1-978-646-2777.

ELSEVIER LICENSE

TERMS AND CONDITIONS

Jan 23, 2017

This Agreement between Kalpana Rose ("You") and Elsevier ("Elsevier") consists of your license details and the terms and conditions provided by Elsevier and Copyright Clearance Center.

License Number

4021510750584

License date

Jan 03, 2017

Licensed Content Publisher

Elsevier

Licensed Content Publication

Microvascular Research

Licensed Content Title

The impact of hypercapnia on retinal capillary blood flow assessed by scanning laser Doppler flowmetry

Licensed Content Author

Subha T. Venkataraman,Chris Hudson,Joseph A. Fisher,John G. Flanagan

Licensed Content Date

May 2005

Licensed Content Volume Number

69

Licensed Content Issue Number

3

Licensed Content Pages

7

Start Page

149

End Page

155

Type of Use

reuse in a thesis/dissertation

Portion

figures/tables/illustrations

Number of figures/tables/illustrations

1

Format

electronic

Are you the author of this Elsevier article?

No

Will you be translating?

No

Order reference number

Original figure numbers

Fig. 1

Title of your thesis/dissertation

RETINAL PERFUSION CHANGES IN CHOROIDAL MELANOMA POST BRACHYTHERAPY

Expected completion date

Jun 2017

Estimated size (number of pages)

200

Elsevier VAT number

GB 494 6272 12

Requestor Location

Kalpana Rose

200 University avenue east

Waterloo, ON N2L3G1

Canada

Attn: Kalpana Rose

Total

0.00 USD

Terms and Conditions

INTRODUCTION

1. The publisher for this copyrighted material is Elsevier. By clicking "accept" in connection with completing this licensing transaction, you agree that the following terms and conditions apply to this transaction (along with the Billing and Payment terms and conditions established by Copyright Clearance Center, Inc. ("CCC"), at the time that you opened your Rightslink account and that are available at any time at http://myaccount.copyright.com).

GENERAL TERMS

2. Elsevier hereby grants you permission to reproduce the aforementioned material subject to the terms and conditions indicated.

3. Acknowledgement: If any part of the material to be used (for example, figures) has appeared in our publication with credit or acknowledgement to another source, permission must also be sought from that source. If such permission is not obtained then that material may not be included in your publication/copies. Suitable acknowledgement to the source must be made, either as a footnote or in a reference list at the end of your publication, as follows:
"Reprinted from Publication title, Vol /edition number, Author(s), Title of article / title of chapter, Pages No., Copyright (Year), with permission from Elsevier [OR APPLICABLE SOCIETY COPYRIGHT OWNER]." Also Lancet special credit - "Reprinted from The Lancet, Vol. number, Author(s), Title of article, Pages No., Copyright (Year), with permission from Elsevier."

4. Reproduction of this material is confined to the purpose and/or media for which permission is hereby given.

5. Altering/Modifying Material: Not Permitted. However figures and illustrations may be altered/adapted minimally to serve your work. Any other abbreviations, additions, deletions

and/or any other alterations shall be made only with prior written authorization of Elsevier Ltd. (Please contact Elsevier at permissions@elsevier.com). No modifications can be made to any Lancet figures/tables and they must be reproduced in full.

6. If the permission fee for the requested use of our material is waived in this instance, please be advised that your future requests for Elsevier materials may attract a fee.

7. Reservation of Rights: Publisher reserves all rights not specifically granted in the combination of (i) the license details provided by you and accepted in the course of this licensing transaction, (ii) these terms and conditions and (iii) CCC's Billing and Payment terms and conditions.

8. License Contingent Upon Payment: While you may exercise the rights licensed immediately upon issuance of the license at the end of the licensing process for the transaction, provided that you have disclosed complete and accurate details of your proposed use, no license is finally effective unless and until full payment is received from you (either by publisher or by CCC) as provided in CCC's Billing and Payment terms and conditions. If full payment is not received on a timely basis, then any license preliminarily granted shall be deemed automatically revoked and shall be void as if never granted. Further, in the event that you breach any of these terms and conditions or any of CCC's Billing and Payment terms and conditions, the license is automatically revoked and shall be void as if never granted. Use of materials as described in a revoked license, as well as any use of the materials beyond the scope of an unrevoked license, may constitute copyright infringement and publisher reserves the right to take any and all action to protect its copyright in the materials.

9. Warranties: Publisher makes no representations or warranties with respect to the licensed material.

10. Indemnity: You hereby indemnify and agree to hold harmless publisher and CCC, and their respective officers, directors, employees and agents, from and against any and all claims arising out of your use of the licensed material other than as specifically authorized pursuant to this license.

11. No Transfer of License: This license is personal to you and may not be sublicensed, assigned, or transferred by you to any other person without publisher's written permission.

12. No Amendment Except in Writing: This license may not be amended except in a writing signed by both parties (or, in the case of publisher, by CCC on publisher's behalf).
13. Objection to Contrary Terms: Publisher hereby objects to any terms contained in any purchase order, acknowledgment, check endorsement or other writing prepared by you, which terms are inconsistent with these terms and conditions or CCC's Billing and Payment terms and conditions. These terms and conditions, together with CCC's Billing and Payment terms and conditions (which are incorporated herein), comprise the entire agreement between you and publisher (and CCC) concerning this licensing transaction. In the event of any conflict between your obligations established by these terms and conditions and those established by CCC's Billing and Payment terms and conditions, these terms and conditions shall control.
14. Revocation: Elsevier or Copyright Clearance Center may deny the permissions described in this License at their sole discretion, for any reason or no reason, with a full refund payable to you. Notice of such denial will be made using the contact information provided by you. Failure to receive such notice will not alter or invalidate the denial. In no event will Elsevier or Copyright Clearance Center be responsible or liable for any costs, expenses or damage incurred by you as a result of a denial of your permission request, other than a refund of the amount(s) paid by you to Elsevier and/or Copyright Clearance Center for denied permissions.

LIMITED LICENSE

The following terms and conditions apply only to specific license types:
15. **Translation**: This permission is granted for non-exclusive world **English** rights only unless your license was granted for translation rights. If you licensed translation rights you may only translate this content into the languages you requested. A professional translator must perform all translations and reproduce the content word for word preserving the integrity of the article.
16. **Posting licensed content on any Website**: The following terms and conditions apply as follows: Licensing material from an Elsevier journal: All content posted to the web site must maintain the copyright information line on the bottom of each image; A hyper-text must be included to the Homepage of the journal from which you are licensing at http://www.sciencedirect.com/science/journal/xxxxx or the Elsevier homepage for books at http://www.elsevier.com; Central Storage: This license does not include permission for a

scanned version of the material to be stored in a central repository such as that provided by Heron/XanEdu.

Licensing material from an Elsevier book: A hyper-text link must be included to the Elsevier homepage at http://www.elsevier.com . All content posted to the web site must maintain the copyright information line on the bottom of each image.

Posting licensed content on Electronic reserve: In addition to the above the following clauses are applicable: The web site must be password-protected and made available only to bona fide students registered on a relevant course. This permission is granted for 1 year only. You may obtain a new license for future website posting.

17. **For journal authors:** the following clauses are applicable in addition to the above:

Preprints:

A preprint is an author's own write-up of research results and analysis, it has not been peer-reviewed, nor has it had any other value added to it by a publisher (such as formatting, copyright, technical enhancement etc.).

Authors can share their preprints anywhere at any time. Preprints should not be added to or enhanced in any way in order to appear more like, or to substitute for, the final versions of articles however authors can update their preprints on arXiv or RePEc with their Accepted Author Manuscript (see below).

If accepted for publication, we encourage authors to link from the preprint to their formal publication via its DOI. Millions of researchers have access to the formal publications on ScienceDirect, and so links will help users to find, access, cite and use the best available version.

Please note that Cell Press, The Lancet and some society-owned have different preprint policies. Information on these policies is available on the journal homepage.

Accepted Author Manuscripts: An accepted author manuscript is the manuscript of an article that has been accepted for publication and which typically includes author-incorporated changes suggested during submission, peer review and editor-author communications.

Authors can share their accepted author manuscript:

- □ immediately

- via their non-commercial person homepage or blog
- by updating a preprint in arXiv or RePEc with the accepted manuscript
- via their research institute or institutional repository for internal institutional uses or as part of an invitation-only research collaboration work-group
- directly by providing copies to their students or to research collaborators for their personal use
- for private scholarly sharing as part of an invitation-only work group on commercial sites with which Elsevier has an agreement

- after the embargo period
  - via non-commercial hosting platforms such as their institutional repository
  - via commercial sites with which Elsevier has an agreement

In all cases accepted manuscripts should:

- link to the formal publication via its DOI
- bear a CC-BY-NC-ND license - this is easy to do
- if aggregated with other manuscripts, for example in a repository or other site, be shared in alignment with our hosting policy not be added to or enhanced in any way to appear more like, or to substitute for, the published journal article.

Published journal article (JPA): A published journal article (PJA) is the definitive final record of published research that appears or will appear in the journal and embodies all value-adding publishing activities including peer review co-ordination, copy-editing, formatting, (if relevant) pagination and online enrichment.

Policies for sharing publishing journal articles differ for subscription and gold open access articles:

Subscription Articles: If you are an author, please share a link to your article rather than the full-text. Millions of researchers have access to the formal publications on ScienceDirect, and so links will help your users to find, access, cite, and use the best available version.

Theses and dissertations which contain embedded PJAs as part of the formal submission can be posted publicly by the awarding institution with DOI links back to the formal publications on ScienceDirect.

If you are affiliated with a library that subscribes to ScienceDirect you have additional private sharing rights for others' research accessed under that agreement. This includes use for classroom teaching and internal training at the institution (including use in course packs and courseware programs), and inclusion of the article for grant funding purposes.

Gold Open Access Articles: May be shared according to the author-selected end-user license and should contain a CrossMark logo, the end user license, and a DOI link to the formal publication on ScienceDirect.

Please refer to Elsevier's posting policy for further information.

18. **For book authors** the following clauses are applicable in addition to the above: Authors are permitted to place a brief summary of their work online only. You are not allowed to download and post the published electronic version of your chapter, nor may you scan the printed edition to create an electronic version. **Posting to a repository:** Authors are permitted to post a summary of their chapter only in their institution's repository.

19. **Thesis/Dissertation**: If your license is for use in a thesis/dissertation your thesis may be submitted to your institution in either print or electronic form. Should your thesis be published commercially, please reapply for permission. These requirements include permission for the Library and Archives of Canada to supply single copies, on demand, of the complete thesis and include permission for Proquest/UMI to supply single copies, on demand, of the complete thesis. Should your thesis be published commercially, please reapply for permission. Theses and dissertations which contain embedded PJAs as part of the formal submission can be posted publicly by the awarding institution with DOI links back to the formal publications on ScienceDirect.

Elsevier Open Access Terms and Conditions

You can publish open access with Elsevier in hundreds of open access journals or in nearly 2000 established subscription journals that support open access publishing. Permitted third party re-use of these open access articles is defined by the author's choice of Creative Commons user license. See our open access license policy for more information.

Terms & Conditions applicable to all Open Access articles published with Elsevier:

of Open Access articles published with a CC BY NC SA or CC BY NC ND license requires permission from Elsevier and will be subject to a fee.

Commercial reuse includes:

- Associating advertising with the full text of the Article
- Charging fees for document delivery or access
- Article aggregation
- Systematic distribution via e-mail lists or share buttons

Posting or linking by commercial companies for use by customers of those companies.

20. **Other Conditions**:

v1.9

Questions? customercare@copyright.com or +1-855-239-3415 (toll free in the US) or +1-978-646-2777.

Dear Kalpana Rose,

Permission is hereby granted to reprint the following article in your Doctoral thesis for the University of Waterloo:

Rose K, Kulasekara SI, Hudson C. Intervisit Repeatability of Retinal Blood Oximetry and Total Retinal Blood Flow Under Varying Systemic Blood Gas Oxygen Saturations. Invest Ophthalmol Vis Sci. 2016;57:188-197.

(You don't really need ARVO's permission, though, because your article is open access, and you and the other authors own the copyright.)

Best regards,
Debbie Chin
ARVO Journals

-----Original Message-----
From: Marco Stoutamire
Sent: Tuesday, January 24, 2017 10:41 AM
To: Debbie Chin <dchin@arvo.org>
Subject: FW: Request to reprint
-----Original Message-----
From: k3rose@uwaterloo.ca [mailto:k3rose@uwaterloo.ca]
Sent: Tuesday, January 24, 2017 10:31 AM
To: IOVS Email Account <IOVS@arvo.org>
Subject: Request to reprint

HI,
I am the first author of the following paper titled...

"Intervisit Repeatability of Retinal Blood Oximetry and Total Retinal Blood Flow Under Varying Systemic Blood Gas Oxygen Saturations.
Kalpana Rose; Susith I. Kulasekara; Christopher Hudson Invest Ophthalmol Vis Sci 57 (1), 188-197."
I would like to reuse this paper as a part of my Doctoral thesis work.
Could you please grant me permission to do so.

Thank you,
Kalpana Rose

References

Chapter1 Reference List

1. Orgül S, Cioffi G. Embryology, anatomy, and histology of the optic nerve vasculature. *J Glaucoma*. 1996; 5(4):285-294.
2. Kur J, Newman EA, Chan-Ling T. Cellular and physiological mechanisms underlying blood flow regulation in the retina and choroid in health and disease. *Prog Retin Eye Res.* 2012; 31(5):377-406.
3. Cogan DG, Toussaint D, Kuwabara T. Retinal vascular patterns: IV. Diabetic retinopathy. *Arch Ophthalmol.* 1961; 66(3):366-378.
4. Hildebrand GD, Fielder AR. Anatomy and physiology of the retina. In: *Pediatric retina.* Springer; 2011:39-65.
5. Haefliger I O, Flammer J. Endothelium dependent vasoactive modulation in the ophthalmic circulation. *Prog Retin Eye Res.* 2001; 20(2):209-225.
6. Pournams CJ. Autoregulation of ocular blood flow. *Ocular blood flow: new insights into the pathogenesis of ocular diseases.* 1996:40.
7. Guyton AC, Carrier O, jr, Walker jr. Evidence for Tissue oxygen demand as the major factor causing autoregulation. *Circ Res.* 1964; 15: SUPPL: 60-69.
8. Schulte K, Wolf S, Arend O, Harris A, Henle C, Reim M. Retinal hemodynamics during increased intraocular pressure. *Ger J Ophthalmol*. 1996; 5(1):1-5.
9. Robinson F, Riva CE, Grunwald JE, Petrig BL, Sinclair SH. Retinal blood flow autoregulation in response to an acute increase in blood pressure. *Invest Ophthalmol Vis Sci*. 1986; 27(5):722-726.

10. Jeppesen P, Aalkjær C, Bek T. Myogenic response in isolated porcine retinal arterioles. *Curr Eye Res.* 2003; 27(4):217-222.
11. Pournaras CJ. Regulation of retinal blood flow in health and disease. *Prog Retin Eye Res.* 2008; 27(3):284-330.
12. Harris A, Ciulla TA, Chung HS, Martin B. Regulation of retinal and optic nerve blood flow. *Arch Ophthalmol.* 1998; 116(11):1491-1495.
13. Yu D, Su E, Cringle SJ, Paula KY. Isolated preparations of ocular vasculature and their applications in ophthalmic research. *Prog Retin Eye Res.* 2003; 22(2):135-169.
14. Meyer P, Flammer J, Lüscher T. Endothelium-dependent regulation of the ophthalmic microcirculation in the perfused porcine eye: role of nitric oxide and endothelins. *Invest Ophthalmol Vis Sci.* 1993; 34(13):3614-3621.
15. Gilmore ED, Hudson C, Nrusimhadevara RK, et al. Retinal arteriolar diameter, blood velocity, and blood flow response to an isocapnic hyperoxic provocation in early sight-threatening diabetic retinopathy. *Invest Ophthalmol Vis Sci.* 2007; 48(4):1744-1750.
16. Grunwald J, Riva C, Brucker A, Sinclair S, Petrig B. Altered retinal vascular response to 100% oxygen breathing in diabetes mellitus. *Ophthalmology.* 1984; 91(12):1447-1452.
17. Mishra A, Newman EA. Inhibition of inducible nitric oxide synthase reverses the loss of functional hyperemia in diabetic retinopathy. *Glia.* 2010; 58(16):1996-2004.
18. Mandecka A, Dawczynski J, Blum M, et al. Influence of flickering light on the retinal vessels in diabetic patients. *Diabetes Care.* 2007; 30(12):3048-3052.

19. Venkataraman ST, Hudson C, Rachmiel R, et al. Retinal arteriolar vascular reactivity in untreated and progressive primary open-angle glaucoma. *Invest Ophthalmol Vis Sci.* 2010; 51(4):2043-2050.
20. Harris A, Kagemann L, Ehrlich R, Rospigliosi C, Moore D, Siesky B. Measuring and interpreting ocular blood flow and metabolism in glaucoma. *Canadian Journal of Ophthalmology/Journal Canadien d'Ophtalmologie.* 2008; 43(3):328-336.
21. Kohner EM, Patel V, Rassam SM. Role of blood flow and impaired autoregulation in the pathogenesis of diabetic retinopathy. *Diabetes.* 1995; 44(6):603-607.
22. Grunwald J, Riva C, Stone R, Keates E, Petrig B. Retinal autoregulation in open-angle glaucoma. *Ophthalmology.* 1984; 91(12):1690-1694.
23. Krebs W, Krebs I. Primate retina and choroid: atlas of fine structure in man and monkey. *Springer Science & Business Media*; 2012.
24. Nickla DL, Wallman J. The multifunctional choroid. *Prog Retin Eye Res.* 2010; 29(2):144-168.
25. Gilmore ED, Hudson C, Venkataraman ST, Preiss D, Fisher J. Comparison of different hyperoxic paradigms to induce vasoconstriction: Implications for the investigation of retinal vascular reactivity. *Invest Ophthalmol Vis Sci.* 2004; 45(9):3207-3212.
26. Rose K, Kulasekara SI, Hudson C. Intervisit repeatability of retinal blood oximetry and total retinal blood flow under varying systemic blood gas oxygen saturations. *Invest Ophthalmol Vis Sci.* 2016; 57(1):188-97.
27. Garhöfer G, Resch H, Sacu S, et al. Effect of regular smoking on flicker induced retinal vasodilatation in healthy subjects. *Microvasc Res.* 2011; 82(3):351-355.

28. Tayyari F, Khuu LA, Flanagan JG, Singer S, Brent MH, Hudson C. Retinal blood flow and retinal blood oxygen saturation in mild to moderate diabetic retinopathy. *Invest Ophthalmol Vis Sci.* 2015; 56(11):6796-6800.
29. Hafez AS, Bizzarro RL, Lesk MR. Evaluation of optic nerve head and peripapillary retinal blood flow in glaucoma patients, ocular hypertensives, and normal subjects. *Am J Ophthalmol.* 2003; 136(6):1022-1031.
30. Friedman E. Update of the vascular model of AMD. *Br J Ophthalmol*. 2004; 88(2):161-163.
31. Friedman E. A hemodynamic model of the pathogenesis of age-related macular degeneration. *Am J Ophthalmol.* 1997; 124(5):677-682.
32. Rooke TW, Sparks H. An overview of circulation and hemodynamics. *Medical physiology*. Boston: Little, Brown and Company. 1995:230-241.
33. Feke GT, Tagawa H, Deupree DM, Goger DG, Sebag J, Weiter J. Blood flow in the normal human retina. *Invest Ophthalmol Vis Sci.* 1989; 30(1):58-65.
34. Gowers WR. The state of the arteries in Bright's disease. *Br Med J.* 1876; 2(832):743-745.
35. Haessler FH, Squier TL. Measurements of Retinal Vessels in Early Hypertension. *Trans Am Ophthalmol Soc.* 1931; 29:254-262.
36. Kristinsson JK, Gottfredsdottir MS, Stefansson E. Retinal vessel dilatation and elongation precedes diabetic macular edema. *Br J Ophthalmol.* 1997; 81(4):274-278.
37. Garhofer G, Bek T, Boehm AG, et al. Use of the retinal vessel analyzer in ocular blood flow research. *Acta Ophthalmol*. 2010; 88(7):717-722.

38. Briers JD. Laser Doppler, speckle and related techniques for blood perfusion mapping and imaging. *Physiol Meas.* 2001; 22(4):R35.

39. Feke GT, Goger DG, Tagawa H, Delori FC. Laser Doppler technique for absolute measurement of blood speed in retinal vessels. *Biomedical Engineering, IEEE Transactions on.* 1987(9):673-800.

40. Guan K1, Hudson C, Flanagan JG. Variability and repeatability of retinal blood flow measurements using the Canon Laser Blood Flowmeter. *Microvasc Res.* 2003 May; 65(3):145-151.

41. Bonner R, Nossal R. Model for laser Doppler measurements of blood flow in tissue. *Appl Opt.* 1981; 20(12):2097-2107.

42. Pechauer AD, Huang D, Jia Y. Detecting blood flow response to stimulation of the human eye. *Biomed Res Int.* 2015; 2015:121973. doi: 10.1155/2015/121973.

43. Kagemann L, Harris A, Chung HS, Evans D, Buck S, Martin B. Heidelberg retinal flowmetry: factors affecting blood flow measurement. *Br J Ophthalmol*. 1998; 82(2):131-136.

44. Holló G, Thomas JTP, van den Berg, Greve EL. Scanning laser Doppler flowmetry in glaucoma. *Int Ophthalmol*. 1996;20(1):63-70

45. Fujimoto JG. Optical coherence tomography for ultrahigh resolution in vivo imaging. *Nat Biotechnol*. 2003; 21(11):1361-1367.

46. Swanson EA, Izatt J, Lin C, et al. In vivo retinal imaging by optical coherence tomography. *Opt Lett*. 1993; 18(21):1864-1866.

47. Chen Z, Milner TE, Dave D, Nelson JS. Optical Doppler tomographic imaging of fluid flow velocity in highly scattering media. *Opt Lett.* 1997; 22(1):64-66.
48. Wang Y, Bower BA, Izatt JA, Tan O, Huang D. Retinal blood flow measurement by circumpapillary Fourier domain Doppler optical coherence tomography. *J Biomed Opt.* 2008; 13(6):064003-064003-9.
49. Liu G, Chen Z. Advances in Doppler OCT. *Chinese Optics Letters.* 2013; 11(1):011702.
50. Leitgeb R, Hitzenberger C, Fercher A. Performance of Fourier domain vs. time domain optical coherence tomography. *Optics Express.* 2003; 11(8):889-894.
51. Leitgeb R, Drexler W, Unterhuber A, et al. Ultrahigh resolution Fourier domain optical coherence tomography. *Optics Express.* 2004; 12(10):2156-2165.
52. Haindl R, Trasischker W, Wartak A, Baumann B, Pircher M, Hitzenberger CK. Total retinal blood flow measurement by three beam Doppler optical coherence tomography. *Biomed Opt Express.* 2016; 7(2):287-301.
53. Drexler W, Liu M, Kumar A, Kamali T, Unterhuber A, Leitgeb RA. Optical coherence tomography today: speed, contrast, and multimodality. *J Biomed Opt.* 2014; 19(7):071412-071412.
54. Drexler W, Fujimoto JG. State-of-the-art retinal optical coherence tomography. *Prog Retin Eye Res.* 2008; 27(1):45-88.
55. Riva C, Petrig B. Blue field entoptic phenomenon and blood velocity in the retinal capillaries. *J Opt Soc Am.* 1980; 70(10):1234-1238.
56. Hurley BR, Regillo CD. Fluorescein angiography: general principles and interpretation. In: *Retinal Angiography and Optical Coherence Tomography.* Springer; 2009:27-42.

57. Baxter GM, Williamson TH. Color Doppler imaging of the eye: normal ranges, reproducibility, and observer variation. *J Ultrasound Med.* 1995; 14(2):91-96.

58. Bill A, Sperber G, Ujiie K. Physiology of the choroidal vascular bed. *Int Ophthalmol.* 1983; 6(2):101-107.

59. Kiel J, Van Heuven W. Ocular perfusion pressure and choroidal blood flow in the rabbit. *Invest Ophthalmol Vis Sci*. 1995; 36(3):579-585.

60. Yu D, Alder VA, Cringle SJ, Brown MJ. Choroidal blood flow measured in the dog eye in vivo and in vitro by local hydrogen clearance polarography: validation of a technique and response to raised intraocular pressure. *Exp Eye Res.* 1988; 46(3):289-303.

61. Hitchings R. The ocular pulse. *Br J Ophthalmol.* 1991; 75(2):65.

62. Zion IB, Harris A, Siesky B, Shulman S, McCranor L, Garzozi HJ. Pulsatile ocular blood flow: relationship with flow velocities in vessels supplying the retina and choroid. *Br J Ophthalmol*. 2007; 91(7):882-884.

63. Riva CE, Cranstoun SD, Grunwald JE, Petrig BL. Choroidal blood flow in the foveal region of the human ocular fundus. *Invest Ophthalmol Vis Sci*. 1994; 35(13):4273-4281.

64. Slakter JS, Yannuzzi LA, Guyer DR, Sorenson JA, Orlock DA. Indocyanine-green angiography. *Curr Opin Ophthalmol*. 1995; 6(3):25-32.

65. Hirata Y, Nishiwaki H. The choroidal circulation assessed by laser-targeted angiography. *Prog Retin Eye Res*. 2006; 25(2):129-147.

66. Považay B, Hermann B, Unterhuber A, et al. Three-dimensional optical coherence tomography at 1050nm versus 800nm in retinal pathologies: enhanced performance and choroidal penetration in cataract patients. *J Biomed Opt*. 2007; 12(4):041211-041217.

67. Jia Y, Bailey ST, Hwang TS, et al. Quantitative optical coherence tomography angiography of vascular abnormalities in the living human eye. *Proc Natl Acad Sci U S A*. 2015; 112(18):E2395-E2402.

68. Spaide RF, Koizumi H, Pozonni MC. Enhanced depth imaging spectral-domain optical coherence tomography. *Am J Ophthalmol*. 2008; 146(4):496-500.

69. Jaillon F, Makita S, Min E, Lee BH, Yasuno Y. Enhanced imaging of choroidal vasculature by high-penetration and dual-velocity optical coherence angiography. *Biomed Opt Express.* 2011; 2(5):1147-1158.

70. Mordant D, Al-Abboud I, Muyo G, et al. Spectral imaging of the retina. *Eye.* 2011; 25(3):309-320.

71. Pedersen DB, Jensen PK, la Cour M, et al. Carbonic anhydrase inhibition increases retinal oxygen tension and dilates retinal vessels. *Graefes Arch Clin Exp Ophthalmol*. 2005; 243(2):163-168.

72. Shonat R, Wilson D, Riva C, Cranstoun S. Effect of acute increases in intraocular pressure on intravascular optic nerve head oxygen tension in cats. *Invest Ophthalmol Vis Sci.* 1992; 33(11):3174-3180.

73. Drabkin DL, Schmidt CF. Spectrophotometric studies XII. Observation of circulating blood in vivo, and the direct determination of the saturation of hemoglobin in arterial blood. *J Biol Chem.* 1945; 157(1):69-84.

74. Beach JM, Schwenzer KJ, Srinivas S, Kim D, Tiedeman JS. Oximetry of retinal vessels by dual-wavelength imaging: calibration and influence of pigmentation. *J Appl Physiol (1985)*. 1999; 86(2):748-758.

75. Hammer M, Vilser W, Riemer T, Schweitzer D. Retinal vessel oximetry-calibration, compensation for vessel diameter and fundus pigmentation, and reproducibility. J *Biomed Opt.* 2008; 13(5):054015.
76. Delori FC. Noninvasive technique for oximetry of blood in retinal vessels. *Appl Opt.* 1988; 27(6):1113-1125.
77. Smith MH, Denninghoff KR, Lompado A, Woodruff JB, Hillman LW. Minimizing the influence of fundus pigmentation on retinal vessel oximetry measurements. 2001: *SPIE* 4245, Ophthalmic Technologies XI, (2001); doi: 10.1117/12.429265135-145.
78. Hardarson SH, Harris A, Karlsson RA, et al. Automatic retinal oximetry. *Invest Ophthalmol Vis Sci.* 2006; 47(11):5011-5016.
79. Mordant DJ. Human retinal oximetry using spectral imaging. 2012. *Doctoral thesis,* UCL (University College London).
80. Schweitzer D, Hammer M, Kraft J, Thamm E, Konigsdorffer E, Strobel J. In vivo measurement of the oxygen saturation of retinal vessels in healthy volunteers. *IEEE transactions on biomedical engineering.* 1999; 46(12):1454-1465.
81. Patel SR, Flanagan JG, Shahidi AM, Sylvestre J, Hudson C. A prototype hyperspectral system with a tunable laser source for retinal vessel imaging. *Invest Ophthalmol Vis Sci.* 2013; 54(8):5163-5168.
82. Desjardins M, Sylvestre J, Jafari R, et al. Preliminary investigation of multispectral retinal tissue oximetry mapping using a hyperspectral retinal camera. *Exp Eye Res.* 2016; 146:330-340.

83. Drewes JJ. Four-wavelength retinal vessel oximetry. 1999. *Thesis (PhD).* University of Alabama in Huntsville.

84. Tsuchihashi T, Mori K, Peyman G, Shimada Y, Yoneya S. Photodynamic effects on retinal oxygen saturation, blood flow, and electrophysiological function in patients with neovascular age-related macular degeneration. *Retina.* 2009; 29(10):1450-1456.

85. Hickam JB, Sieker HO, Frayser R. Studies of retinal circulation and A-V oxygen difference in man. *Trans Am Clin Climatol Assoc*. 1959; 71:34-44.

86. Broadfoot KD, Gloster J, Greaves DP. Photoelectric Method of Investigating the Amount and Oxygenation of Blood in the Fundus Oculi. *Br J Ophthalmol.* 1961; 45(3):161-182.

87. Kristjansdottir JV, Hardarson SH, Harvey AR, Olafsdottir OB, Eliasdottir TS, Stefánsson E. Choroidal oximetry with a noninvasive spectrophotometric oximeter. *Invest Ophthalmol Vis Sci.* 2013; 54(5):3234-3239.

88. Hammer M, Vilser W, Riemer T, et al. Diabetic patients with retinopathy show increased retinal venous oxygen saturation. *Graefe's Archive for Clinical and Experimental Ophthalmology.* 2009; 247(8):1025-1030.

89. Hardarson SH, Stefansson E. Retinal oxygen saturation is altered in diabetic retinopathy. *Br J Ophthalmol*. 2012; 96(4):560-563.

90. Olafsdottir OB, Vandewalle E, Abegao Pinto L, et al. Retinal oxygen metabolism in healthy subjects and glaucoma patients. *Br J Ophthalmol*. 2014; 98(3):329-333.

91. Ito M, Murayama K, Deguchi T, et al. Oxygen saturation levels in the juxta-papillary retina in eyes with glaucoma. *Exp Eye Res*. 2008; 86(3):512-518.

92. Williamson TH, Grewal J, Gupta B, Mokete B, Lim M, Fry CH. Measurement of PO_2 during vitrectomy for central retinal vein occlusion, a pilot study. *Graefe's Archive for Clinical and Experimental Ophthalmology*. 2009; 247(8):1019-1023.
93. Yoneya S, Saito T, Nishiyama Y, et al. Retinal oxygen saturation levels in patients with central retinal vein occlusion. *Ophthalmology*. 2002; 109(8):1521-1526.
94. Yu D, Cringle SJ. Oxygen distribution and consumption within the retina in vascularized and avascular retinas and in animal models of retinal disease. *Prog Retin Eye Res.* 2001; 20(2):175-208.
95. Kaur C, Foulds WS, Ling EA. Hypoxia-ischemia and retinal ganglion cell damage. *Clin Ophthalmol*. 2008; 2(4):879-889.
96. Galvin O, Gardiner T, McDonald D, McDonald. Mechanisms of Hyperoxia-induced Retinal Endothelial Cell Death and Senescence. *Invest Ophthalmol Vis Sci.* June 2013; 54, 5573.
97. Yu DY, Cringle SJ, Alder VA, Su EN. Intraretinal oxygen distribution in rats as a function of systemic blood pressure. *Am J Physiol*. 1994; 267(6 Pt 2):H2498-H2507.
98. Yu D, Cringle SJ, Paula KY, Su E. Intraretinal oxygen distribution and consumption during retinal artery occlusion and graded hyperoxic ventilation in the rat. *Invest Ophthalmol Vis Sci*. 2007; 48(5):2290-2296.
99. Werkmeister RM, Schmidl D, Aschinger G, et al. Retinal oxygen extraction in humans. *Sci Rep*. 2015; 5:15763.

100. Palkovits S, Told R, Schmidl D, et al. Regulation of retinal oxygen metabolism in humans during graded hypoxia. *Am J Physiol Heart Circ Physiol*. 2014; 307(10):H1412-H1418.

101. Teng P, Wanek J, Blair NP, Shahidi M. Inner retinal oxygen extraction fraction in Rat. *Invest Ophthalmol Vis Sci*. 2013; 54(1):647-651.

102. Palkovits S, Lasta M, Told R, et al. Retinal oxygen metabolism during normoxia and hyperoxia in healthy subjects. *Invest Ophthalmol Vis Sci*. 2014; 55(8):4707-4713.

103. Nguyen TT, Wang JJ, Islam FM, et al. Retinal arteriolar narrowing predicts incidence of diabetes: the Australian Diabetes, Obesity and Lifestyle (AusDiab) Study. *Diabetes.* 2008; 57(3):536-539.

104. Cheung N, Rogers SL, Donaghue KC, Jenkins AJ, Tikellis G, Wong TY. Retinal arteriolar dilation predicts retinopathy in adolescents with type 1 diabetes. *Diabetes Care.* 2008; 31(9):1842-1846.

105. Wong TY, Islam FA, Klein R, et al. Retinal vascular caliber, cardiovascular risk factors, and inflammation: the multi-ethnic study of atherosclerosis (MESA). *Invest Ophthalmol Vis Sci*. 2006; 47(6):2341-2350.

106. Wang Y, Fawzi A, Tan O, Gil-Flamer J, Huang D. Retinal blood flow detection in diabetic patients by Doppler Fourier domain optical coherence tomography. *Optics express*. 2009; 17(5):4061-4073.

107. Shahidi AM, Hudson C, Tayyari F, Flanagan JG. Retinal oxygen saturation in patients with primary open-angle glaucoma using a non-flash hyperspectral camera. *Curr Eye Res*. 2016:1-5.

108. Michelson G, Scibor M. Intravascular oxygen saturation in retinal vessels in normal subjects and open-angle glaucoma subjects. *Acta Ophthalmol Scand.* 2006; 84(3):289-295.

109. Hwang JC, Konduru R, Zhang X, et al. Relationship among visual field, blood flow, and neural structure measurements in Glaucoma. *Invest Ophthalmol Vis Sci*. 2012; 53(6):3020-3026.

110. Hu D, Yu G, McCormick SA, Schneider S, Finger PT. Population-based incidence of uveal melanoma in various races and ethnic groups. *Am J Ophthalmol*. 2005; 140(4):612-617.

111. Margo CE. The collaborative ocular melanoma study: an overview. *Cancer Control*. 2004; 11(5):304-309.

112. Garcia-Valenzuela, Enrique. "Choroidal Melanoma": Practice Essentials, Overview, Pathophysiology. *Medscape,* 17 June 2016. Web. 05 Oct. 2016.

113. Koutsandrea C, Moschos MM, Dimissianos M, Georgopoulos G, Ladas I, Apostolopoulos M. Metastasis rates and sites after treatment for choroidal melanoma by proton beam irradiation or by enucleation. *Clin Ophthalmol.* 2008; 2(4):989-995.

114. Finger PT. Radiation therapy for choroidal melanoma. *Surv Ophthalmol.* 1997; 42(3):215-232.

115. Krema H, Heydarian M, Beiki-Ardakani A, et al. A comparison between ^{125}Iodine brachytherapy and stereotactic radiotherapy in the management of juxtapapillary choroidal melanoma. *Br J Ophthalmol*. 2013; 97(3):327-332.

116. Verschueren KM, Creutzberg CL, Schalij-Delfos NE, et al. Long-term outcomes of eye-conserving treatment with Ruthenium 106 brachytherapy for choroidal melanoma. *Radiotherapy and Oncology*. 2010; 95(3):332-338.
117. Fernandes BF, Weisbrod D, Yücel YH, et al. Neovascular glaucoma after stereotactic radiotherapy for juxtapapillary choroidal melanoma: histopathologic and dosimetric findings. *International Journal of Radiation Oncology* Biology* Physics.* 2011; 80(2):377-384.
118. Gündüz K, Shields CL, Shields JA, Cater J, Freire JE, Brady LW. Radiation retinopathy following plaque radiotherapy for posterior uveal melanoma. *Arch Ophthalmol*. 1999; 117(5):609-614.
119. Krema H, Xu W, Payne D, Vasquez LM, Pavlin CJ, Simpson R. Factors predictive of radiation retinopathy post 125 Iodine brachytherapy for uveal melanoma. *Canadian Journal of Ophthalmology/Journal Canadien d'Ophtalmologie.* 2011; 46(2):158-163.
120. Zamber RW, Kinyoun JL. Radiation retinopathy. *West J Med*. 1992; 157(5):530-533.
121. Irvine AR, Alvarado JA, Wara WM, Morris BW, Wood IS. Radiation retinopathy: an experimental model for the ischemic--proliferative retinopathies. *Trans Am Ophthalmol Soc*. 1981; 79:103-122.
122. Archer D, Amoaku W, Gardiner T. Radiation retinopathy—clinical, histopathological, ultrastructural and experimental correlations. *Eye*. 1991; 5(Pt 2):239-251.
123. Archer DB. Responses of retinal and choroidal vessels to ionizing radiation. *Eye*. 1993; 7(1):1-13.

124. Brown GC, Shields JA, Sanborn G, Augsburger JJ, Savino PJ, Schatz NJ. Radiation retinopathy. *Ophthalmology*. 1982; 89(12):1494-1501.

125. Neal H. Atebara, John H. Drouilhet and Gary C. Brown. Chapter 36A: Radiation Retinopathy. *Duane's ophthalmology on CD-ROM*. Lippincott Williams & Wilkins. 2006.

126. Boldt HC, Melia BM, Liu JC, Reynolds SM, Collaborative Ocular Melanoma Study Group. I-125 brachytherapy for choroidal melanoma: photographic and angiographic abnormalities: *the Collaborative Ocular Melanoma Study*: COMS Report No. 30. Ophthalmology. 2009; 116(1):106-115.

127. Groenewald, C; Konstantinidis, L; Damato, B. Effects of radiotherapy on uveal melanomas and adjacent tissues. *Eye (Lond)*. 2013 Feb; 27(2):163-71.

128. Giuliari GP, Sadaka A, Hinkle DM, Simpson ER. Current treatments for radiation retinopathy. *Acta Oncol*. 2011; 50(1):6-13.

129. Werkmeister RM, Dragostinoff N, Pircher M, Götzinger E, Hitzenberger CK, Leitgeb RA, Schmetterer L. Bidirectional Doppler Fourier-domain optical coherence tomography for measurement of absolute flow velocities in human retinal vessels. *Opt Lett.* 2008 Dec 15; 33(24):2967-9.

130. Polak K, Polska E, Luksch A, Dorner G, Fuchsjäger-Mayrl G, Findl O, Eichler HG, Wolzt M, Schmetterer L. Choroidal blood flow and arterial blood pressure. *Eye (Lond)*. 2003 Jan; 17(1):84-8.

131. Schindelin J, Arganda-Carreras I, Frise E, et al. Fiji: an open-source platform for biological-image analysis. *Nature methods*. 2012; 9(7):676-682.

132. Sponsel WE, DePaul KL, Zetlan S. Retinal hemodynamic effects of carbon dioxide, hyperoxia, and mild hypoxia. *Invest Ophthalmol Vis Sci*. 1992; 33(6):1864-1869.

133. Gilmore ED, Hudson C, Venkataraman ST, Preiss D, Fisher J. Comparison of different hyperoxic paradigms to induce vasoconstriction: implications for the investigation of retinal vascular reactivity. *Invest Ophthalmol Vis Sci*. 2004; 45(9):3207-3212.

134. Roff EJ, Harris A, Chung HS, et al. Comprehensive assessment of retinal, choroidal and retrobulbar hemodynamics during blood gas perturbation. *Graefe's archive for clinical and experimental ophthalmology.* 1999; 237(12):984-990.

135. Luksch A, Garhofer G, Imhof A, et al. Effect of inhalation of different mixtures of O(2) and CO(2) on retinal blood flow. *Br J Ophthalmol*. 2002; 86(10):1143-1147.

136. Becker HF, Polo O, McNamara SG, Berthon-Jones M, Sullivan CE. Effect of different levels of hyperoxia on breathing in healthy subjects. *J Appl Physiol (1985)*. 1996; 81(4):1683-1690.

137. Slessarev M, Han J, Mardimae A, et al. Prospective targeting and control of end-tidal CO2 and O2 concentrations. *J Physiol (Lond)*. 2007; 581(3):1207-1219.

138. Slessarev M, Somogyi R, Preiss D, Vesely A, Sasano H, Fisher JA. Efficiency of oxygen administration: sequential gas delivery versus "flow into a cone" methods. *Crit Care Med.* 2006; 34(3):829-834.

Chapter 2 Reference List

1. Cringle SJ, Yu D, Yu PK, Su E. Intraretinal oxygen consumption in the rat in vivo. *Invest Ophthalmol Visual Sci*. 2002; 43(6):1922-1927.
2. Alder VA, Ben-Nun J, Cringle SJ. PO2 profiles and oxygen consumption in cat retina with an occluded retinal circulation. *Invest Ophthalmol Vis Sci.* 1990; 31(6):1029-1034.
3. Yu D, Cringle SJ. Oxygen distribution and consumption within the retina in vascularized and avascular retinas and in animal models of retinal disease. *Prog Retin Eye Res*. 2001; 20(2):175-208.
4. Patel SR, Flanagan JG, Shahidi AM, Sylvestre J, Hudson C. A prototype hyperspectral system with a tunable laser source for retinal vessel imaging. *Invest Ophthalmol Vis Sci.* 2013; 54(8):5163-5168.
5. Desjardins M, Sylvestre J, Jafari R, et al. Preliminary investigation of multispectral retinal tissue oximetry mapping using a hyperspectral retinal camera. *Exp Eye Res.* 2016; 146:330-340.
6. Feke GT, Tagawa H, Deupree DM, Goger DG, Sebag J, Weiter J. Blood flow in the normal human retina. *Invest Ophthalmol Vis Sci*. 1989; 30(1):58-65.
7. Feke GT, Goger DG, Tagawa H, Delori FC. Laser Doppler technique for absolute measurement of blood speed in retinal vessels. *Biomedical Engineering, IEEE Transactions on.* 1987(9):673-800.
8. Wang Y, Bower BA, Izatt JA, Tan O, Huang D. Retinal blood flow measurement by circumpapillary Fourier domain Doppler optical coherence tomography. *J Biomed Opt.* 2008; 13(6):064003-064003-9.
9. Liu G, Chen Z. Advances in Doppler OCT. *Chinese Optics Letters.* 2013; 11(1):011702.

10. Kagemann L, Harris A, Chung HS, Evans D, Buck S, Martin B. Heidelberg retinal flowmetry: factors affecting blood flow measurement. *Br J Ophthalmol.* 1998; 82(2):131-136.
11. Holló G, Thomas JTP, Van den Berg, Greve EL. Scanning laser Doppler flowmetry in glaucoma. *Int Ophthalmol.* 1996;20(1):63-70
12. Briers JD. Laser Doppler, speckle and related techniques for blood perfusion mapping and imaging. *Physiol Meas*. 2001; 22(4):R35.
13. Archer D, Amoaku W, Gardiner T. Radiation retinopathy—clinical, histopathological, ultrastructural and experimental correlations. *Eye.* 1991; 5(Pt 2):239-251.
14. Irvine AR, Alvarado JA, Wara WM, Morris BW, Wood IS. Radiation retinopathy: an experimental model for the ischemic--proliferative retinopathies. *Trans Am Ophthalmol Soc*. 1981; 79:103-122.
15. Brown GC, Shields JA, Sanborn G, Augsburger JJ, Savino PJ, Schatz NJ. Radiation retinopathy. *Ophthalmology.* 1982; 89(12):1494-1501.
16. Neal H. Atebara, John H. Drouilhet and Gary C. Brown. Chapter 36A: Radiation Retinopathy. *Duane's ophthalmology on CD-ROM.* Lippincott Williams & Wilkins. 2006.
17. Gilmore ED, Hudson C, Nrusimhadevara RK, et al. Retinal arteriolar diameter, blood velocity, and blood flow response to an isocapnic hyperoxic provocation in early sight-threatening diabetic retinopathy. *Invest Ophthalmol Vis Sci*. 2007; 48(4):1744-1750.
18. Grunwald J, Riva C, Brucker A, Sinclair S, Petrig B. Altered retinal vascular response to 100% oxygen breathing in diabetes mellitus. *Ophthalmology*. 1984; 91(12):1447-1452.

19. Tayyari F, Khuu LA, Flanagan JG, Singer S, Brent MH, Hudson C. Retinal blood flow and retinal blood oxygen saturation in mild to moderate diabetic retinopathy. *Invest Ophthalmol Vis Sci.* 2015; 56(11):6796-6800.
20. Patz A. Retinal neovascularization: early contributions of Professor Michaelson and recent observations. *Br J Opthahlmol.* 1984 Jan; 68(1): 42-46.
21. Heitmar R, Cubbidge RP. The impact of flash intensity on retinal vessel oxygen saturation measurements using dual wavelength oximetry. *Invest Ophthalmol Vis Sci.* 2013; 54: 2807-2811.
22. Slessarev M, Han J, Mardimae A, et al. Prospective targeting and control of end-tidal CO_2 and O_2 concentrations. *J Physiol (Lond).* 2007; 581(3):1207-1219.
23. Slessarev M, Somogyi R, Preiss D, Vesely A, Sasano H, Fisher JA. Efficiency of oxygen administration: sequential gas delivery versus "flow into a cone" methods. *Crit Care Med.* 2006; 34(3):829-834.

Chapter 3 Reference List

1. Riva CE, Alm A, Pournaras CJ. Ocular circulation. In: Alm A, Kaufman PL, et.al. *Adler's Physiology of the Eye*. 11th ed. St. Louis: Mosby; 2011:243-246.

2. Robinson F, Riva CE, Grunwald JE, Petrig BL, Sinclair SH. Retinal blood flow autoregulation in response to an acute increase in blood pressure. *Invest Ophthalmol Vis Sci*. 1986; 27(5):722-726.

3. Schulte K, Wolf S, Arend O, Harris A, Henle C, Reim M. Retinal hemodynamics during increased intraocular pressure. *Ger J Ophthalmol*. 1996; 5(1):1-5.

4. Grunwald JE, Sinclair SH, Riva CE. Autoregulation of the retinal circulation in response to decrease of intraocular pressure below normal. *Invest Ophthalmol Vis Sci*. 1982; 23(1):124-127.

5. Johnson PC. Brief Review: Autoregulation of blood flow. *Circ Res*. 1986; 59:483-495.

6. Lester M, Torre PG, Bricola G, Bagnis A, Calabria G. Retinal blood flow autoregulation after dynamic exercise in healthy young subjects. *Ophthalmologica*. 2007; 221(3):180-185.

7. Guyton AC, Carrier O,Jr, Walker JR. Evidence for Tissue Oxygen Demand as the Major Factor Causing Autoregulation. *Circ Res*. 1964; 15: SUPPL: 60-9.

8. Sponsel WE, DePaul KL, Zetlan S. Retinal hemodynamic effects of carbon dioxide, hyperoxia, and mild hypoxia. *Invest Ophthalmol Vis Sci*. 1992; 33(6):1864-1869.

9. Harino S, Grunwald JE, Petrig BJ, Riva CE. Rebreathing into a bag increases human retinal macular blood velocity. *Br J Ophthalmol*. 1995; 79(4):380-383.

10. Roff EJ, Harris A, Chung HS, et al. Comprehensive assessment of retinal, choroidal and retrobulbar haemodynamics during blood gas perturbation. *Graefe's archive for clinical and experimental ophthalmology*. 1999; 237(12):984-990.

11. Dorner GT, Garhofer G, Kiss B, et al. Nitric oxide regulates retinal vascular tone in humans. *Am J Physiol Heart Circ Physiol*. 2003; 285(2):H631-6.

12. Gilmore ED, Hudson C, Preiss D, Fisher J. Retinal arteriolar diameter, blood velocity, and blood flow response to an isocapnic hyperoxic provocation. *Am J Physiol Heart Circ Physiol*. 2005; 288(6):H2912-7.

13. Gilmore ED, Hudson C, Venkataraman ST, Preiss D, Fisher J. Comparison of different hyperoxic paradigms to induce vasoconstriction: implications for the investigation of retinal vascular reactivity. *Invest Ophthalmol Vis Sci*. 2004; 45(9):3207-3212.

14. Venkataraman ST, Hudson C, Fisher JA, Rodrigues L, Mardimae A, Flanagan JG. Retinal arteriolar and capillary vascular reactivity in response to isoxic hypercapnia. *Exp Eye Res*. 2008; 87(6):535-542.

15. Kisilevsky M, Mardimae A, Slessarev M, Han J, Fisher J, Hudson C. Retinal arteriolar and middle cerebral artery responses to combined hypercarbic/hyperoxic stimuli. *Invest Ophthalmol Vis Sci*. 2008; 49:5503-5509.

16. Luksch A, Garhofer G, Imhof A, et al. Effect of inhalation of different mixtures of O(2) and CO(2) on retinal blood flow. *Br J Ophthalmol*. 2002; 86(10):1143-1147.

17. Garhöfer G, Resch H, Sacu S, et al. Effect of regular smoking on flicker induced retinal vasodilatation in healthy subjects. *Microvasc Res*. 2011; 82(3):351-355.

18. Garhofer G, Zawinka C, Resch H, Kothy P, Schmetterer L, Dorner GT. Reduced response of retinal vessel diameters to flicker stimulation in patients with diabetes. *Br J Ophthalmol*. 2004; 88(7):887-891.

19. Gilmore ED, Hudson C, Nrusimhadevara RK, et al. Retinal arteriolar diameter, blood velocity, and blood flow response to an isocapnic hyperoxic provocation in early sight-threatening diabetic retinopathy. *Invest Ophthalmol Vis Sci.* 2007; 48(4):1744-1750.

20. Venkataraman ST, Flanagan JG, Hudson C. Vascular reactivity of optic nerve head and retinal blood vessels in glaucoma—a review. *Microcirculation*. 2010; 17(7):568-581.

21. Palkovits S, Told R, Schmidl D, et al. Regulation of retinal oxygen metabolism in humans during graded hypoxia. *Am J Physiol Heart Circ Physiol*. 2014; 307(10):H1412-8.

22. Wanek J, Teng PY, Blair NP, Shahidi M. Inner retinal oxygen delivery and metabolism under normoxia and hypoxia in rat. *Invest Ophthalmol Vis Sci*. 2013; 54(7):5012-5019.

23. Kur J, Newman EA, Chan-Ling T. Cellular and physiological mechanisms underlying blood flow regulation in the retina and choroid in health and disease. *Prog Retin Eye Res*. 2012; 31(5):377-406.

24. Harris A, Ciulla TA, Chung HS, Martin B. Regulation of retinal and optic nerve blood flow. *Arch Ophthalmol*. 1998; 116(11):1491-1495.

25. Venkataraman ST, Hudson C, Rachmiel R, et al. Retinal arteriolar vascular reactivity in untreated and progressive primary open-angle glaucoma. *Invest Ophthalmol Vis Sci*. 2010; 51(4):2043-2050.

26. Rose K, Flanagan JG, Patel SR, Cheng R, Hudson C. Retinal blood flow and vascular reactivity in chronic smokers. *Invest Ophthalmol Vis Sci*. 2014; 55(7):4266-4276.

27. Wimpissinger B, Resch H, Berisha F, Weigert G, Schmetterer L, Polak K. Response of retinal blood flow to systemic hyperoxia in smokers and nonsmokers. *Graefes Arch Clin Exp Ophthalmol*. 2005; 243(7):646-652.

28. Riva C, Ross B, Benedek GB. Laser Doppler measurements of blood flow in capillary tubes and retinal arteries. *Invest Ophthalmol*. 1972; 11(11):936-944.

29. Feke GT, Goger DG, Tagawa H, Delori FC. Laser Doppler technique for absolute measurement of blood speed in retinal vessels. *Biomedical Engineering, IEEE Transactions on*. 1987(9):673-800.

30. Guan K, Hudson C, Flanagan JG. Variability and repeatability of retinal blood flow measurements using the Canon Laser Blood Flowmeter. *Microvasc Res*. 2003; 65(3):145-151.

31. Feke GT. Laser Doppler instrumentation for the measurement of retinal blood flow: theory and practice. *Bull Soc Belge Ophtalmol*. 2006; 302:171-184.

32. Wang Y, Bower BA, Izatt JA, Tan O, Huang D. In vivo total retinal blood flow measurement by Fourier domain Doppler optical coherence tomography. *J Biomed Opt*. 2007; 12(4):041215-041215-8.

33. Wang Y, Fawzi A, Tan O, Gil-Flamer J, Huang D. Retinal blood flow detection in diabetic patients by Doppler Fourier domain optical coherence tomography. *Optics express*. 2009; 17(5):4061-4073.

34. Garhofer G, Werkmeister R, Dragostinoff N, Schmetterer L. Retinal blood flow in healthy young subjects. *Invest Ophthalmol Vis Sci*. 2012; 53(2):698-703.

35. Olafsdottir OB, Hardarson SH, Gottfredsdottir MS, Harris A, Stefánsson E. Retinal oximetry in primary open-angle glaucoma. *Invest Ophthalmol Vis Sci*. 2011; 52(9):6409-6413.

36. Hammer M, Vilser W, Riemer T, et al. Diabetic patients with retinopathy show increased retinal venous oxygen saturation. *Graefes Arch Clin Exp Ophthalmol*. 2009; 247(8):1025-1030.

37. Geirsdottir A, Hardarson SH, Olafsdottir OB, Stefánsson E. Retinal oxygen metabolism in exudative age-related macular degeneration. *Acta Ophthalmol*. 2014; 92(1):27-33.

38. Fong AY, Wachman E. Hyperspectral imaging for the life sciences. *Biophoton Int*. 2008; 15(3):38.

39. Slessarev M, Han J, Mardimae A, et al. Prospective targeting and control of end-tidal CO2 and O2 concentrations. *J Physiol (Lond)*. 2007; 581(3):1207-1219.

40. Slessarev M, Somogyi R, Preiss D, Vesely A, Sasano H, Fisher JA. Efficiency of oxygen administration: sequential gas delivery versus "flow into a cone" methods. *Crit Care Med*. 2006; 34(3):829-834.

41. Tan O, Wang Y, Konduru RK, Zhang X, Sadda S, Huang D. Doppler optical coherence tomography of retinal circulation. *Journal of visualized experiments: JoVE*. 2011(67):e3524-e3524.

42. Konduru RK, Tan O, Nittala MG, Huang D, Sadda SR. Reproducibility of retinal blood flow measurements derived from semi-automated Doppler OCT analysis. . *Ophthalmic Surg Lasers Imaging*. 2012; 43(1):25-31.

43. Rose K, Jong M, Yusof F, et al. Grader learning effect and reproducibility of Doppler Spectral-Domain Optical Coherence Tomography derived retinal blood flow measurements. *Acta Ophthalmol*. 2014; 92(8):e630-e636.

44. Tayyari F, Yusof F, Vymyslicky M, et al. Variability and Repeatability of Quantitative, Fourier-Domain Optical Coherence Tomography Doppler Blood Flow in Young and Elderly Healthy Subjects Doppler FD-OCT Repeatability in Healthy Subjects. *Invest Ophthalmol Vis Sci*. 2014; 55(12):7716-7725.

45. Patel SR, Flanagan JG, Shahidi AM, Sylvestre J, Hudson C. A Prototype Hyperspectral System with a Tunable Laser Source for Retinal Vessel Imaging A Prototype Hyperspectral System. *Invest Ophthalmol Vis Sci*. 2013; 54(8):5163-5168.

46. Schindelin J, Arganda-Carreras I, Frise E, et al. Fiji: an open-source platform for biological-image analysis. *Nature methods*. 2012; 9(7):676-682.

47. Yoshida A, Feke GT, Mori F, et al. Reproducibility and clinical application of a newly developed stabilized retinal laser Doppler instrument. *Am J Ophthalmol*. 2003; 135(3):356-361.

48. Harris A, Jonescu-Cuypers C, Kagemann L, Ciulla T, Krieglstein G. Vascular anatomy, pathophysiology, and metabolism. *Atlas of Ocular Blood Flow*. 2003(Philadelphia: Butterworth Heinemann).

49. Lieb WE, Cohen SM, Merton DA, Shields JA, Mitchell DG, Goldberg BB. Color Doppler imaging of the eye and orbit: technique and normal vascular anatomy. *Arch Ophthalmol*. 1991; 109(4):527-531.

50. Cringle SJ, Yu D, Yu PK, Su E. Intraretinal oxygen consumption in the rat in vivo. *Invest Ophthalmol Visual Sci*. 2002; 43(6):1922-1927.

51. Eliasdottir TS, Geirsdottir A, Palsson O, et al. Retinal Vessel Oxygen Saturation In Healthy Individuals. *Invest Ophthalmol Vis Sci*. 2012; 53(14):2172-2172.

52. Beach JM, Schwenzer KJ, Srinivas S, Kim D, Tiedeman JS. Oximetry of retinal vessels by dual-wavelength imaging: calibration and influence of pigmentation. *J Appl Physiol (1985)*. 1999; 86(2):748-758.

53. Mordant D, Al-Abboud I, Muyo G, et al. Spectral imaging of the retina. *Eye*. 2011; 25(3):309-320.

54. Hardarson SH, Harris A, Karlsson RA, et al. Automatic retinal oximetry. *Invest Ophthalmol Visual Sci*. 2006; 47(11):5011.

55. Heitmar R, Cubbidge RP. The impact of flash intensity on retinal vessel oxygen saturation measurements using dual wavelength oximetry. *Invest Ophthalmol Vis Sci*. 2013; 54: 2807-2811.

56. Hammer M, Vilser W, Riemer T, Schweitzer D. Retinal vessel oximetry-calibration, compensation for vessel diameter and fundus pigmentation, and reproducibility. *J Biomed Opt*. 2008; 13(5):054015-054015-7.

57. Hardarson SH, Harris A, Karlsson RA, et al. Automatic retinal oximetry. *Invest Ophthalmol Visual Sci*. 2006; 47(11):5011.

58. Becker HF, Polo O, McNamara SG, Berthon-Jones M, Sullivan CE. Effect of different levels of hyperoxia on breathing in healthy subjects. *J Appl Physiol (1985)*. 1996; 81(4):1683-1690.

59. Dallinger S, Dorner GT, Wenzel R, et al. Endothelin-1 contributes to hyperoxia-induced vasoconstriction in the human retina. *Invest Ophthalmol Vis Sci*. 2000; 41(3):864-869.

60. ZHU Y, Park T, GIDDAY JM. Mechanisms of hyperoxia-induced reductions in retinal blood flow in newborn pig. *Exp Eye Res*. 1998; 67(3):357-369.

61. Ishizaki E, Fukumoto M, Puro DG. Functional KATP channels in the rat retinal microvasculature: topographical distribution, redox regulation, spermine modulation and diabetic alteration. *J Physiol (Lond)*. 2009; 587(10):2233-2253.

62. Yamanishi S, Katsumura K, Kobayashi T, Puro DG. Extracellular lactate as a dynamic vasoactive signal in the rat retinal microvasculature. *Am J Physiol Heart Circ Physiol*. 2006; 290(3):H925-34.

63. Delaey C, Boussery K, Van de Voorde J. A retinal-derived relaxing factor mediates the hypoxic vasodilation of retinal arteries. *Invest Ophthalmol Vis Sci*. 2000; 41(11):3555-3560.

64. Delaey C. Retinal tissue modulates retinal arterial tone through the release of a potent vasodilating factor. *Verh K Acad Geneeskd Belg*. 2001; 63(4):335-357.

65. Brown MM, Wade JP, Marshall J. Fundamental importance of arterial oxygen content in the regulation of cerebral blood flow in man. *Brain*. 1985; 108 (Pt 1):81-93.

66. Stoyka W, Frankel D, Kay J. The linear relation of cerebral blood flow to arterial oxygen saturation in hypoxic hypoxia induced with nitrous oxide or nitrogen. *Canadian Anaesthetists' Society Journal*. 1978; 25(6):474-478.

67. Wangsa-Wirawan ND, Linsenmeier RA. Retinal oxygen: fundamental and clinical aspects. *Arch Ophthalmol*. 2003; 121(4):547-57.

68. Wolbarsht ML, Stefansson E, Landers 3rd. MB. Retinal oxygenation from the choroid in hyperoxia. *Exp Biol*. 1987; 47(1):49-52.

69. Palkovits S, Lasta M, Told R, et al. Retinal oxygen metabolism during normoxia and hyperoxia in healthy subjects. *Invest Ophthalmol Vis Sci*. 2014; 55(8):4707-4713.

70. Palkovits S, Told R, Boltz A, et al. Effect of increased oxygen tension on flicker-induced vasodilatation in the human retina. *Journal of Cerebral Blood Flow & Metabolism*. 2014; 34(12):1914-1918.

71. Mishra A, Hamid A, Newman EA. Oxygen modulation of neurovascular coupling in the retina. *Proc Natl Acad Sci U S A*. 2011; 108(43):17827-17831.

72. Shahidi AM, Patel SR, Flanagan JG, Hudson C. Regional variation in human retinal vessel oxygen saturation. *Exp Eye Res.* 2013; 113:143-147.

Chapter 4 Reference List

1. Cringle SJ, Yu D, Yu PK, Su E. Intraretinal oxygen consumption in the rat in vivo. *Invest Ophthalmol Visual Sci*. 2002; 43(6):1922-1927.
2. Bill A. Blood circulation and fluid dynamics in the eye. *Physiol Rev*. 1975; 55(3):383-417.
3. Törnquist P, Alm A. Retinal and choroidal contribution to retinal metabolism in vivo. A study in pigs. *Acta Physiol Scand*. 1979; 106(3):351-357.
4. Watanabe D, Suzuma K, Matsui S, et al. Erythropoietin as a retinal angiogenic factor in proliferative diabetic retinopathy. *N Engl J Med*. 2005; 353(8):782-792.
5. Krock BL, Skuli N, Simon MC. Hypoxia-Induced Angiogenesis Good and Evil. *Genes & cancer*. 2011; 2(12):1117-1133.
6. Inoue Y, Yanagi Y, Matsuura K, Takahashi H, Tamaki Y, Araie M. Expression of hypoxia-inducible factor 1alpha and 2alpha in choroidal neovascular membranes associated with age-related macular degeneration. *Br J Ophthalmol*. 2007; 91(12):1720-1721.
7. Venkataraman ST, Hudson C, Rachmiel R, et al. Retinal arteriolar vascular reactivity in untreated and progressive primary open-angle glaucoma. *Invest Ophthalmol Vis Sci.* 2010; 51(4):2043-2050.
8. Gross RL, Hensley SH, Gao F, Wu SM. Retinal ganglion cell dysfunction induced by hypoxia and glutamate: potential neuroprotective effects of β-blockers. *Surv Ophthalmol*. 1999; 43:S162-S170.
9. Wanek J, Teng PY, Blair NP, Shahidi M. Inner retinal oxygen delivery and metabolism under normoxia and hypoxia in rat. *Invest Ophthalmol Vis Sci.* 2013; 54(7):5012-5019.

10. Yu D, Cringle SJ, Yu PK, Su E. Intraretinal oxygen distribution and consumption during retinal artery occlusion and graded hyperoxic ventilation in the rat. *Invest Ophthalmol Visual Sci*. 2007; 48(5):2290.
11. Alder VA, Ben-Nun J, Cringle SJ. PO2 profiles and oxygen consumption in cat retina with an occluded retinal circulation. *Invest Ophthalmol Vis Sci.* 1990; 31(6):1029-1034.
12. Yu D, Cringle SJ. Oxygen distribution and consumption within the retina in vascularized and avascular retinas and in animal models of retinal disease. *Prog Retin Eye Res.* 2001; 20(2):175-208.
13. Palkovits S, Lasta M, Told R, et al. Retinal oxygen metabolism during normoxia and hyperoxia in healthy subjects. *Invest Ophthalmol Vis Sci.* 2014; 55(8):4707-4713.
14. Ekstraksiyon, Serebrovasküler Hastalıklı Hastalarda Oksijen, Fraksiyonunun M, ve Sonrası CÖ. Quantitative Measurement of Oxygen Extraction Fraction by MRI in Patients with Cerebrovascular Disease: Pre-and Post-Surgery. *Turk Neurosurg.* 2015; 25(1):21-28.
15. Ragan DK, McKinstry R, Benzinger T, Leonard J, Pineda JA. Depression of whole-brain oxygen extraction fraction is associated with poor outcome in pediatric traumatic brain injury. *Pediatr Res.* 2011; 71(2):199-204.
16. Heiss W, Sobesky J. Comparison of PET and DW/PW-MRI in acute ischemic stroke. *Keio J Med.* 2008; 57(3):125-131.
17. Yamauchi H, Fukuyama H, Nagahama Y, et al. Significance of increased oxygen extraction fraction in five-year prognosis of major cerebral arterial occlusive diseases. *Journal of Nuclear Medicine*. 1999; 40(12):1992-1998.

18. London A, Benhar I, Schwartz M. The retina as a window to the brain—from eye research to CNS disorders. *Nature Reviews Neurology.* 2013; 9(1):44-53.
19. Steuer H, Jaworski A, Elger B, et al. Functional characterization and comparison of the outer blood-retina barrier and the blood-brain barrier. *Invest Ophthalmol Vis Sci.* 2005; 46(3):1047-1053.
20. Wang Y, Bower BA, Izatt JA, Tan O, Huang D. In vivo total retinal blood flow measurement by Fourier domain Doppler optical coherence tomography. *J Biomed Opt.* 2007; 12(4):041215-041215-8.
21. Tan O, Nittala MG, Sadda SR, Huang D. Reproducibility of Retinal Blood Flow Measurements Derived from Semi-Automated Doppler OCT Analysis. *Invest Ophthalmol Vis Sci.* 2011; 52(14):1710-1710.
22. Tan O, Wang Y, Konduru RK, Zhang X, Sadda S, Huang D. Doppler optical coherence tomography of retinal circulation. *Journal of visualized experiments: JoVE.* 2011(67):e3524-e3524.
23. Rose K, Jong M, Yusof F, et al. Grader learning effect and reproducibility of Doppler Spectral-Domain Optical Coherence Tomography derived retinal blood flow measurements. *Acta Ophthalmol.* 2014; 92(8):e630-e636.
24. Tayyari F, Yusof F, Vymyslicky M, et al. Variability and Repeatability of Quantitative, Fourier-Domain Optical Coherence Tomography Doppler Blood Flow in Young and Elderly Healthy Subjects. *Invest Ophthalmol Vis Sci.* 2014; 55(12):7716-7725.

25. Patel SR, Flanagan JG, Shahidi AM, Sylvestre J, Hudson C. A prototype hyperspectral system with a tunable laser source for retinal vessel imaging. *Invest Ophthalmol Vis Sci.* 2013; 54(8):5163-5168.
26. Schindelin J, Arganda-Carreras I, Frise E, et al. Fiji: an open-source platform for biological-image analysis. *Nature methods*. 2012; 9(7):676-682.
27. Slessarev M, Han J, Mardimae A, et al. Prospective targeting and control of end-tidal CO_2 and O_2 concentrations. *J Physiol (Lond).* 2007; 581(3):1207-1219.
28. Slessarev M, Somogyi R, Preiss D, Vesely A, Sasano H, Fisher JA. Efficiency of oxygen administration: sequential gas delivery versus "flow into a cone" methods. *Crit Care Med.* 2006; 34(3):829-834.
29. Gilmore ED, Hudson C, Preiss D, Fisher J. Retinal arteriolar diameter, blood velocity, and blood flow response to an isocapnic hyperoxic provocation. *Am J Physiol Heart Circ Physiol.* 2005; 288(6):H2912-7.
30. McLellan S, Walsh T. Oxygen delivery and hemoglobin. *Continuing Education in Anaesthesia, Critical Care & Pain*. 2004; 4(4):123-126.
31. Balaban DY, Duffin J, Preiss D, et al. The in-vivo oxyhemoglobin dissociation curve at sea level and high altitude. *Respiratory physiology & neurobiology.* 2013; 186(1):45-52.
32. Pittman RN. Matching Oxygen Supply to Oxygen Demand. In: *Regulation of Tissue Oxygenation.* Morgan & Claypool Life Sciences; 2011: Chapter 8.
33. Palkovits S, Told R, Schmidl D, et al. Regulation of retinal oxygen metabolism in humans during graded hypoxia. *Am J Physiol Heart Circ Physiol*. 2014; 307(10):H1412-H1418.

34. Pittman RN. Matching Oxygen Supply to Oxygen Demand. In: *Regulation of Tissue Oxygenation.* Morgan & Claypool Life Sciences; 2011: Chapter 7.
35. Wangsa-Wirawan ND, Linsenmeier RA. Retinal oxygen: fundamental and clinical aspects. *Arch Ophthalmol.* 2003; 121(4):547-557.
36. Shahidi M, Shakoor A, Blair NP, Mori M, Shonat RD. A method for chorioretinal oxygen tension measurement. *Curr Eye Res*. 2006; 31(4):357-366.
37. Cheng RW, Yusof F, Tsui E, et al. Relationship between Retinal Blood Flow and Arterial Oxygen. *J Physiol (Lond).* 2015.
38. Ito H, Kanno I, Kato C, et al. Database of normal human cerebral blood flow, cerebral blood volume, cerebral oxygen extraction fraction and cerebral metabolic rate of oxygen measured by positron emission tomography with 15O-labelled carbon dioxide or water, carbon monoxide and oxygen: a multicenter study in Japan. *European journal of nuclear medicine and molecular imaging.* 2004; 31(5):635-643.
39. Berkowitz BA, Luan H, Gupta RR, et al. Regulation of the early subnormal retinal oxygenation response in experimental diabetes by inducible nitric oxide synthase. *Diabetes.* 2004; 53(1):173-178.
40. Teng PY, Wanek J, Blair NP, Shahidi M. Inner retinal oxygen extraction fraction in rat. *Invest Ophthalmol Vis Sci.* 2013; 54(1):647-651.
41. Zhu X, Chen JM, Tu T, Chen W, Song S. Simultaneous and noninvasive imaging of cerebral oxygen metabolic rate, blood flow and oxygen extraction fraction in stroke mice. *Neuroimage*. 2013; 64:437-447.

42. Gupta A, Baradaran H, Schweitzer AD, et al. Oxygen extraction fraction and stroke risk in patients with carotid stenosis or occlusion: a systematic review and meta-analysis. *AJNR Am J Neuroradiol*. 2014; 35(2):250-255.
43. Wang S, Linsenmeier RA. Hyperoxia improves oxygen consumption in the detached feline retina. *Invest Ophthalmol Vis Sci.* 2007; 48(3):1335-1341.
44. Milley JR, Rosenberg AA, Jones MD. Retinal and choroidal blood flows in hypoxic and hypercarbic newborn lambs. *Pediatr Res.* 1984; 18(5):410-414.
45. Werkmeister RM, Schmidl D, Aschinger G, et al. Retinal oxygen extraction in humans. *Sci Rep*. 2015; 5:15763.
46. Bengtsson J, Bake B, Johansson Å, Bengtson J. End-tidal to arterial oxygen tension difference as an oxygenation index. *Acta Anaesthesiol Scand.* 2001; 45(3):357-363.
47. Chong SP, Merkle CW, Leahy C, Srinivasan VJ. Cerebral metabolic rate of oxygen (CMRO 2) assessed by combined Doppler and spectroscopic OCT. *Biomedical optics express.* 2015; 6(10):3941-3951.
48. Song W, Wei Q, Liu W, et al. A combined method to quantify the retinal metabolic rate of oxygen using photoacoustic ophthalmoscopy and optical coherence tomography. *Scientific reports.* 2014; 4.

Chapter 5 Reference list

1. Stallard H. Radiant Energy as (a) a Pathogenic, (b) a Therapeutic Agent in Ophthalmic Disorders. The Gifford Edmonds Prize Essay for 1932. *PP-London.-British Journal of Ophthalmology*; 1933.
2. Irvine AR, Alvarado JA, Wara WM, Morris BW, Wood IS. Radiation retinopathy: an experimental model for the ischemic--proliferative retinopathies. *Trans Am Ophthalmol Soc.* 1981; 79:103-122.
3. Krema H, Xu W, Payne D, Vasquez LM, Pavlin CJ, Simpson R. Factors predictive of radiation retinopathy post 125 Iodine brachytherapy for uveal melanoma. *Canadian Journal of Ophthalmology/Journal Canadien d'Ophtalmologie.* 2011; 46(2):158-163.
4. Finger PT. Radiation therapy for choroidal melanoma. *Surv Ophthalmol.* 1997; 42(3):215-232.
5. Higginson DS, Sahgal A, Lawrence MV, et al. External Beam Radiotherapy for Head and Neck Cancers Is Associated with Increased Variability in Retinal Vascular Oxygenation. *PloS one.* 2013; 8(8):e69657.
6. Margo CE. The collaborative ocular melanoma study: an overview. *Cancer Control.* 2004; 11(5):304-309.
7. Melia BM, Abramson DH, Albert DM, et al. Collaborative ocular melanoma study (COMS) randomized trial of I-125 brachytherapy for medium choroidal melanoma. I. Visual acuity after 3 years COMS report no. 16. *Ophthalmology.* 2001; 108(2):348-366.
8. Shields JA, Shields CL. *Current management of posterior uveal melanoma.* 1993; 68(12):1196-1200.

9. Gündüz K, Shields CL, Shields JA, Cater J, Freire JE, Brady LW. Radiation retinopathy following plaque radiotherapy for posterior uveal melanoma. *Arch Ophthalmol.* 1999; 117(5):609-614.
10. Archer D, Amoaku W, Gardiner T. Radiation retinopathy—clinical, histopathological, ultrastructural and experimental correlations. *Eye.* 1991; 5(Pt 2):239-251.
11. Atebara NH, Drouilhet JH, and Brown, GC. Chapter 36A: Radiation Retinopathy. Duane's ophthalmology on CD-ROM Lippincott Williams & Wilkins. 2006.
12. Reichstein D. Current treatments and preventive strategies for radiation retinopathy. *Curr Opin Ophthalmol.* 2015; 26(3):157-166.
13. Giuliari GP, Sadaka A, Hinkle DM, Simpson ER. Current treatments for radiation retinopathy. *Acta Oncol.* 2011; 50(1):6-13.
14. Faryan T, Lee-Anne K, Flanagan JG, Shaun S, Brent MH, Christopher H. Retinal blood flow and retinal blood oxygen saturation in mild to moderate diabetic retinopathy retinal blood flow and SO_2 in early DR. *Invest Ophthalmol Vis Sci.* 2015;56(11):6796-6800.
15. Hammer M, Vilser W, Riemer T, et al. Diabetic patients with retinopathy show increased retinal venous oxygen saturation. *Graefes Arch Clin Exp Ophthalmol.* 2009; 247(8):1025-1030.
16. Hardarson SH, Stefansson E. Retinal oxygen saturation is altered in diabetic retinopathy. *Br J Ophthalmol.* 2012; 96(4):560-563.
17. Hardarson SH, Elfarsson A, Agnarsson BA, Stefánsson E. Retinal oximetry in central retinal artery occlusion. *Acta Ophthalmol.* 2013; 91(2):189-190.

18. Eliasdottir TS, Bragason D, Hardarson SH, Kristjansdottir G, Stefánsson E. Venous oxygen saturation is reduced and variable in central retinal vein occlusion. *Graefe's Archive for Clinical and Experimental Ophthalmology*. 2015; 253(10):1653-1661.
19. Shahidi AM, Hudson C, Tayyari F, Flanagan JG. Retinal oxygen saturation in patients with primary open-angle glaucoma using a non-flash hyperspectral camera. *Curr Eye Res*. 2016:1-5.
20. Resch H, Garhofer G, Fuchsjäger-Mayrl G, Hommer A, Schmetterer L. Endothelial dysfunction in glaucoma. *Acta Ophthalmol.* 2009; 87(1):4-12.
21. Flammer J, Orgül S, Costa VP, et al. The impact of ocular blood flow in glaucoma. *Prog Retin Eye Res.* 2002; 21(4):359-393.
22. Patel SR, Flanagan JG, Shahidi AM, Sylvestre J, Hudson C. A prototype hyperspectral system with a tunable laser source for retinal vessel imaging. *Invest Ophthalmol Vis Sci*. 2013; 54(8):5163-5168.
23. Rose K, Kulasekara SI, Hudson C. Intervisit Repeatability of retinal blood oximetry and total retinal blood flow under varying systemic blood gas oxygen saturations. *Invest Ophthalmol Vis Sci.* 2016; 57(1):188-197.
24. Cheng RW, Yusof F, Tsui E, et al. Relationship between retinal blood flow and arterial oxygen. *J Physiol (Lond).* 2016; 594(3):625-640.
25. Khuu L, Flanagan JG, Tayyari F, et al. Retinal blood flow is reduced in patients with non-proliferative diabetic retinopathy. *Invest Ophthalmol Vis Sci.* 2014; 55(13):4342-4342.

26. Wang Y, Fawzi A, Tan O, Gil-Flamer J, Huang D. Retinal blood flow detection in diabetic patients by Doppler Fourier domain optical coherence tomography. *Optics express.* 2009; 17(5):4061-4073.
27. Wang Y, Bower BA, Izatt JA, Tan O, Huang D. In vivo total retinal blood flow measurement by Fourier domain Doppler optical coherence tomography. *J Biomed Opt. 2007*; 12(4):041215-041215-8.
28. Wang Y, Fawzi AA, Varma R, et al. Pilot study of optical coherence tomography measurement of retinal blood flow in retinal and optic nerve diseases. *Invest Ophthalmol Vis Sci.* 2011; 52(2):840-845.
29. Tan O, Nittala MG, Sadda SR, Huang D. Reproducibility of Retinal Blood Flow Measurements Derived from Semi-Automated Doppler OCT Analysis. *Invest Ophthalmol Vis Sci.* 2011; 52(14):1710-1710.
30. Tan O, Wang Y, Konduru RK, Zhang X, Sadda SR, Huang D. Doppler optical coherence tomography of retinal circulation. *JoVE.* 2012(67):e3524-e3524.
31. Konduru RK, Tan O, Nittala MG, Huang D, Sadda SR. Reproducibility of retinal blood flow measurements derived from semi-automated Doppler OCT analysis. *Ophthalmic Surgery, Lasers and Imaging Retina.* 2012; 43(1):25-31.
32. Schindelin J, Arganda-Carreras I, Frise E, et al. Fiji: an open-source platform for biological-image analysis. *Nature methods.* 2012; 9(7):676-682.
33. Khoobehi B, Firn K, Thompson H, Reinoso M, Beach J. Retinal arterial and venous oxygen saturation is altered in diabetic patients. *Invest Ophthalmol Vis Sci.* 2013; 54(10):7103-7106.

34. Rassam SM, Patel V, Kohner EM. The effect of experimental hypertension on retinal vascular autoregulation in humans: a mechanism for the progression of diabetic retinopathy. *Exp Physiol.* 1995; 80(1):53-68.
35. Chahal P, Inglesby DV, Sleightholm M, Kohner EM. Blood pressure and the progression of mild background diabetic retinopathy. *Hypertension.* 1985; 7(6 Pt 2):II79-83.
36. Rilvén S, Torp TL, Grauslund J. Retinal oximetry in patients with ischaemic retinal diseases. *Acta Ophthalmol.* 2016. Sep 1. doi: 10.1111/aos.13229. [Epub ahead of print].
37. Groenewald C, Konstantinidis L, Damato B. Effects of radiotherapy on uveal melanomas and adjacent tissues. *Eye.* 2013; 27(2):163-171.
38. Ward J. The complexity of DNA damage: relevance to biological consequences. *Int J Radiat Biol.* 2009.
39. Archerz D, Gardiner T. Ionizing radiation and the retina. *Curr Opin Ophthalmol.* 1994; 5(3):59-65.
40. Nguyen V, Waleed Gaber M, Sontag MR, F Kiani M. Late effects of ionizing radiation on the microvascular networks in normal tissue. *Radiat Res.* 2000; 154(5):531-536.
41. Roth NM, Sontag MR, Kiani MF. Early effects of ionizing radiation on the microvascular networks in normal tissue. *Radiat Res.* 1999; 151(3):270-277.
42. Pogrzebielski A, Starzycka M, Romanowska-Dixon B, Jakubowska B, Szpakowicz U. The analysis of I125 brachytherapy complications in cases of uveal melanoma. *Klin Oczna.* 2005; 107(1-3):49-53.

43. Parsons JT, Bova FJ, Fitzgerald CR, Mendenhall WM, Million RR. Radiation retinopathy after external-beam irradiation: analysis of time-dose factors. *International Journal of Radiation Oncology* Biology* Physics.* 1994; 30(4):765-773.
44. Fernandes BF, Weisbrod D, Yücel YH, et al. Neovascular glaucoma after stereotactic radiotherapy for juxtapapillary choroidal melanoma: histopathologic and dosimetric findings. *International Journal of Radiation Oncology* Biology* Physics.* 2011; 80(2):377-384.
45. Hayreh SS. Post-radiation retinopathy. A fluorescence fundus angiographic study. *Br J Ophthalmol.* 1970; 54(11):705-714.

Chapter 6 Reference list

1. Acker J, Marks LB, Spencer D, et al. Serial in vivo observations of cerebral vasculature after treatment with a large single fraction of radiation. *Radiat Res*. 1998; 149(4):350-359.

2. Archer D, Amoaku W, Gardiner T. Radiation retinopathy—clinical, histopathological, ultrastructural and experimental correlations. *Eye*. 1991; 5(Pt 2):239-251.

3. Archerz D, Gardiner T. Ionizing radiation and the retina. *Curr Opin Ophthalmol*. 1994; 5(3):59-65.

4. Bianciotto C, Shields CL, Pirondini C, Mashayekhi A, Furuta M, Shields JA. Proliferative radiation retinopathy after plaque radiotherapy for uveal melanoma. *Ophthalmology*. 2010; 117(5):1005-1012.

5. Char DH, Castro JR, Kroll SM, Irvine AR, Quivey JM, Stone RD. Five-year follow-up of helium ion therapy for uveal melanoma. *Arch Ophthalmol*. 1990; 108(2):209-214.

6. Chee PH. Radiation retinopathy. *Am J Ophthalmol*. 1968; 66(5):860-865.

7. Damato B, Foulds W. Tumor-associated retinal pigment epitheliopathy. *Eye*. 1990; 4(2):382-387.

8. Gragoudas ES, Egan KM, Seddon JM, et al. Survival of Patents with Metastases from Uveal Melanoma. *Ophthalmology*. 1991; 98(3):383-390.

9. Griewank KG, Murali R. Pathology and genetics of uveal melanoma. *Pathology*. 2013; 45(1):18-27. doi: 10.1097/PAT.0b013e32835c6505 [doi].

10. Hammer M, Vilser W, Riemer T, et al. Diabetic patients with retinopathy show increased retinal venous oxygen saturation. *Graefe's Archive for Clinical and Experimental Ophthalmology*. 2009; 247(8):1025-1030.

11. Hardarson SH, Elfarsson A, Agnarsson BA, Stefánsson E. Retinal oximetry in central retinal artery occlusion. *Acta Ophthalmol*. 2013; 91(2):189-190.

12. Hardarson SH, Harris A, Karlsson RA, et al. Automatic retinal oximetry. *Invest Ophthalmol Vis Sci*. 2006; 47(11):5011-5016.

13. Hardarson SH, Stefansson E. Retinal oxygen saturation is altered in diabetic retinopathy. *Br J Ophthalmol*. 2012; 96(4):560-563. doi: 10.1136/bjophthalmol-2011-300640 [doi].

14. Iwamoto T, Jones IS, Howard GM. Ultrastructural comparison of spindle A, spindle B, and epithelioid-type cells in uveal malignant melanoma. *Invest Ophthalmol Vis Sci*. 1972; 11(11):873-889.

15. Konduru RK, Tan O, Nittala MG, Huang D, Sadda SR. Reproducibility of retinal blood flow measurements derived from semi-automated Doppler OCT analysis. *Ophthalmic Surgery, Lasers and Imaging Retina*. 2012; 43(1):25-31.

16. Krema H, Xu W, Payne D, Vasquez LM, Pavlin CJ, Simpson R. Factors predictive of radiation retinopathy post 125 Iodine brachytherapy for uveal melanoma. *Canadian Journal of Ophthalmology/Journal Canadien d'Ophtalmologie*. 2011; 46(2):158-163.

17. Krema H, Heydarian M, Beiki-Ardakani A, et al. A comparison between (1)(2)(5)Iodine brachytherapy and stereotactic radiotherapy in the management of juxtapapillary choroidal melanoma. *Br J Ophthalmol*. 2013; 97(3):327-332. doi: 10.1136/bjophthalmol-2012-302808 [doi].

18. Lumbroso-Le Rouic L, Chefchaouni MC, Levy C, et al. ^{125}I plaque brachytherapy for anterior uveal melanomas. *Eye*. 2004; 18(9):911-916.

19. Margo CE. The collaborative ocular melanoma study: an overview. *Cancer Control*. 2004; 11(5):304-309.

20. Miller B, Abrahams C, Cole GC, Proctor NS. Ocular malignant melanoma in South African blacks. *Br J Ophthalmol*. 1981; 65(10):720-722.

21. Nguyen V, Waleed Gaber M, Sontag MR, F Kiani M. Late effects of ionizing radiation on the microvascular networks in normal tissue. *Radiat Res*. 2000; 154(5):531-536.

22. Patel SR, Flanagan JG, Shahidi AM, Sylvestre J, Hudson C. A Prototype Hyperspectral System With a Tunable Laser Source for Retinal Vessel ImagingA Prototype Hyperspectral System. *Invest Ophthalmol Vis Sci*. 2013; 54(8):5163-5168.

23. Resch H, Garhöfer G, Schmetterer L, Zehetmayer M, Dorner GT. Choroidal perfusion in eyes with untreated choroidal melanoma. *Acta Ophthalmol*. 2008; 86(4):404-407.

24. Roth NM, Sontag MR, Kiani MF. Early effects of ionizing radiation on the microvascular networks in normal tissue. *Radiat Res*. 1999; 151(3):270-277.

25. Schindelin J, Arganda-Carreras I, Frise E, et al. Fiji: an open-source platform for biological-image analysis. *Nature methods*. 2012; 9(7):676-682.

26. Scotto J, Fraumeni JF,Jr, Lee JA. Melanomas of the eye and other noncutaneous sites: epidemiologic aspects. *J Natl Cancer Inst*. 1976; 56(3):489-491.

27. Singh P, Singh A. Choroidal melanoma. *Oman J Ophthalmol*. 2012; 5(1):3-9. doi: 10.4103/0974-620X.94718 [doi].

28. Stallard H. Radiant Energy as (a) a Pathogenic,(b) a Therapeutic Agent in Ophthalmic Disorders. *The Gifford Edmonds Prize Essay for 1932.* PP-London.- *Br J Ophthalmol*; 1933.

29. Tan O, Nittala MG, Sadda SR, Huang D. Reproducibility of Retinal Blood Flow Measurements Derived from Semi-Automated Doppler OCT Analysis. *Invest Ophthalmol Vis Sci*. 2011; 52(14):1710-1710.

30. Tan O, Wang Y, Konduru RK, Zhang X, Sadda SR, Huang D. Doppler optical coherence tomography of retinal circulation. *JoVE*. 2012(67):e3524-e3524.

31. Vecsei PV, Kircher K, Nagel G, et al. Ocular arterial blood flow of choroidal melanoma eyes before and after stereotactic radiotherapy using Leksell gamma knife: 2 year follow up. *Br J Ophthalmol*. 1999; 83(12):1324-1328.

32. Wang Y, Bower BA, Izatt JA, Tan O, Huang D. In vivo total retinal blood flow measurement by Fourier domain Doppler optical coherence tomography. *J Biomed Opt*. 2007; 12(4):041215-041215-8.

33. Wang Y, Fawzi AA, Varma R, et al. Pilot study of optical coherence tomography measurement of retinal blood flow in retinal and optic nerve diseases. *Invest Ophthalmol Vis Sci*. 2011; 52(2):840-845.

34. Wang Y, Fawzi A, Tan O, Gil-Flamer J, Huang D. Retinal blood flow detection in diabetic patients by Doppler Fourier domain optical coherence tomography. *Optics express*. 2009; 17(5):4061-4073.

35. Wen JC, Oliver SC, McCannel TA. Ocular complications following I-125 brachytherapy for choroidal melanoma. *Eye*. 2009; 23(6):1254-1268.

36. Yang Y, Kent D, Fenerty C, Kosmin A, Damato B. Pulsatile ocular blood flow in eyes with untreated choroidal melanoma. *Eye-London-Ophthalmological Soceity Of The United Kingdom Then Royal College Of Ophthalmologists-*. 1997; 11:331-334.

37. Desjardins, L. Proton beam radiotherapy of uveal melanomas. *Acta Ophthalmol*. 2014; 92: s253.

Chapter 7 Reference List

1. Feke GT. Laser Doppler instrumentation for the measurement of retinal blood flow: theory and practice. *Bull Soc Belge Ophtalmol*. 2006; 302:171-184.
2. Guan K, Hudson C, Flanagan JG. Variability and repeatability of retinal blood flow measurements using the Canon Laser Blood Flowmeter. *Microvasc Res*. 2003; 65(3):145-151.
3. Garhofer G, Werkmeister R, Dragostinoff N, Schmetterer L. Retinal blood flow in healthy young subjects. *Invest Ophthalmol Vis Sci.* 2012; 53(2):698-703.
4. Russell RR. Evidence for autoregulation in human retinal circulation. *The Lancet*. 1973; 302(7837):1048-1050.
5. Pechauer AD, Huang D, Jia Y. Detecting blood flow response to stimulation of the human eye. *BioMed research international*. 2015; 2015:121973. doi: 10.1155/2015/121973.
6. Dorner G, Garhoefer G, Zawinka C, Kiss B, Schmetterer L. Response of retinal blood flow to CO_2-breathing in humans. *Eur J Ophthalmol*. 2002; 12(6):459-466.
7. Gilmore ED, Hudson C, Preiss D, Fisher J. Retinal arteriolar diameter, blood velocity, and blood flow response to an isocapnic hyperoxic provocation. *Am J Physiol Heart Circ Physiol*. 2005; 228(6):2912-2917.
8. Riva CE, Sinclair SH, Grunwald JE. Autoregulation of retinal circulation in response to decrease of perfusion pressure. *Invest Ophthalmol Vis Sci*. 1981; 21(1):34.

9. Gilmore ED, Hudson C, Nrusimhadevara RK, et al. Retinal arteriolar diameter, blood velocity, and blood flow response to an isocapnic hyperoxic provocation in early sight-threatening diabetic retinopathy. *Invest Ophthalmol Vis Sci*. 2007; 48(4):1744-1750.
10. Pournaras CJ, Rungger-Brändle E, Riva CE, Hardarson SH, Stefansson E. Regulation of retinal blood flow in health and disease. *Prog Retin Eye Res*. 2008; 27(3):284-330.
11. Venkataraman ST, Flanagan JG, Hudson C. Vascular reactivity of optic nerve head and retinal blood vessels in glaucoma—a review. *Microcirculation*. 2010; 17(7):568-581.
12. Rose K, Flanagan JG, Patel SR, Cheng R, Hudson C. Retinal blood flow and vascular reactivity in chronic smokers. *Invest Ophthalmol Vis Sci*. 2014; 55(7):4266-4276.
13. Slessarev M, Han J, Mardimae A, et al. Prospective targeting and control of end-tidal CO_2 and O_2 concentrations. *J Physiol (Lond)*. 2007; 581(3):1207-1219.
14. Slessarev M, Somogyi R, Preiss D, Vesely A, Sasano H, Fisher JA. Efficiency of oxygen administration: Sequential gas delivery versus" flow into a cone" methods. *Crit Care Med*. 2006; 34(3):829-834.
15. Sponsel WE, DePaul KL, Zetlan S. Retinal hemodynamic effects of carbon dioxide, hyperoxia, and mild hypoxia. *Invest Ophthalmol Vis Sci*. 1992; 33(6):1864.
16. Roff EJ, Harris A, Chung HS, et al. Comprehensive assessment of retinal, choroidal and retrobulbar hemodynamics during blood gas perturbation. *Graefe's archive for clinical and experimental ophthalmology*. 1999; 237(12):984-990.
17. Alder VA, Ben-Nun J, Cringle SJ. PO_2 profiles and oxygen consumption in cat retina with an occluded retinal circulation. *Invest Ophthalmol Vis Sci*. 1990; 31(6):1029-1034.

18. Zhu Y, Park T, Gidday JM. Mechanisms of hyperoxia-induced reductions in retinal blood flow in newborn pig. *Exp Eye Res*. 1998; 67(3):357-369.
19. Cringle SJ, Yu D, Yu PK, Su E. Intraretinal oxygen consumption in the rat in vivo. *Invest Ophthalmol Visual Sci*. 2002; 43(6):1922-1927.
20. Chong SP, Merkle CW, Leahy C, Srinivasan VJ. Cerebral metabolic rate of oxygen (CMRO 2) assessed by combined Doppler and spectroscopic OCT. *Biomedical optics express*. 2015; 6(10):3941-3951.
21. Song W, Wei Q, Liu W, et al. A combined method to quantify the retinal metabolic rate of oxygen using photoacoustic ophthalmoscopy and optical coherence tomography. *Sci Rep*. 2014; 4:6525. doi: 10.1038/srep06525.
22. GilmoreED, HudsonC, VenkataramanST, et al. Comparison of different hyperoxic paradigms to induce vasoconstriction: implications for the investigation of retinal vascular reactivity. *Invest Ophthalmol Vis Sci*. 2004; 45:3207–3212.